Republic of Iraq
Ministry of Higher Education and Scientific Research
University of Babylon
College of Engineering
Civil Engineering Department

Investigation of Effectiveness of Different Types of Blocks In Dissipating of Energy Within Stilling Basins

A Thesis

Submitted to the College of Engineering \ University of Babylon in Partial Fulfillment of the Requirements for the Degree of Master in Civil Engineering \Water Resources Engineering

By

Mohammed Jawad Kadhim Al-Fatlawi

(B.Sc. 2016)

Supervised By

Prof. Dr. Abdul Hassan K. Al-Shuker

2023

وَمَا تَوْفِيقِي إِلَّا بِاللَّهِ ۚ عَلَيْهِ تَوَكَّلْتُ
وَإِلَيْهِ أُنِيبُ

[هود من الآية:88]

Certificate

I certify that this thesis entitled **''Investigation of Effectiveness of Different Types of Blocks In Dissipating of Energy Within Stilling Basins''** is prepared by **Muhammad Jawad Kadhim Al-Fatlawi** under my supervision at the College of Engineering, University of Babylon in partial fulfillment of the requirements for the degree of Master of science in Civil Engineering / Water Resources Engineering.

Supervisor

Signature:

Name: Prof. Dr. Abdul Hassan K. Al-Shuker

Date: / / 2023

EXAMINATION COMMITTEE CERTIFICATE

We certify that we have read this thesis entitled ***"Investigation of Effectiveness of Different Types of Blocks In Dissipating of Energy Within Stilling Basins"*** presented by ***"Muhammad Jawad Kadhim Al-Fatlawi"*** and as an examining committee, we examined the student in its content and in what is connected with it, and that in our opinion it meets standard of a thesis for the degree of Master of Science in Civil Engineering / Water Resources Engineering.

Signature

Name: ***Prof. Dr. Riyadh Z. Azzubaidi***

(Chairman)

Date:

Signature

Name: ***Prof. Dr. Nisreen J. Al-Mansori***

(Member)

Date:

Signature

Name: ***Assist Prof. Dr. Najah K. Abbas***

(Member)

Date:

Signature:

Name: ***Prof. Dr. Abdul Hassan K. Al-Shuker***

(Member and Supervisor)

Date:

Approved by the Head of the Civil Engineering Department

Signature:

Name: ***Prof. Dr .Thair J. Alfatlawi***

Date:

Approved by the Dean of College of Engineering

Signature:

Name: ***Prof. Dr. Hatem H. Al-Taie***

Data:

Abstract

Spillway is one of the most significant components of the dam to ensure safety during a flood. The identification of hydraulic characteristics for a spillway is a difficult issue because it is exposed to different types of flow throughout its service life. Ogee spillway is the most important type of spillway, due it is widely used in many earthen and concrete dams, as well as it needs precise and complex design details. The scouring problem caused by the flow movement in the downstream areas of hydraulic structures is an issue that keeps its actuality. In order to prevent these scouring to occur, various types of energy dissipaters are placed downstream of the hydraulic structures, especially in stilling basins. Factors such as sediment type, the velocity of the stream, and flow regime play an important role in scouring. To prevent scouring, the flow's energy must be dissipated before meeting the sediment.

This study aims to reduce the amount of scour occurred downstream of the ogee spillway using different block configurations such as baffle blocks, triangle blocks, and stepped blocks. These dissipated blocks have been distributed at stilling basin with three new proposed types of distributions, as one, two, and three rows.

The flow and scouring events on the spillway were carried out in the laboratory as experimental works. Each configuration was tested under Froude numbers ranging from 2.75 to 9.25 at which the hydraulic jump was located within a description of oscillating and steady jump. During the tests, the sequent depths, transverse velocity distributions, and scour depths were measured. The findings were compared for the proposed block distributions and the results were discussed in this respect.

The results showed that the baffle block configuration appeared with good

results in minimizing flow velocities within the stilling basin in accordance with proposed distributions, especially with the range of Froude number 4.5-9.25. Also, using the triangle block distribution has demonstrated that this distribution produces a uniform flow along the stilling basin, with a range of 5.75–9.25 of the Froude number, which dissipated (45-70) %. Stepped block distribution appeared with better results in reducing the sequent depth ratios and the flow velocities compared to the baffle block and triangle block, as it can be seen that there is a decrease in velocities up to (73-85) %. The transverse local velocity distribution across the flume width, when using the stepped block configuration, tends to become more uniform across the width while these values seem greater than those that were observed with the other configurations.

Acknowledgments

First and foremost, all praises and thanks are due to **Allah** (subhanaho wa taala) for bestowing me with health**,** knowledge and patience to complete this work. Many peace and blessings of Allah be upon **Prophet Muhammad** (PBUH), **his family** and **righteous**, for providing me the spiritual support to pass master's study.

I would like to express my sincerely and cordial thanks to my supervisor Dr. Abdul Hassan Khadr Al-Shuker who provided me with invaluable guidance, encouragement, suggestions, ideas and continued support throughout the preparation of this work.

I am very grateful to my family for everything. Also, I wish to express how I am thankful to my friends and staff of Civil Engineering Laboratories, College of Engineering, Babylon University, IRAQ.

Mohammed Al-Fatlawi

List of Contents

List of Abbreviations

Abbreviations	Description
3D	Three-Dimensional.
CFD	Computational Fluid Dynamics
CFD	Computational Fluid Dynamics.
DDBs	Direction-Diverting Blocks
FEM	Finite Element Method
FSL	Full Supply Level
ICOLD	International Commission On Large Dams
T.P	Tangential Point
USACE	United States Army Corps Of Engineers
USBR	United States Bureau of Reclamation
VOF	Volume Of Fluid

List of symbols

Symbol	Description	*Unit*
δ_C	settlement due to consolidation	*M*
C_C	compression index	*Dimensionless*
e_0	initial void ratio	*dimensionless*
σ_{zf}	final vertical stress	*N/m²*
σ_{zo}	initial vertical stress.	*N/m²*
H	height of the compressible soil	*m*
C r	recompression index	*dimensionless*
σ_{zc}	pre-consolidation stress of the soil	*N/m²*
p_w	density of the distilled water	*kg/m³*
p_s	density of the soil particles	*kg/m³*
K	temperature correction factor	*dimensionless*

List of Figures

List of Tables

CHAPTER ONE
INTRODUCTION

1.1 General

The increasing need for water supply, flood control, and hydroelectric power generation has prompted governments to build dams as a top priority around the world. As water is of critical importance to protect, technological improvements in the design and analysis of dams are needed for better management of water resources (Foroudi and Barati 2022). All dams are equipped with spillways as a safety measure against overtopping. They are provided to safely carry water away from the reservoir when water levels exceed the full supply level. The ogee spillway, which is also known as an overflow or S-shaped spillway, is the most common type of spillway that is used to release water from a dam or levee reservoir to the downstream channels, as presented in Figure (1.1).

Figure 1.1: An Ogee Spillway(https://www.shutterstock.com).

1.2 Background and Motivation

Hydraulic jump is a common phenomenon generally observed in open channel flow, especially at the toe of hydraulic structures e.g., spillways. One of the main applications of a hydraulic jump is dissipating the excess kinetic

energy downstream of the hydraulic structures. The stilling basin is the most common form of structure to contain the hydraulic jump to achieve the required dissipation of kinetic energy (Muhsun and Al-Sharify 2018). Water flowing over an ogee spillway crest always remains in contact with the spillway surface as it smoothly flows downstream. Water flowing over an ogee spillway contains high kinetic energy that can cause erosion at its end and leads to dam failure (Peltier et al., 2018; Daneshfaraz et al., 2020). Therefore, stilling basins of different designs are used to dissipate the energy of the flowing water and establish safe flow conditions to protect the downstream end of the spillway from erosion. These basins are usually equipped with different types of blocks and end sills to stabilize, reduce the length of the hydraulic jump, and improve its performance (Morales et al., 2012; Saneie et al., 2016; Yildiz et al., 2020). The standard stilling basin, which uses the baffle blocks as a main feature for dissipating the surplus kinetic energy, is introduced in the late 1950s by Bradley and Peterka and there study was further generalized and published as Reclamation Engineering Monograph No. 25 by Peterka A. J. on September 1958 (last re-print at May 1984). Scour is the process of water removing particles from the riverbed and banks of a river or channel. Many scholars have looked at the elements that influence this phenomenon to figure out what causes it and how to fix it (Azmathullah et al., 2006; Hong et al., 2010; Samadi et al., 2015; Ghaderi et al., 2020; Nou et al., 2021; Asadi et al., 2022).

Different experimental studies have been conducted to determine the appropriate characterization for each case of development that took place in the stilling basin. Eloubaidy et al. (1999) was the first adopted a cubic baffle block to investigate the effect of location, relative size, and curvature curved (in plan) on the hydraulic jump properties and dissipation of energy. It was found that the baffle blocks have the efficiency for dissipation regarding the excess kinetic energy for all flow conditions. Maatooq (2006) explained an

experimental hydraulic model to evaluate the performance of an overflow spillway. The spillway tested has a standard ogee profile with continuous steps cut into a straight portion of the downstream face from a tangential point to the toe. The preliminary results indicated that the average increase in energy dissipation was approximately 37%, which would imply a significant reduction in the size of downstream stilling basins. Al-Zubaidy (2014) investigate the effects of applying the direction- diverting blocks fixed on an ogee spillway surface with different slopes on energy dissipation. The configurations differ in spacing between rows of blocks and the number of rows. When blocks were used, the maximum reduction in Froude Number was 36%, 89%, and 93% for spillway models with slopes 1:1, 0.85:1, and 0.75:1, respectively. Valero et al. (2018) carried out an experimental study on the baffle block with a sloping vertical face arranged downstream of a sluice gate, to investigate its effect on the length of the hydraulic jump. The results of this study show that baffle blocks with a sloping front face can reduce the jump's length compared with the free jump. Saki and Shafai (2022) used wedge-shaped and baffle blocks to find their effect on the hydraulic jump properties. The results show a reduction in the length of jump and sequent depth ratio compared to those with smooth beds. Baffle block tests showed that the scour processes were faster in contrast to wedge block, which was marked by slower changes in bed profile.

Although the laboratory results give good results, they are generally costly, require effort, and are prone to errors. Therefore, numerical methods are resorted to ensure the validity of the laboratory model and to ensure the accuracy of laboratory experiments. Numerical models are generally applied to verify the river stage and the water surface profile upstream and along the length of the spillway (Mohammed and Qasim 2012). Alwan et al., 2016 developed numerical models for spillways installed into the water in the channel and conducted underflow and clear-water conditions by using

uniform cohesion less soil as bed material with medium grain size (d_{50} = 0.65 mm). The results proved that the scour increases with increasing discharge due to an increase in water energy. Elnikhely (2018) explained local scour downstream of the ogee spillway due to hydraulic jumps. Simulations were performed using different diameters, lengths, and arrangements of baffle blocks with different discharges. The data collected proved that the use of concrete baffle blocks improved the design of spillways. Ghaderi et al., 2021 simulated the flow over the ogee spillway by solving a modified form of the shallow water equation in one dimension and a reasonable agreement was achieved. Therefore, the hydraulic field of the ogee spillway, in terms of scour and energy dissipation, becomes attractive for further studies.

1.3 Research Objectives

The main purpose of this work is to carry out an experimental program for investigating the energy dissipation and sediment scour downstream of the ogee spillway, under different discharges and Froude Numbers, and to validate these experimental results with previous works. The specific objectives of this research include:

1. Conduct experimental tests on physical models installed in the laboratory flume, to investigate the effect of blockage distance with the presence of one, two, and three rows of baffle blocks, triangle blocks, and stepped blocks on the hydraulic performance.
2. Obtain the basic parameters such as velocity distribution at end of the jump and scour effect downstream of the stilling basin.
3. Implement other experimental works in the analysis of scour with different geometries of blocks downstream of the stilling basin.

1.4 Research Limitations

The limitations of this study are:

1 The slope of the straight line part of the ogee spillway was H 0.75:V 1.

2 Maximum and minimum applied initial Froude Number was limited by a range from 2.75 to 9.25.

3 The length and width of the models are limited by the laboratory canal width of 0.3m.

1.5 Research Outline

This research project is subdivided into six chapters and structured as stated below: **Chapter One,** namely the introduction, presents the background and motivation for carrying out this research, its objectives, and the research outline. **Chapter Two** consists of literature with basic details on experimental, analytical, and numerical methods carried out in the past about flow over ogee spillways. This chapter includes the hydraulics of spillways in general and ogee spillways in particular. The recent advances in the numerical modelling of spillways are also described. **Chapter Three** provides an insight into the physical modelling concepts. It also provides the laboratory investigations executed on these models installed in a laboratory flume. **Chapter Four,** consists of the results of the physical modelling and their discussion. In **Chapter Five,** the results are discussed and conclusions are drawn. Recommendations for future research are also presented here.

CHAPTER TWO
LITERATURE REVIEW

2.1 General

This chapter presents the literature review of the study on spillways in general and ogee spillways in particular. It details different aspects that are considered while designing an ogee spillway, the discharge computation, hydraulic jump, blocks, and end sill along stilling basin as well as the factors defining the hydraulic scour performance downstream of stilling basin. It also includes a conceptual description of Computational Fluid Dynamics (CFD) where the design and methodology used for designing and testing an ogee spillway are examined. This section also presents the underlying theory of CFD modelling and the advantages of using CFD in flow modelling. Finally, a summary of this chapter and the current study contribution are discussed

2.2 Dam Appurtenances

Spillways are control appurtenances that are constructed at the dams and/ or impounding reservoirs to provide the controlled release of flows exceeding the dam's full supply level (FSL) to the downstream side. Excess water is conveyed downstream while an appropriate structure dissipates the high kinetic energy of the flow that may lead to serious scour of the channel bed. If the scour is not properly controlled at the spillway toe, it may extend backward and endanger the entire spillway as well as the dam. In some cases, the energy dissipaters are included along its slope for reducing the amount of space required to efficiently discharge the flow without jeopardizing the dam (Mohtar et al., 2020).

Of all dam safety measures, the spillway capacity is of paramount importance for different kinds of dams, especially earthfill and rockfill

dams, which may probably fail once overtopped.

Concrete spillways must be built with adequate structural protection from frost damage and erosion/abrasion from water and water-borne debris.

Ruskin Dam spillway in Canada, as a prototype case, was resurfaced to repair concrete damages (Lihe, et al., 2011). Such remedies must be avoided as they are very expensive.

Thus, each dam needs to have a sufficient overtopping prevention mechanism. throughout the past, there have been several major occurrences throughout Asia that have caused property damage and the loss of life. Slope instability, overtopping, and earthquakes seem to be the main factors in events involving active dams (ICOLD, 2001).

Apart from the functions discussed here above, BANERJEE (2018) provided seven more functions of a safe spillway:

1. Maintaining normal river water functions

2. Discharging water for utilization

3. Maintaining the initial water level in the flood-control operation

4. Controlling floods

5. Controlling additional floods

6. Releasing surplus water

7. Lowering water levels (depleting water levels in an emergency).

2.3 Spillway Classification

There are many types of spillways such as ogee spillways (overflow), chute spillways, shaft/tunnel spillways, siphon spillways, labyrinth spillways, stepped spillways, etc. Spillways can be classified based on various factors: Function (service spillway and auxiliary spillways); regulatory or control structure (Gated spillway, ungated spillways, and orifice of sluice spillway) with the latter being the most pertinent feature (Khatsuria, 2005).

According to Şentrürk (1994), while selecting a spillway type, the following factors should be considered:

- Type of the dam to be constructed,
- Dam storage and outlet capacity,
- Topography and geological conditions of the spillway site,
- Hydrological and hydraulic factors, and
- Cost and risks involved.

2.4 Ogee or Overflow Spillways

2.4.1 Definition

Several types of spillways currently exist, as discussed in the preceding section, but only the uncontrolled ogee-shaped spillways will be reviewed in this thesis, as others are outside of the scope of this thesis.

Ogee spillway is suitable for a variety of situations because of its high efficiency to control flows (Savage and Johnson 2001), such as in most control crests of other spillways and high dams.

An ogee spillway, as shown in Figure (2.1), exhibits a control weir that is in form of an ogee or S-shaped profile (USBR, 1987). According to

USACE (1990), the crest of an ogee spillway is a sharp-crested weir with a space below the lower nappe replaced with concrete.

The shapes are based on a simple parabola designed conditionally to fit the trajectory of the lower nappe. The profile below the upper curve is prolonged tangentially, along the slope, to support the sheet on the face of the overflow and flow up to the apron of a stilling basin or into the spillway discharge channel (Ribeiro et al., 2020).

Flow over the crest should adhere to the face of the profile, for preventing access of air underneath the sheet. For discharges with a designed head, the flow glides over the crest with no interference from the boundary surface and attains near-maximum discharge efficiency (Ribeiro et al., 2020).

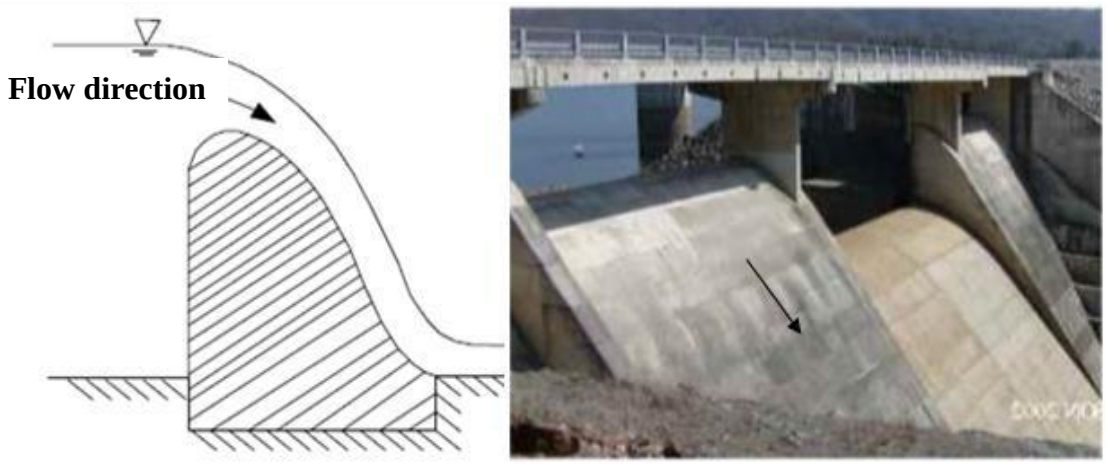

Figure 2.1: Ogee spillway type. A: Ogee spillway front view and B: Sectional view (Chanson, 2002).

2.4.2 Specific Functions of Ogee Spillway

Ogee spillway is the most commonly used type, especially in high dams. Its ability to pass flows efficiently and safely, when properly designed and with relatively good flow measuring capabilities, has enabled engineers to use it in a wide variety of situations (Savage et al. 2001; USBR, 1987).

Based on the regulatory or control structure, three different designs for spillway control are distinguished and can be classified as uncontrolled devices which do not use a hydraulic gate in their operation, movable crest devices, and regulating devices (USBR, 1973).

Uncontrolled crests are generally applied on small spillways and weirs when the release of water is only required in case the reservoir head exceeds the design level. One of the advantages of this design is that the constant supervision of an operator, maintenance, and repair costs are not needed (USBR, 1973).

Movable crest and regulating devices are often employed when there is a sufficiently long uncontrolled crest or when the spillway crest is located under the normal operating level of the reservoir (USBR, 1973).

2.4.3 Ogee Spillway Crest Profile

Considerable work has been conducted to get the shape of the crest of an overflow spillway and different design approaches have been provided that are based on the relative height and the slope of the spillway upstream face. As cited by Horton (1907), Bazin (1888) completed an extensive laboratory investigation which was the first study to determine the ogee shape. These experiments have served as the basis of many early designs, including various USACE and USBR publications that are considered the most used all over the world (Hariri-Ardebili and Nuss, 2018).

As discussed previously, the ogee-crested shape is derived from the lower surface of an aerated nappe flowing over the sharp-crested weir as illustrated by Loftin (1999) in Figure (2.2).

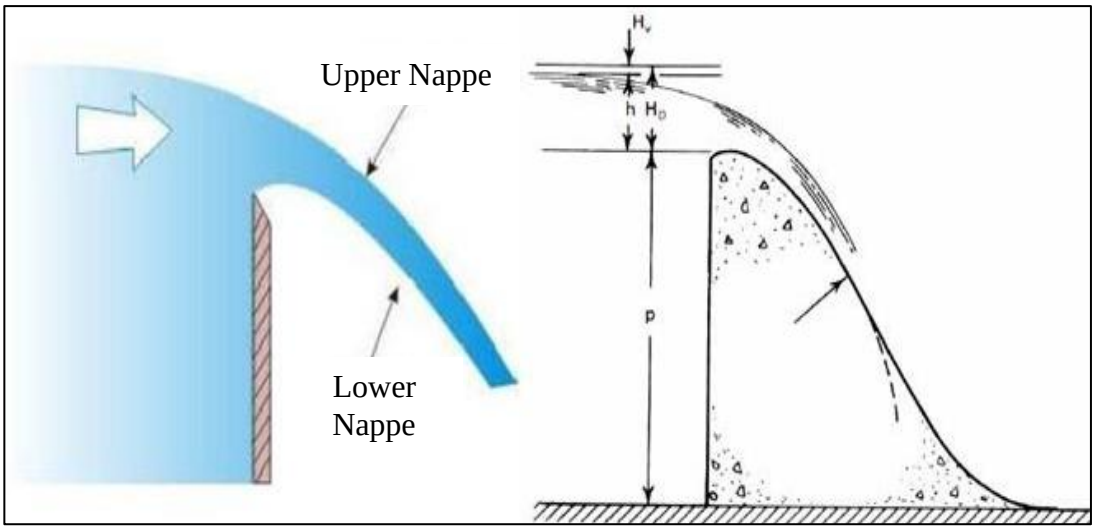

Figure 2.2: Sketch of a sharp-crested and ogee weir (Loftin, 1999).

Şentrürk 1994; Ribeiro et al., 2020, confirm that the stability of this nappe is not altered even if the space underneath the nappe is filled with concrete or other material. The shape of this flow nappe can be interpreted by the principle of the projectile, as depicted in Figure (2.3). It is assumed that the horizontal velocity component is constant and the only acting force on the nappe is gravity. During an interval of time "t", a particle of water in the lower surface of the nappe will cover horizontally a distance– x, from the face of the weir as defined in Equation (2.1):

$$x = v_o \, t \cos \theta \tag{2.1}$$

where

x = Horizontal distance (L)

v_o = Velocity at the point where x = 0 (L/T^{-1})

θ = Angle of inclination of "v_o" with the horizontal (degrees)

t = Time (T)

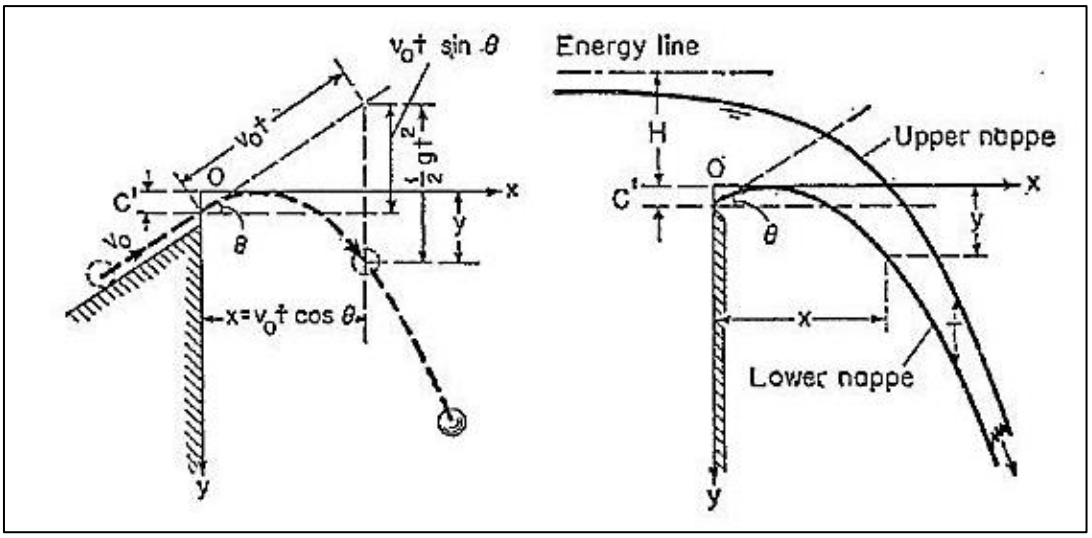

Figure 2.3: Derivation of nappe profile over a sharp-crested weir by the principle of the projectile(Chow, 1959).

The ogee crest is designed for a single total head (energy head), called the design head H_o. When an ogee weir is discharging at the design head, the flow glides over the crest with no interference from the boundary surface and attains near-maximum discharge efficiency (Loftin, 1999). The following sub-section discusses some design approaches that are commonlyapplied.

2.4.4 Design Approaches

The design and/or evaluation of an ogee spillway performance often requires a profound study to confirm its capacity before construction. Many spillway designs have been tested and a compendium of standard operational curves has been published primarily by the USACE and the USBR since the mid-1900s (Savage and Johnson, 2001). The publications from both agencies are considered the basis for the existing information. A wealth of information on ogee-crested spillways is found in Brater et al., 1996; Jafari-Asl et al., 2021.

The flow over an ogee spillway is characterized by the changes in its state from a subcritical to a supercritical regime caused by a sudden change

in its geometry after the crest.

As documented by USBR (1987), in the design of small dams publication, five different flow regimes can occur and they are clearly distinguished below an overflow crest depending on the relative positions of the apron and the downstream water surface:

- A supercritical flow stays attached to the length of the spillway;
- An incomplete hydraulic jump may form directly downstream from the crest;
- A full or true hydraulic jump can occur;
- A drowned jump can occur in which the flow with a high-velocity jet will follow the face of the ogee spillway for a considerable distance under the tailwater and then continue in an unpredictable and fluctuating path; and
- In other cases, no jump may occur. The jet breaks up from the face of the spillway, flows on the spillway surface for a short trajectory, then rides along the surface for a short distance before erratically intermixing with the slow-flowing water below.

2.4.5 Discharge Computations

The most commonly used equation for computing the discharge of ogee spillways was developed from early experiments. This discharge relationship, which is of the same form as other weirs, is often referred to as the "Weir Equation", as shown in Equation (2.2):

$$Q = C_{\circ} L H_e^{1.5} \quad (2.2)$$

Where:

Q = Discharge (L^3/T^{-1})

L = Lateral crest length or width (L)

$C_\circ$ = Discharge coefficient ($L^{0.5}/T^{-1}$)

H_e = The total energy head upstream from the crest

2.4.6 Determination of Discharge Coefficients

An ogee spillway is characterized by a relatively high value of discharge coefficient because of its shape. However, this coefficient is not constant. It is influenced by several factors including the depth of the approach, the relation of the actual crest shape to the ideal nappe shape, the upstream face slope downstream apron interface, and downstream submergence.

As documented by USBR (1987), the design discharge coefficients for ogee weirs with a vertical upstream face are depicted in Figure (2.4). Thence, these coefficients are valid only when the ogee confirms the ideal nappe shape; that is when $H_e/H_o = 1$. When crest shapes are different from the ideal shape or when it has been made for heads greater or smaller than the design head, the coefficient changes as depicted in Figure (2.5).

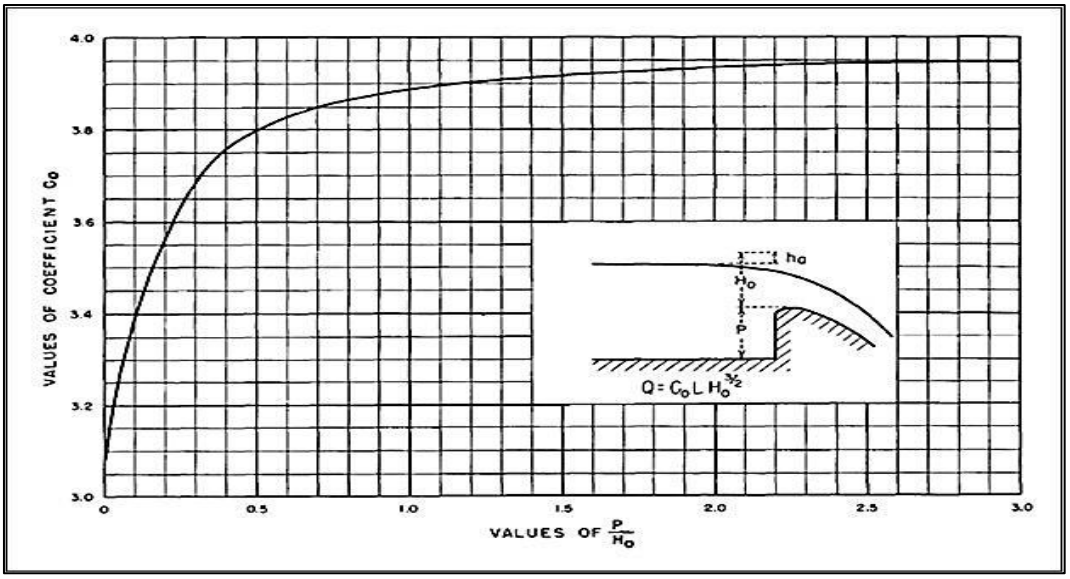

Figure 2.4: Discharge coefficient for vertical-faced ogee crest (USBR, 1987).

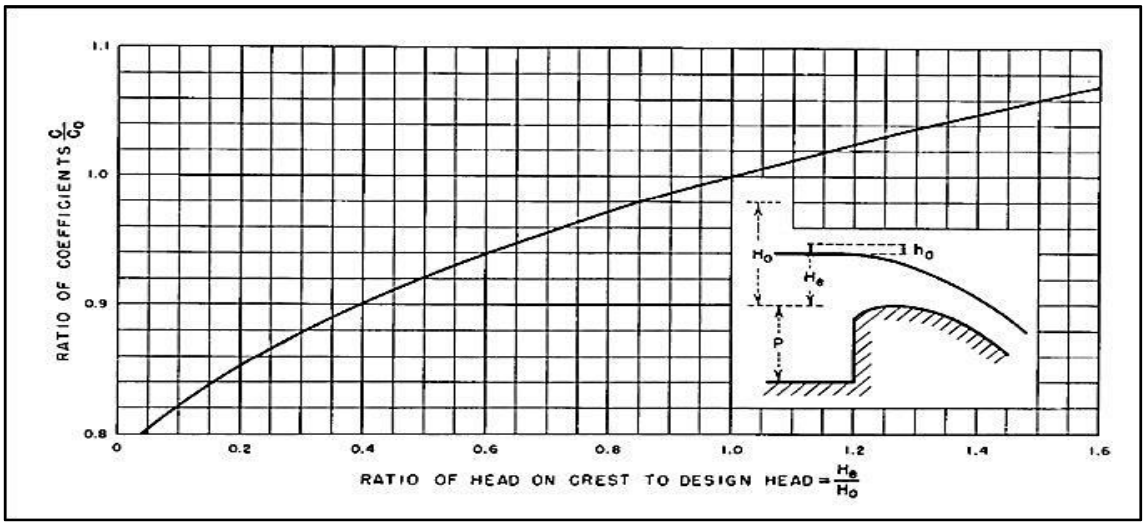

Figure 2.5: Discharge coefficients other than the design head (USBR, 1987).

The upstream sloped face of the spillway causes a change in the coefficient of discharge. According to USBR, (1987), for small ratios of the approach depth to the head on the crest, the inclined upstream face causes an increase in the discharge coefficient, especially for heights other than the design head.

For large ratios, the effect causes a decrease in the coefficient of discharge. Discharge coefficients for an ogee-shaped crest with a sloping upstream face are depicted in Figure (2.6).

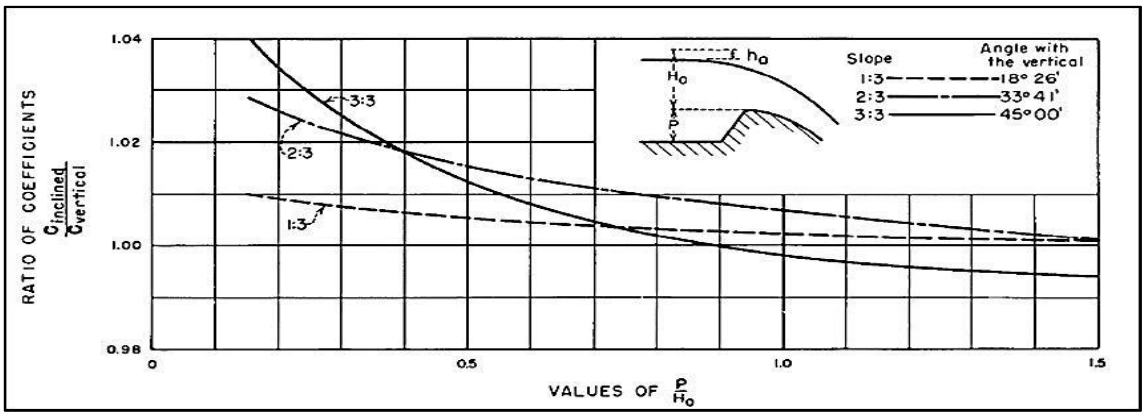

Figure 2.6: Discharge coefficients for ogee-shaped crest with sloping upstream face (USBR, 1987).

Coefficients of discharge are also affected by the downstream apron and spillway submergenceas shown in Figures (2.7 and 2.8), respectively.

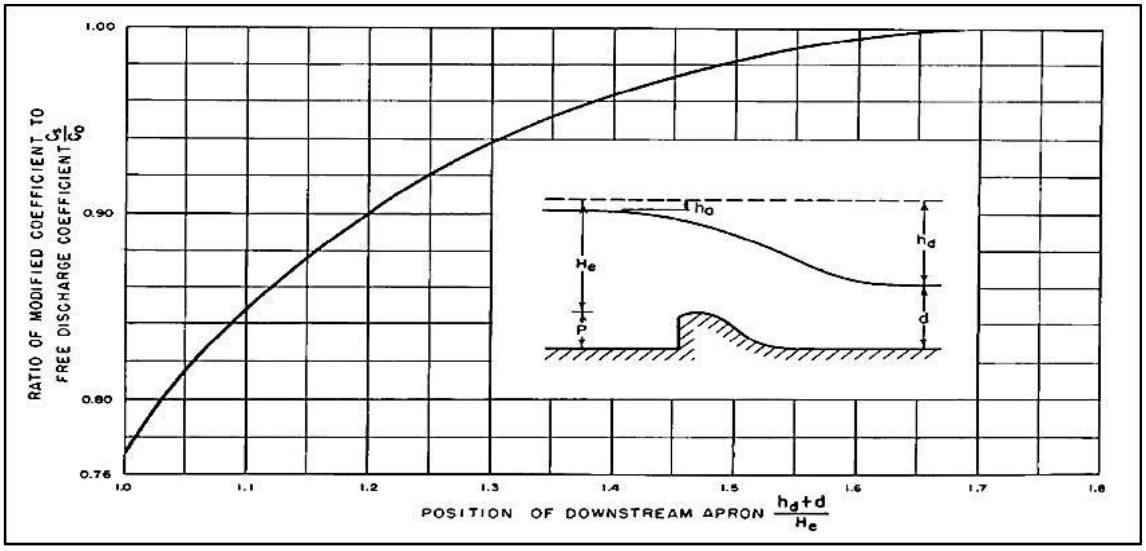

Figure 2.7: Ratio of discharge coefficients resulting from apron effects (USBR, 1987)

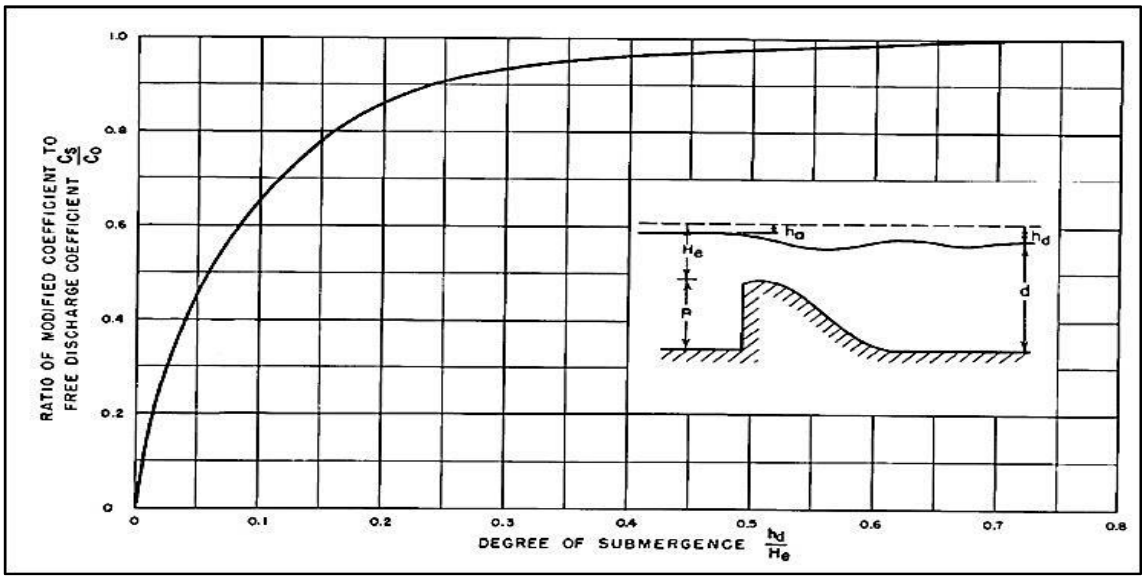

Figure 2.8: Ratio of discharge coefficients caused by tailwater effects (USBR, 1987).

2.5 Hydraulic Jump

The hydraulic jump is a common phenomenon generally observed in open channel flow, especially at the toe of hydraulic structures e.g., sluice

gates and spillways. This phenomenon is divided into two types according to bed characteristics. The first type is a classical hydraulic jump that occurs over a smooth bed and has been studied extensively. This type in honor of the first definition and put the relations between its initial and sequent depth, was named after him as the "Bélanger equation" (USBR, 1987) in the form;

$$\frac{y_2}{y_1} = \frac{1}{2}(\sqrt{1 + 8Fr_1^2} - 1) \qquad (2.3)$$

Where y_2 is the sequent depth or the required tail water to get a free jump over a smooth bed and Fr_1 is the initial Froude number.

The second type is called a forced hydraulic jump, which occurs over a rough bed, and this roughness takes different features and has been studied by many researchers as will be mentioned later. One of the main applications of a hydraulic jump is dissipating the excess kinetic energy downstream of the hydraulic structure. The stilling basin is the most common form of structure to contain the hydraulic jump to achieve the required dissipation of kinetic energy. Moreover, different roughness can be facilitated at its apron to achieve more dissipation of surplus energy within a shorter distance of the basin apron. There are many devices to satisfy these principle criteria such as baffle blocks, sills, roughness elements, corrugated elements, screens, roller buckets, and riprap aprons that are installed into the basin. The standard stilling basin, which uses the baffle blocks as a main feature for dissipating the surplus kinetic energy, is introduced in the late 1950s. The baffled basin was named "Type III" in this Monograph. Type III stilling basin, according to USBR, is conventionally designed for single discharge, which is usually the design discharge, provided the tailwater equals the full sequent depth. This basin provided a conservative design (Frizell and Svoboda, 2012). Accordingly, the hydraulic performance for a range of discharges needs to be tested, and

a specific model study is recommended along with consideration for other possible factors such as higher or lower velocities. The dynamic manner of this hydraulic field becomes attractive for further studies

2.6 Aeration Effects

Naturally, air flows are commonly encountered at the water flow surface. The falling nappe is considered aerated and it is subjected to atmospheric pressures. The aeration observed has led to the suggestion that the point at which aeration commences coincides with the point at which the boundary layer depth meets the free surface (Chanson, 2004). Figure (2.9) depicts boundary layer development in the flow over the ogee spillway.

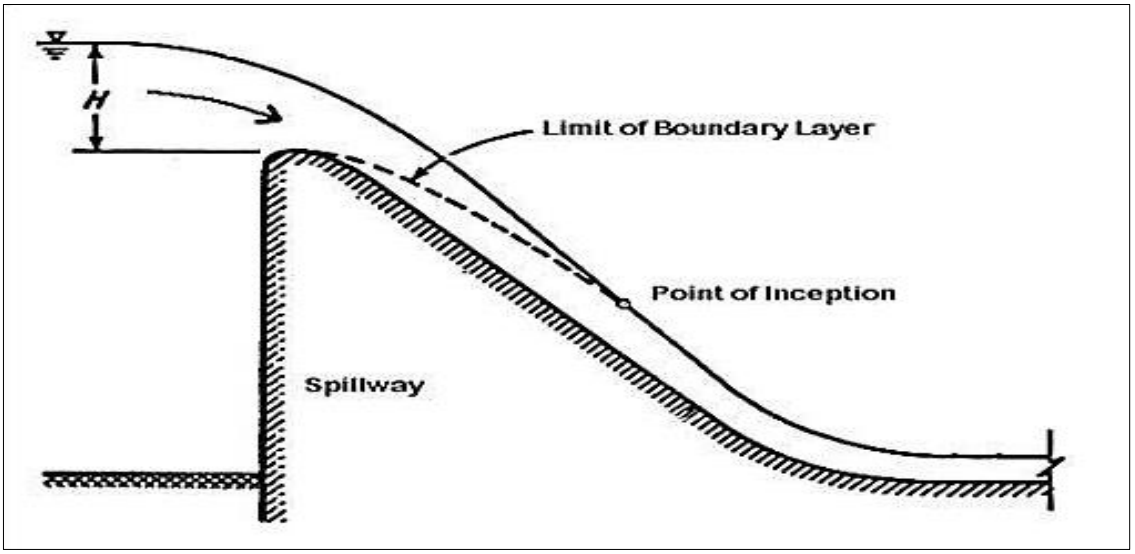

Figure 2.9: Boundary layer developed on ogee spillway flow (Bhajantri et al., 2006)

The insufficient aeration of the nappe will cause a reduction in pressure thereby leading to the abrupt change of the nappe shape for which the spillway crest is designed.

These pressures can theoretically be as low as the vapor pressure of water, which causes structural damage due to destructive cavitation and

vibration, and are therefore to be avoided from an operational and structural point of view.

Wilhelms and Gulliver, 2005 discuss three problems solved for an aerated spillway flow:

- Increase in flow depth due to air entrainment,
- Aeration of the lower nappe avoids pulsating flow,
- The downstream channel is free of cavitation if the lower nappe is aerated.

2.7 Computational Fluid Dynamics Modelling

2.7.1 Definition

Computational Fluid Dynamics (CFD) is a computer-based tool that is used to represent and analyze systems that involve fluid flow, heat transfer, and chemical reactions, by using numerical methods that are based on partial differential equations describing these systems (Versteeg and Malalasekera, 2007).

2.7.2 Background and Development of CFD Modelling

For over 100 years, hydraulic engineering practice has been relying on physical modeling for the design of most hydraulic structures. Because of the rigid and expensive nature of scale models, more alternative methods have been developed for the sake of accuracy and time optimization. Modern Computational Fluid Dynamics (CFD) was born in the 1950s when digital computers were introduced (Chung, 2002). There has been a rush in development and application to all aspects of fluid dynamics since the late 1960s when the aerospace industry profited from its use, especially for the design and manufacturing processes (Chanson 2022).

In hydraulic engineering, computational modelling of spillway flows is

increasingly being usedin the industry. However, validation from a physical model is still required to ensure that the physical processes are accurate. Several approaches have been developed, including modelling in one, two, or three dimensions which use various equations and discretization techniques. One-dimensional models are generally applied to verify the river stage and the water surface profile upstream and along the length of the spillway (Mohammed and Qasim 2012). Ghaderi et al., 2021simulated the flow over a spillway by solving a modified form of the shallow water equation in one dimension, and a reasonable agreement was achieved. On the other hand, one-dimensional model has presented some limitations as it is not adapted to variable-geometric structures such as junctions, steep slopes, curved surfaces, or any other change of size or shape of the channel. However, more details have been found in two- and three-dimensional models which allow perturbations of flow caused by obstructions, curved obstacles, wall boundaries, or other complex geometries. The following subsections detail the basic theory which is behind CFD.

2.7.3 Governing Equations

The fundamental principles for all numerical models remain similar where the problems are stated, physically, by a set of partial differential equations. In the same way, CFD techniques are governed by several equations which must be solved in each control volume. Depending on the properties of fluid flow to simulate, the physical phenomena are represented by mathematical statements that are referred to as governing equations of fluid flow and heat transfer (Versteeg and Malalasekera, 2007). These equations include mass conservation or continuity, momentum, and energy equations also known as the Navier-Stokes equations. Based on the theory documented by Wendet (2009), mass conservation and momentum equations canbe described as follows:

2.7.3.1 Mass Conservation (Continuity) Equation

The mass conservation equation or continuity equation states that the mass of a closed system of substances will remain constant, regardless of the processes acting inside the system. Fluid flow has a fixed mass even if its shape and volume may change as it moves. The illustration is made in Figure (2.10):

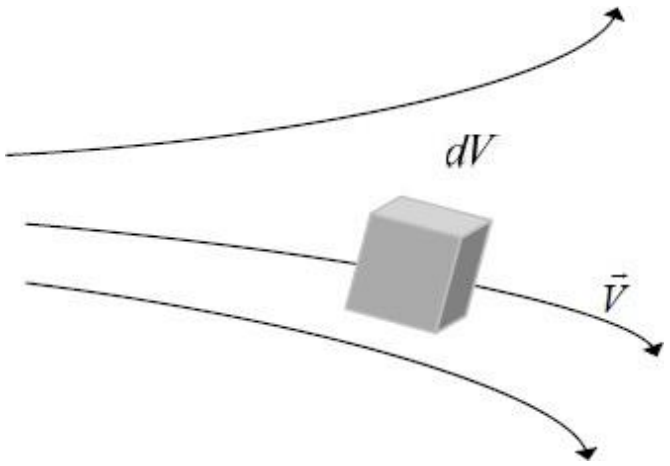

Figure 2.10: Definition sketch for moving fluid (Kositgittiwong, 2012).

2.7.3.2 Momentum Conservation Equation

The momentum equation is a statement of Newton's Second Law and relates the sum of all the forces acting on a particle of fluid (Versteeg & Malalasekera, 2007). The moving fluid element model is sketched with more details in Figure (2.11).

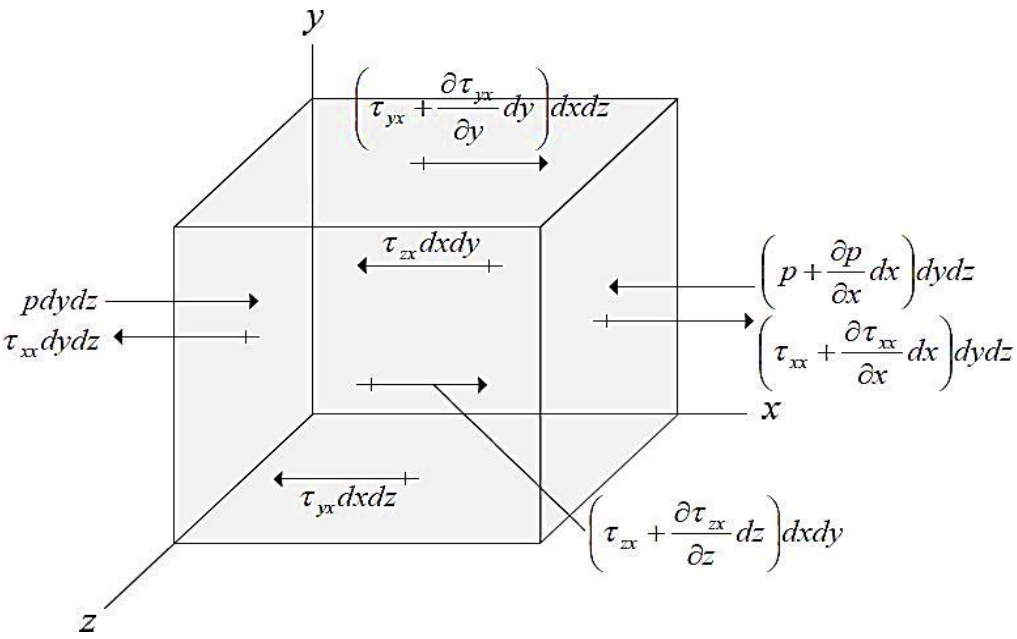

Figure 2.11: Moving particle element model for the x component (Kositgittiwong, 2012).

The general equation for the conservation of momentum can be written as follows:

$$\frac{\partial}{\partial t}=(\rho\vec{v})+\nabla\cdot(\rho\vec{v}\vec{v})=-\left(\frac{\partial P}{\partial t}\right)+\nabla\cdot(\mu\nabla\mu)+S_m \qquad (2.5)$$

Where

P = Static pressure (Pa)

μ = Kinetic viscosity (L^2/T^{-1})

ρ = Density (F/L^3)

S_m= Source term (Constant)

v = Overall velocity vector (L/T^{-1})

The left-hand side of Equation (2.5) contains terms as defined for the mass conservation equation and its right-hand side contains the pressure source term and the diffusion source termrespectively.

2.7.4 Multiphase Modelling

Multiphase modelling is a technique that simulates flow in the simultaneous presence of different phases. All three phases (gas, liquid and solid) are identifiable with a distinct particular inertial response to an interaction with the flow and the potential field. There are four main categories of multiphase flows; gas-liquid, gas-solid, liquid-solid, and three-phase flows (Murrone & Villedieu, 2011). Such complex systems have been made possible with the availability of two broad approaches for numerical calculation, namely the Euler-Euler (Volume of Fluid model or VOF model) and the Euler-Lagrange (Discrete Phase Model) approaches.

The volume of the fluid model is designed for two or more immiscible fluids where the position of the interface between the fluids is of interest. It is an interface-capturing scheme for the free surface flow where the interface of each fluid is the point of focus (Nikseresht et al., 2008). In the VOF model, the phases are treated separately and one set of conservation equations is solved for each phase.

Due to the volume fraction of each phase throughout the same control volume, the fields for velocity, pressure, and temperature are made to be the same.

Thus, conservation equations for each phase are derived to obtain a set of equations, which have a similar structure for all phases

2.7.5 Aeration Effects In Multiphase Modelling

Chatila and Tabbara (2020) conducted a study with a CFD software package called ADINA to compare water surface profiles over an ogee spillway geometrically similar to the physical model. The spillway profile was free of piers and water free surface was measured at the centreline to avoid an influence from the wall boundaries. The results achieved show that,

even if qualitative solutions are reasonably consistent with general flow patterns, an inconsistency was found. In all three simulated discharges, ADINA predicted water surface levels much lower than the experimental water levels along the spillway length. These inconsistencies were found to be caused by air entrainment effects which were not accounted for in the CFD model used. They used different CFD software in their research, called Flow-3D for modelling the Keeyask spillway. The results produced by Flow-3D included the effects of air entrainment because of the use of the volume of fluid method (VOF).

Although some differences appeared at the entrance and exit of the numerical domain, the computed results were in good agreement with those measured in the physical modelling.

2.7.6 Advantages of Using CFD

CFD has grown from a mathematical field to become a crosscutting tool in nearly every branch of fluid dynamics. It assists in the analysis of fluid mechanics and its impact on the structure through/on which water is flowing. In the engineering field, CFD is used to analyze new designs before they are implemented. Some clear advantages can be summarised as follows:

- CFD can give an insight into flow patterns, weight losses, mass and heat transfer, flow separation, etc. Thence, all of these parameters may help implementers with a much better and thorough understanding of what is happening on the field.

- CFD reveals complex features that could not be achieved by physical modelling such as high temperature.

- CFD can be used to test dangerous experiments with cheaper means and without risks such as accident scenarios or safety studies.

2.8 Previous Experimental and Numerical Studies

Maatooq (2006) explained an experimental hydraulic model to evaluate the performance of an overflow spillway. The spillway tested has a standard ogee profile with continuous steps cut into a straight portion of the downstream face from a tangential point (T.P) to the toe. The spillways tested had the form and dimensions shown in Figure (2.12), in which all dimensions are given in centimeters.

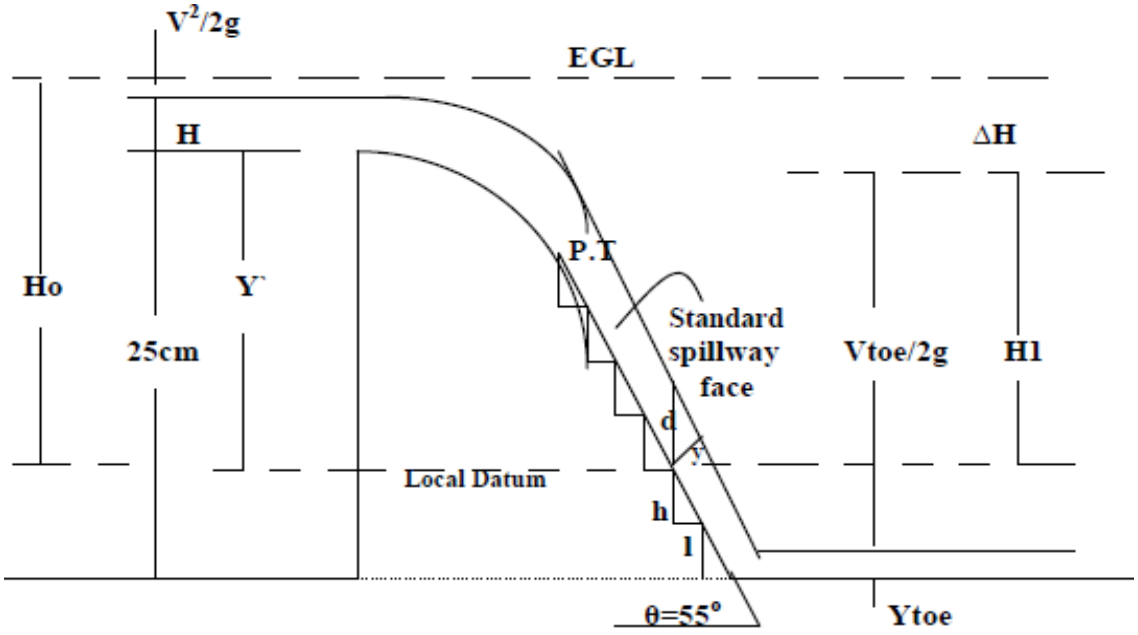

Figure 2.12: Schematic diagram of sloped Spillway tested. (Maatooq 2006).

The preliminary results indicated that the average increase in energy dissipation at the toe is approximately 37%, which would imply a significant reduction in the size of downstream stilling basins. The experimental results indicate that dissipation is highest for the small values of dissipated head yc/Nh tested (i.e at nappe to transition flow), also the dissipation ratio increase with increasing N.

Al-Zubaidy et al., 2014 investigate the effects of applying the direction- diverting blocks fixed on an ogee spillway surface with different slopes on energy dissipation. Three ogee spillway models were

prepared with a slope of 1:1, 0.85:1, and 0.75:1. The blocks were arranged in eighteen configurations for slope 1:1, fourteen configurations for each spillway model with slope 0.85:1 and 0.75:1. The configurations differ in spacing between rows of blocks and the number of rows. Eight hundred and forty-six test runs were carried out to investigate the energy dissipation downstream of the spillway models. When blocks were used, the maximum reduction in Froude Number was 36%, 89%, and 93% for spillway models with slopes 1:1, 0.85:1, and 0.75:1, respectively. Also, a full reduction in the values of hydraulic jump distance was achieved in the three spillway models.

Al- Husseini (2015) showed an experimental study on a flat sloped spillway to specify the efficiency of energy-dissipating of flow (Figure 2.13). Twelve spillways were constructed from plywood and tested to compare various flat-sloped spillways. The results showed that when decreasing both the number of the downstream slops of the spillway will cause an increase in the ratio of flow energy dissipation, and the spillways are more efficient in flow energy dissipation compared with flat sloped spillways.

Figure 2.13: General view of the laboratory flume work (Al-Husseini, 2015).

Abdul-Mehdi (2016) presented a new laboratory study conducted on spillways to investigate their efficiency in dissipating flow energy. Five spillways were constructed from concrete and tested to investigate and compare them. Three were roughed by gravel with different sizes for each one, one of them was sloped without any addition, and the last one was sloped with cavitation. The results proved that the relative energy dissipation was 26.73 % compared with traditional spillways and 16.73 %. When it was compared with a sloped spillway without any addition, the sloped spillways appeared more effective than traditional spillways with a ratio of 10%.

Alwan ey al., 2016 developed physical models for spillways and aprons installed into the water in the channel where conducted under subcritical flow and clear-water conditions by using uniform cohesion less (soil) as bed material with medium grain size (d_{50} = 0.65 mm). Four angles of an apron were used (0˚, 2.73˚, 5.19˚, and 7.43˚) to show the effect of the slope for the apron on local scour. It is found that the slope of an apron is one of the important parameters to reduce the local scour depth and the extent of scour hole. The influence of slope for aprons angle showed a reduction of about (53, 46, and 35) % in the maximum scour depth and about (33, 49, and 33) % in the maximum scour length compared with a horizontal apron for angles (2.73˚, 5.19˚, and 7.43˚), respectively. The results proved that the scour increases with increasing the discharge for each apron due to an increase in water energy. The contour map and 3D development of scour hole are also shown for comparison, see Figure (2.14).

All the tests showed that the scour processes were faster in the early stages of each experiment in contrast to later stages that were marked by slower changes in bed profile. It was clear that the shape of the scour hole changed with time until an equilibrium stage was reached.

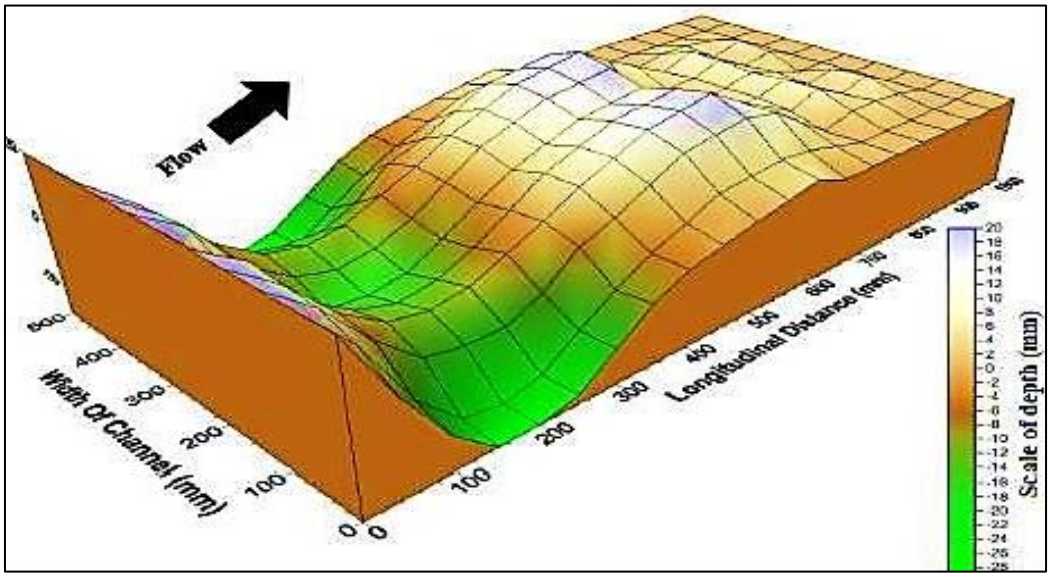

Figure 2.14: Contour map for scour downstream apron (Alwan, 2016).

Al Zubaidy et al., 2016 evaluate the hydraulic performance and efficiency of using direction-diverting blocks DDBs fixed on the surface of an Ogee spillway in reducing the acceleration and dissipating the energy of the incoming supercritical flow. Results indicated that when using the DDBs on a spillway surface, less Froude Number downstream the spillway is obtained and the hydraulic jump occurs at a much shorter distance from the spillway toe compared to the same spillway without DDBs. Depending on the DDBs type, configuration, and the applied discharge, the obtained reduction in Froude Number varied between 4.4 to 19.3% and the reduction in the hydraulic jump distance measured from the spillway toe varied between 54% and 76% compared with that of the standard design of Mandili Dam.

Aydın and Ulu 2018 explained the scouring problem caused by the flow movement in the downstream areas of hydraulic structures is an issue that keeps its actuality. The flow and scouring events on the weir were modeled in two dimensions using Computational Fluid Dynamics (CFD). The findings were compared for different downstream conditions and the

results were discussed in this respect.

Elnikhely (2018) explained local scour downstream of spillways due to hydraulic jumps is considered the most complicated and tedious problem which threats the overall stability of the spillway (Figure 2.15). Throughout this study, eighty experimental runs were carried out to investigate the effect of using cylinder blocks fixed on the back slope of the spillway on the scour hole dimensions downstream of the spillway under different flow conditions. Experiments were performed using different diameters,lengths, and arrangements of cylinder blocks with different discharges. Data collected from the experiments were analyzed and graphically introduced. Furthermore, experimental data for smooth spillways were compared with scour formulae for other researchers. Finally, simple formulae were predicted to estimate the different scour and deposition parameters. The use of concrete cylinder blocks will assist engineers in the design of spillways.

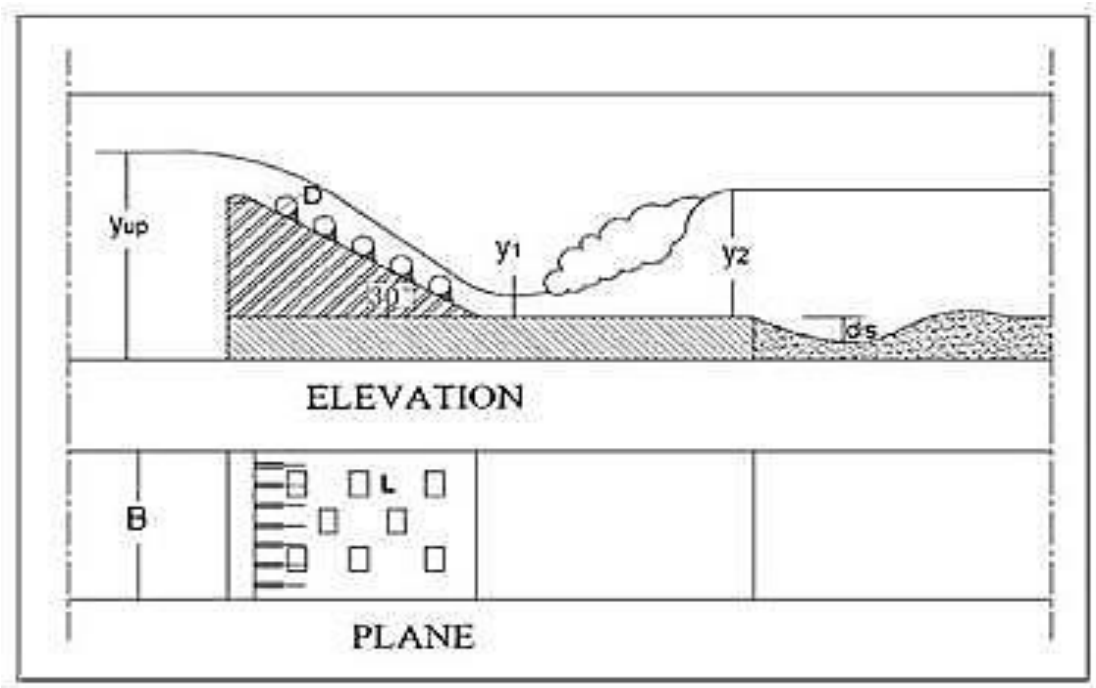

Figure 2.15: Layout of the experimental model (Elnikhely 2018).

Jamel (2018) used Flow-3D software uses to study the energy dissipation for spillways with different end sills. The study is based on

three models. The first model contains rectangular end sills in all steppes. The second model contains rectangular end sills between one step and another. The third model contains triangular end sills in all steppes. Analytical results show that model (3) is the highest energy dissipation for all discharges value (Figure 2.16). Empirical equations extraction to find the energy dissipation for each of these models. The artificial neural network is also adopted to prove the accuracy and efficiency of the analytical results which are at high rates of compatibility with the values of the coefficient of determination for (model 1), (model 2), and (model 3) equal to (93.47%), (88.20%) and (86.00%) respectively. Also, the artificial neural network identifies the most influential factors on energy dissipation, the friction Froude number is the highest impact on energy dissipation.

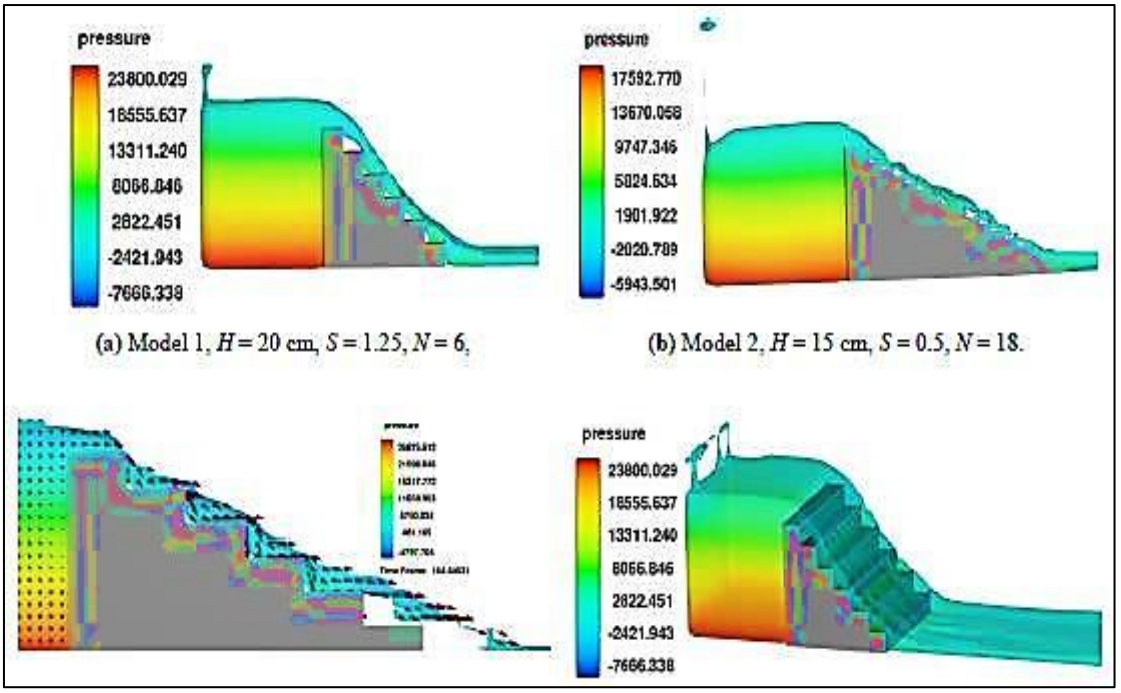

Figure 2.16: Results of models for energy dispersion (Jamel 2018).

Abdel-Mageed et al. (2019) investigate the end sills in the spillway and assessed their effect on energy dissipation. For this purpose, physical models of four steps were built on the spillway. End sills were installed at the end of each step of the spillway. The energy dissipation could be

increased by different behaviors, depending on the characteristics of the end sills (height, shape, and V notch angle). All end sills used enhanced energy dissipation, reduced the relative scour depth, reduced the relative scour length, and reduced the relative scour volume. Increasing the relative height of solid and rectangular partially hollow end sills, enhanced energy dissipation. Minimizing the V notch angle of V notch end sills enhanced energy dissipation.

Rajaa and Kamela (2020) investigations studies of simulating flow over spillways have increased using numerical models. Research findings have shown that CFD (Computational fluid dynamics) models as the numerical method are a perfect alternative for laboratory tests. Performance analysis of the CFD platforms Ansys Fluent-2D and Flow-3D are presented, focusing on finding the variations between the numerical results of the two programs to simulate the flow over the ogee spillway.

Ulu (2021) showed that the energy dissipation performance of a flow separator structure placed in an energy breaker pool was investigated numerically by increasing the shear stresses. A computational fluid dynamics (CFD) program, was used as a method in the study. The program determines fluid motion by solving equations such as the conservation of mass and momentum. A two-dimensional ogee-type spillway with a crest elevation of 5.28 m and a flip-bucket diameter of 2.0 m was used. In the study, a hexahedral 0.05m cell size was used. Analyzes were continued until the flow became completely stable (120 seconds). 1 m downstream water inlet is defined to provide downstream conditions and to observe hydraulic jumps (Figure 2.17). The effect of a flow separator placed in the energy-breaking pools of the spillway structures, which has an important place in the field of hydraulic engineering, on the flow velocities and energy dissipation status was investigated.

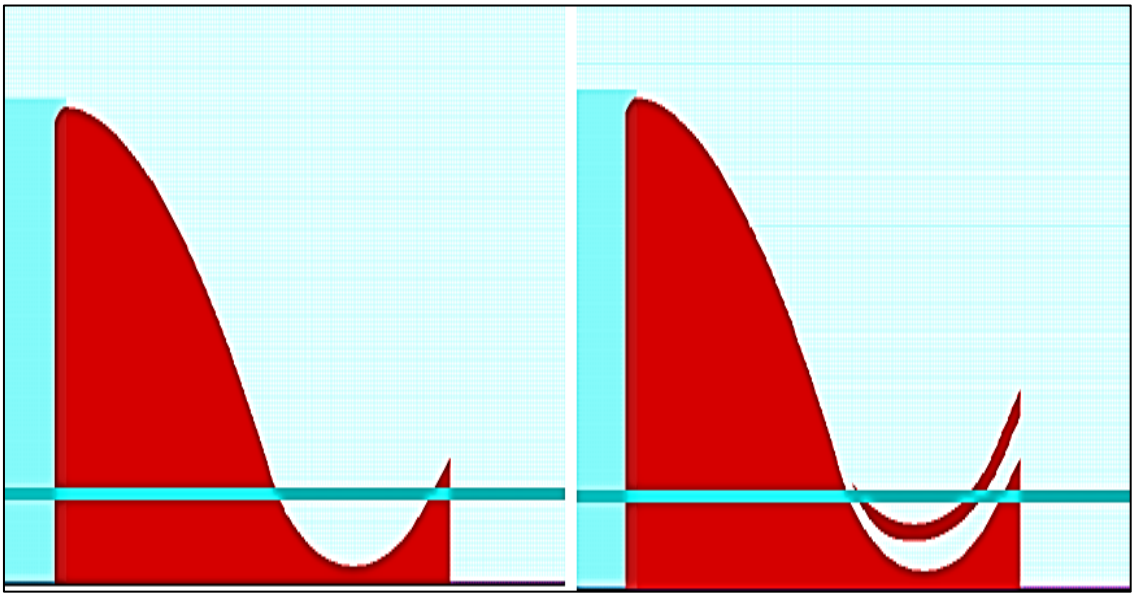

Figure 2.17: Ogee spillway structures of the build models (Ulu and Isik 2021).

Nasralla (2022) explained a study of scour downstream of a free hydraulic jump in the stilling basin of a spillway. This work employed an experimental study to investigate the spillwaywith movable bed material.

The discharge measured at the weirwas installed downstream of the flume, and the used buffers with different dimensions and downstream divergent angles. The effect of the contraction ratio of the sloped spillway was highlighted.

Different downstream divergent angle was studied to minimize the scour depth, and the results showed that the relative scours depth was reduced by 23% for a divergent angle equal to 170°, different shapes of buffer in stilling basin were also studied to reduce the scour depth where the considered buffer decreases the relative scour depth up to 84%.

This study was also simulated by Flow 3D program to analyze the scour hole formed using velocity vectors at the bed.

In conclusion, the majority of the earlier studies—both practical and numerical—sought to enhance the spillway's behavior by largely lowering the speed and scour in the stilling basin. The U.S.B.R.'s fundamental designs and specifications, the distribution of dispersed blocks, their kind, and quantity, as well as a thorough examination of the amount and depth of soil erosion were all left out.

2.9 Summary and Current Study Contribution

The literature review shows that the design process of an ogee spillway is reasonably well understood. Many approaches have been developed by various researchers and most ofthem are based on USBR publications.

These theories provide the design parameters such as the design head (H_O) and the discharge coefficients (C_O) for which the ogee profile can be designed and the discharges computed. However, this is not enough to ensure better performance and stability of a spillway; it is necessary to determine and analyze all hydrodynamic pressures generated from water flows.

The advances in numerical methods as well as the development of computing power are attempting to improve the quantification of hydrodynamic pressures and aeration in thespillway flow.

These factors are very important for improving the spillway performance and limiting negative pressures which could scour the soil surface downstream of the stilling basin of a spillway.

Amongst numerical methods, Computational Fluid Dynamics (CFD) is found to be increasingly used in the spillway flow field. A clear advantage of these methods lies in their ability to simulate the effects of turbulence and multiphase flow since most of the flows in nature are turbulent and

multiphase.

The current study attempted to investigate the experimental effect of the type and distance of blocks with the presence of one, two, and three rows of blocks and end sill structure on the hydraulic jump and scour along and downstream of the ogee spillway stilling basin.

CHAPTER THREE

EXPERIMENTAL WORKS

3.1 Introduction

In this chapter, the detailed presentation of the experimental test process carried out in the laboratory is outlined. The focus is on different considerations and assumptions made concerning obtaining the experimental results for designed dissipated block configurations. The hydraulic aspects that are investigated are mainly the hydrodynamic characteristics of flows and water surcharge upstream and along the spillway downstream face.

3.2 Physical Modeling and Scale Effect

3.2.1 Dimensional Analysis

Dimensional analysis is a mathematical based approach used to analyze a certain phenomenon or problem having differently affected physical quantities to produce a relationship that connects them by identifying their fundamental dimensions. For the simulation of any hydraulic phenomenon, it is necessary to analyze the relevant parameters of the prototype and the laboratory model. Once, the basic (prototype/model) scale ratio is known, collected data from the experimental model can be translated to equivalent value on the prototype depending on dimensionless parameters such as (Reynolds Number, Froude Number, Euler Number, Weber Number, Cauchy Number, etc.).

The current study focuses on the field hydraulic characteristics of the flow concerning the ogee spillway and stilling basin. The factors that affect this phenomenon were described by many studies, which can be arranged in Equations (3.1 to 3.3):

<u>For fluid characteristics</u>

$f_1\ (u, Q, \rho, \mu, \sigma)$ Eq.(3.1)

Where:

u = Velocity of flow; LT^{-1},

Q = Quantity of flow; L^3T^{-1},

ρ = Water density; $FL^{-4}T^2$,

μ = Dynamic viscosity; $FL^{-2}T$, and

σ = Surface tension; FL^{-1}.

For geometric characteristics

f_2 (L , B, h_{st}, y_{up}, y_1, y_2, L_j, D_d, D_s, L_d, L_s, D_{50}) Eq.(3.2)

Where:

L = Length of flume; L,

B = Width of flume; L,

h_{st} = Step height; L,

y_{up} = Upstream water depth; L,

y_1 = Initial depth of jump; L,

y_2 = Sequent depth of jump; L,

L_j = Jump length; L,

D_d = Max. deposition depth; L,

D_s = Max. Scour depth; L,

L_d = Max. deposition length; L,

L_s = Max. scour length; L, and

D_{50} = Sediment diameter; L.

For material characteristics

F_3 (σ, s, E, v) Eq.(3.3)

Where:

σ = Stress; FL^{-2},

s = Strain; LL^{-1},

E = Elastic modulus; FL^{-2}, and

v = Poisson's ratio; LL^{-1}.

Therefore, the variables that are affected by hydraulic characteristics of the flow within the ogee spillway and stilling basin can be summarized as follow:

$$f\left(u, \mathrm{Q}, \rho, \mu, \sigma, \mathrm{L}, \mathrm{B}, \mathrm{hst}, \mathrm{y}_{up}, \mathrm{y}_1, \mathrm{y}_2, \mathrm{L}_j, \mathrm{D}_d, \mathrm{D}_s, \mathrm{L}_d, \mathrm{L}_s, D_{50}, \sigma,\ \mathrm{s}, \mathrm{E}, \mathrm{v}\right) = 0 \quad (3.4)$$

To make sure that the dimensionless quantities governing this problem, Buckingham's theory (π-theorem) is applied using ρ, y_{up} and V_0, Equation (3.4) becomes:

$$\frac{D_s}{y_{up}} = f\left(N, \frac{y_2}{y_1}, \frac{L_j}{y_{up}}, F_{up}, \frac{L_s}{y_{up}}, \frac{L_d}{y_{up}}, \frac{D_d}{y_{up}}\right) \quad (3.5)$$

Similar relationships for the energy loss ratio ($\Delta E/y_{up}$) could be obtained where $\frac{\Delta E}{y_{up}} - E$, E_{up} is the upstream energy and E_2 is the energy at sequent depth.

3.2.2 Similitude Principles

The correlation between physical quantities in the model and the prototype is called similitude. For complete similarity between model and prototype, three similarities must be satisfied; they are geometric, kinematic, and dynamic similitudes. An important consideration in the design of the experimental model is the length scale ratio, several factors and limitations must be included and taken into account to choose a suitable length scale ratio such as the available space, construction cost, and the limitations of other parameters similarity. Physical hydraulic models are commonly used during design stages to optimize a structure and to ensure the safe operation of the structure (Sorensen, 2020). In civil engineering applications, a physical hydraulic model is usually a smaller-size representation of the prototype. Other applications of model studies (e.g. water treatment plant, flotation column) may require the use of models (with controlled flow conditions) to predict the behavior of prototype flow situations which means similarity of geometric and motion (kinematic similarity) and similarity of forces (dynamic similarity) (Sorensen, 2020). There is a multitude of phenomena that might be important in hydraulic flow such as viscous effects, surface tension, and gravity effect. The use of the same fluid on both prototype and model prohibits simultaneously satisfying the Froude, Reynolds, and Weber numbers scaling criteria. The Froude Number similarity requires that $V_r = \sqrt{L_r}$, the Reynolds

Number scaling implies that $V_r = 1/L_r$, and the Weber Number similarity requires $V_r = 1/\sqrt{L_r}$, where $Lr = Lp/Lm$. V refer to approach flow velocity and L refer to unit length of model. The subscript r refers to the ratio of prototype to model quantity and the subscripts P and M refer to prototype and model parameters, respectively. Froude Number modeling is typically used when friction losses are small and the flow is highly turbulent: e.g. spillways, overflow weirs, and flow past bridge piers. In each case, only the most dominant mechanism is modeled. In free-surface flow, gravity effects are always important and Froude Number modeling is used, hence viscous and surface tension effects are negligible in the prototype, according to Chow (Tuna,2012), the model flow must behave as a prototype for Reynolds Number is larger than 2000, and Weber Number is higher than 11, according to (Young, 2022).

If scale effects will become significant in a model, a smaller prototype-to-model scale ratio should be used to minimize the scale effects. For example, in a $100:1$ scale model of an open channel, the gravity effect is predominant but the viscous effect might be significant. In a geometric scale ratio of $50:1$ or $25:1$, the gravity effect is predominant but the viscous effect might be eliminated (Sorensen, 2020). Under this limit and the dimensions of the laboratory channel are used, then physical models are constructed with dimensions that accomplish a turbulent flow and a high Weber Number with a geometric scale of $30:1$. With this geometrical scale, hydraulic model ratios are listed in Table (3.1).

Table 3.1: Physical similitude relations.

Parameter	Relations
Discharge	$Q_r = V_r {L_r}^2 = {L_r}^{2.5}$
Velocity	$V_r = \sqrt{L_r}$
Energy	$E_r = {L_r}^4$
Reynolds number	$R_r = {L_r}^{1.5}$
Pressure	$P_r = F_r/{L_r}^2$

3.3 Physical Model Set-Up and Laboratory Facilities

The physical modelling tests for this study were carried out in the Hydraulic Laboratory of Babylon University, located in Babil governorate, Republic of Iraq. Thephysical modelling consisted of one ogee spillway installed, in a glass flume of 0.45m high, 0.30 m wide, and 12 m in length. The flow rate that could be obtained in the laboratory is up to 12m^3/min., which gives the initial Froude from 2.75 to 9.25. The laboratory set-up was a closed loop system whereby the outflow system was set up in a way that allowed the flow to be re-used. The conceptual laboratory and physical model setup are shown in Figure (3.1).

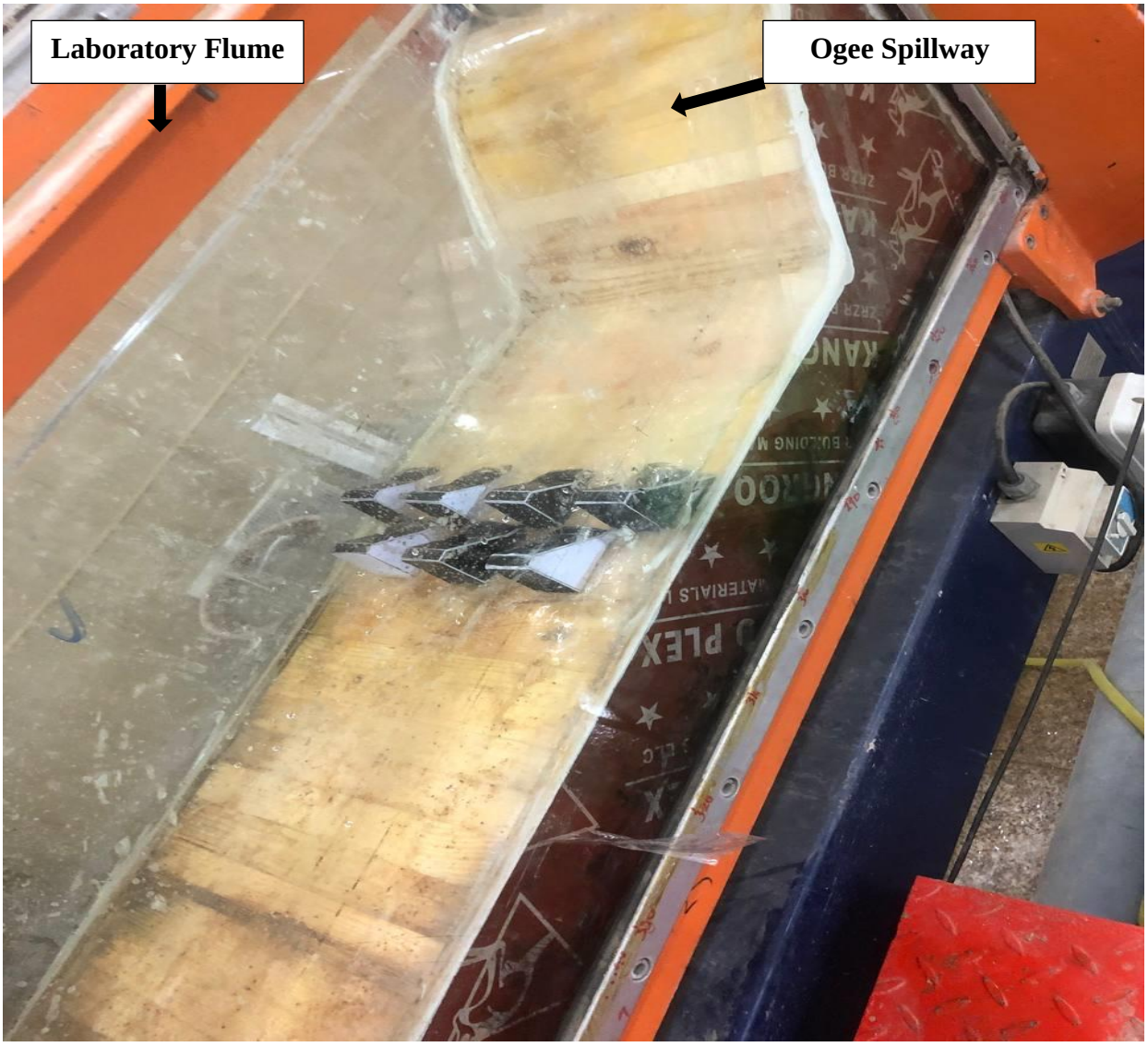

Figure 3.1: Laboratory and selected model set-up.

To complete the laboratory work, a number of instruments were used. A manually operated trolley system equipped with a needle gauge (point), which allowed vertical movement along the flume, was selected as a better way to measure water discharge along the ogee spillway. This needle gauge had one degree of freedom, that is, to operate vertically and perpendicularlyto the channel bed of the flume.

The flow meter and adjustable valve installed in the supply system were used to regulate different flows. To obtain enough flow, however, a system composed of two high-capacity pumps pumping water from an underground tank to the constant head tank, and a reticulation pipe with a flow control valve were used to provide the release of different flows. In addition, video and photograph recordings were made to record the flow patterns on all sides of the physical model.

3.4 Physical Model Design and Dimensions

In this section, the hydraulic and geometric designs of the ogee spillway that was used for physical modeling, are detailed. The design approach was based on the procedure documented in Small Dam Design by USBR (1987).

In this research, the primary spillway model is the 30:1 scale of a large-sized prototype. The spillway model is ten times the size of the upper part of the primary model as depicted in Figure (3.2). This scenario was performed with the hoping to obtain more details at the crest of an ogee spillway.

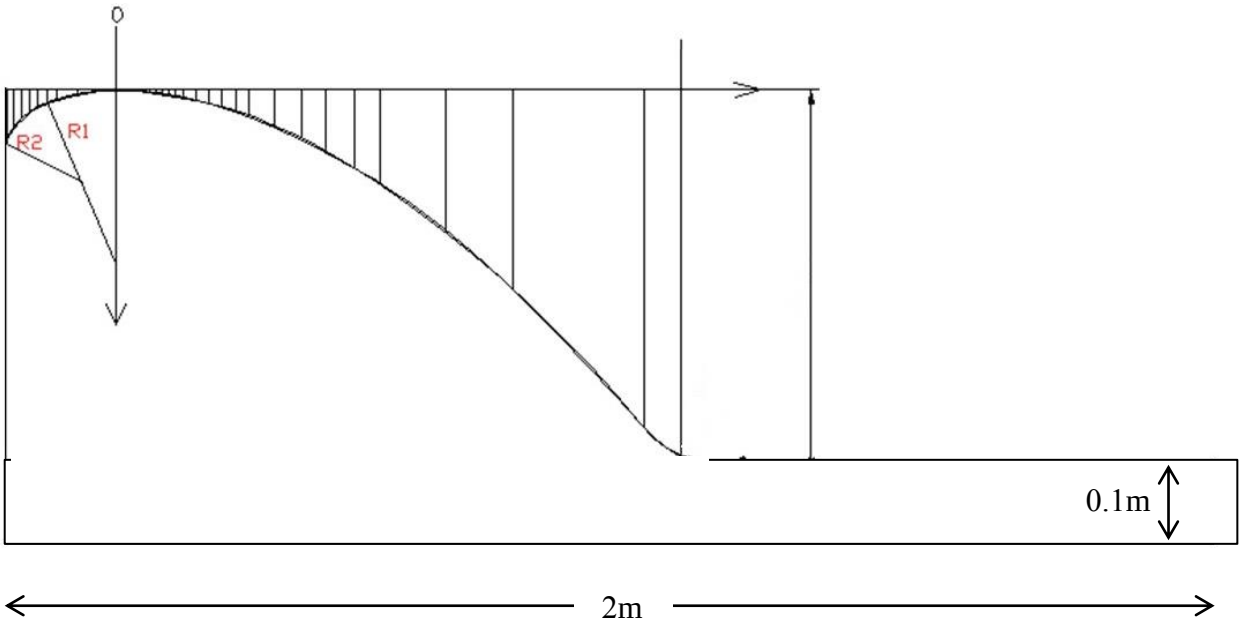

Figure 3.2: Schematic representation of the spillway and scale model.

Upon the completion of the model construction, it was necessary to carry out a geometric survey in order to check that the design dimensions were not altered. To achieve this, a topographic survey with an accurate total station was used as the most trusted technique to obtain all the dimensions with a minimum of errors.

The geometric dimensions for the selected case were summarized in Table (3.2). It is noted that since the same flume of 0.3 m wide was used in the laboratory, the prototype width modeled by the1:3 model is 3*0.3=0.9 m and that for the 1:30 model is 30*0.3=9 m.

Table 3.2: Model dimensions.

Spillway length (m)	Spillway depth (m)	Crest width (m)	Spillway radius (m)	
			R_1	R_2
2.0	0.45	0.3	0.05	0.02

3.5 Configuration and Arrangement of Standard USBR

The shape and dimensions of the block as recommended by USBR at which the upper longitudinal dimension and width of the block are selected as a

function of block height (Peterka, 1978). The blocks have been arranged at a blockage ratio "η" so they do not exceed 0.5. The calculation of the blockage ratio is according to;

$$\eta = \sum W_b / \sum (W_b + S) \quad (3.6)$$

Where the W_b, is the width of the block, and S, is the clear spacing between the adjacent blocks.

3.5.1 Baffle Blocks

The blocks were made from timber fixed at the height of 5cm for the entire Froude number range so that the width is 3.75 cm, the length of the base is manufactured at 6 cm, and the upper longitudinal dimension of the baffle blocks is 1 cm, as presented in Figure (3.3). The space between the first block and the wall of the flume was equal to $0.5W_b$ for each side. Figure (3.4) represents a general sketch of the hydraulic jump over the USBR baffle block.

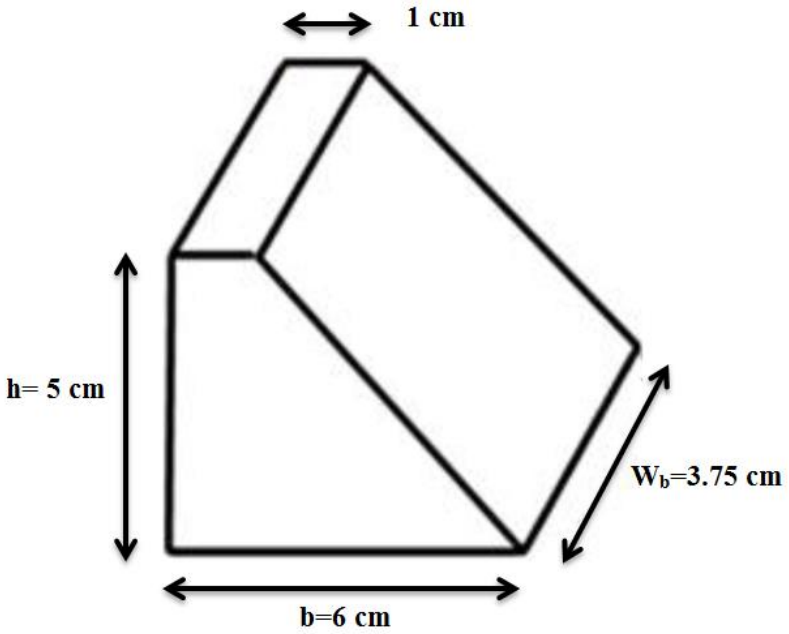

Figure 3.3:The configuration and dimensions of baffle block.

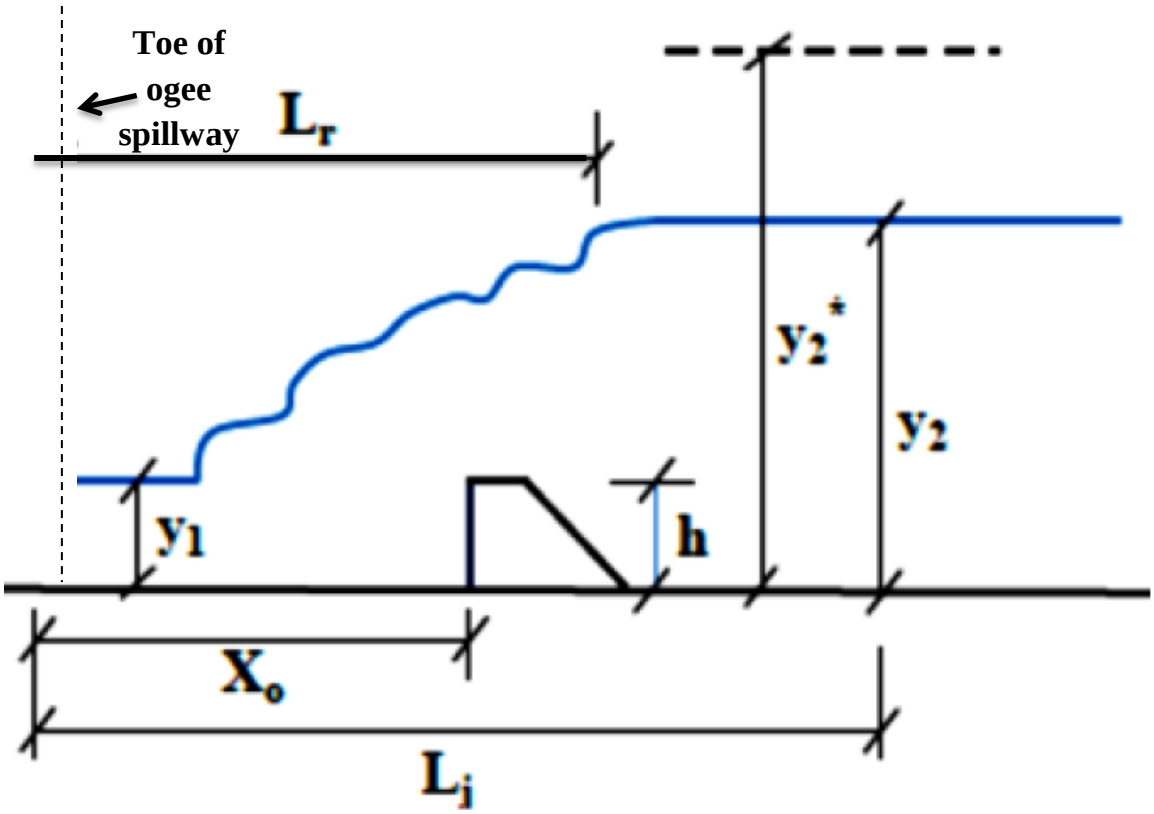

Figure 3.4: Schematic diagram for the forced hydraulic jump.

Different configurations have been arranged in single row, double rows, and complex rows. The location of the first baffle block from the toe spillway was selected equal to X_0/y_2^*= 1.3, it was adopted as recommended by Eloubaidy et al. (1999), where the X_0 related to the sequent depth of jump that was calculated by the Belanger equation. Since the maximum y_2^* is 17.11 cm according to the minimum incoming water level spillway and incoming Froude number X_0 was fixed at 22.24 cm downstream of the spillway for all runs undertaken.

Three groups of baffle block models were used; the first group is one row of baffles with two blockage ratios, the second group installed at two rows includes three different distance ratios $\bar{X}$/b, and the third group installed at three rows includes fixed distance ratios $\bar{X}$/b, where $\bar{X}$ is a distance from the front face of blocks of the first row to the front of the second row. All of these configurations were installed with different blockage ratios.

Table (3.3) consists of these three groups, and Figure (3.5) presents the view of configuration-A1 for the one-row configuration. The blockage ratio of 37.5% was used with the two configurations on the single row. The same number of blocks have been used for configurations A2 and A3 but there was a difference in spacing. The other types of distributions are shown in Figures (3.5 to 3.10). The test, as presented in Figure (3.11), was performed in order to select the most efficient one for improving the characteristics of a hydraulic jump such as depth ratio and transverse velocity distribution.

Table 3.3: Characteristics of the models tested.

Group	Configuration	No. of Rows	Blockage Ratio	Dimensions (cm)			S1 cm	S2 cm	S3 cm	S4 cm	$\bar{X}$ /b
				h	b	W_b					
A	A1	One row	37.5%(1)	5	6	3.75	5.625	3.75	-	-	-
	A2	One row	37.5%(1I)	5	6	3.75	1.875	7.5	-	-	-
	A3	One row	50%	5	6	3.75	1.875	3.75	-	-	-
B	B1	Two rows	50&37.5% (II)	5	6	3.75	1.875	3.75	5.625	3.75	1
	B2	Two rows	50&37.5% (II)	5	6	3.75	1.875	3.75	5.625	3.75	2
C	C1	Three rows	50&37.5 % (II)	5	6	3.75	1.875	3.75	5.625	3.75	3

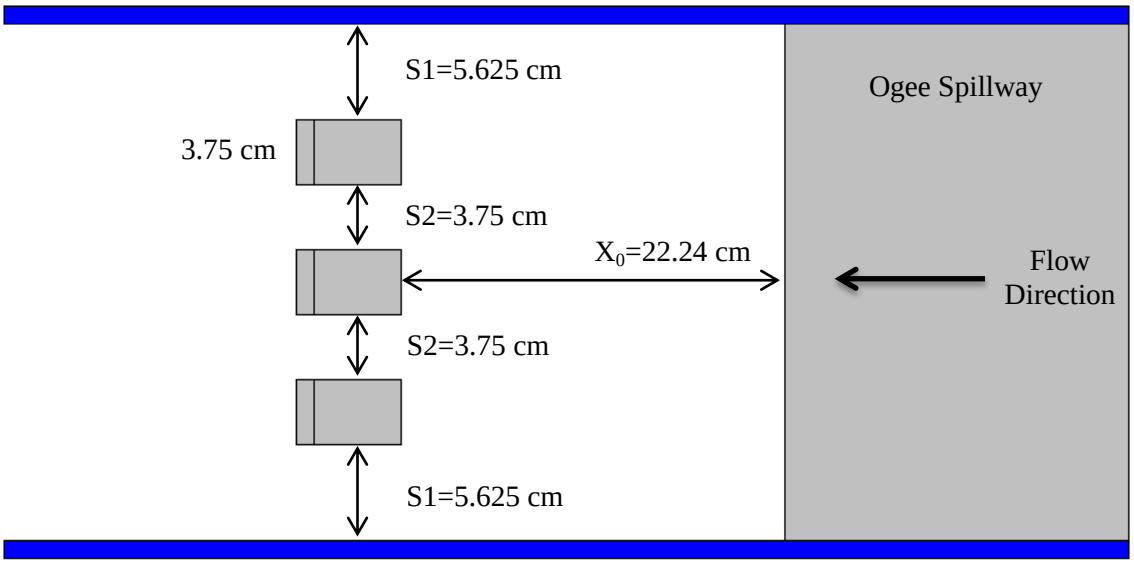

Figure 3.5: Baffle blocks arrangements-A1 one row.

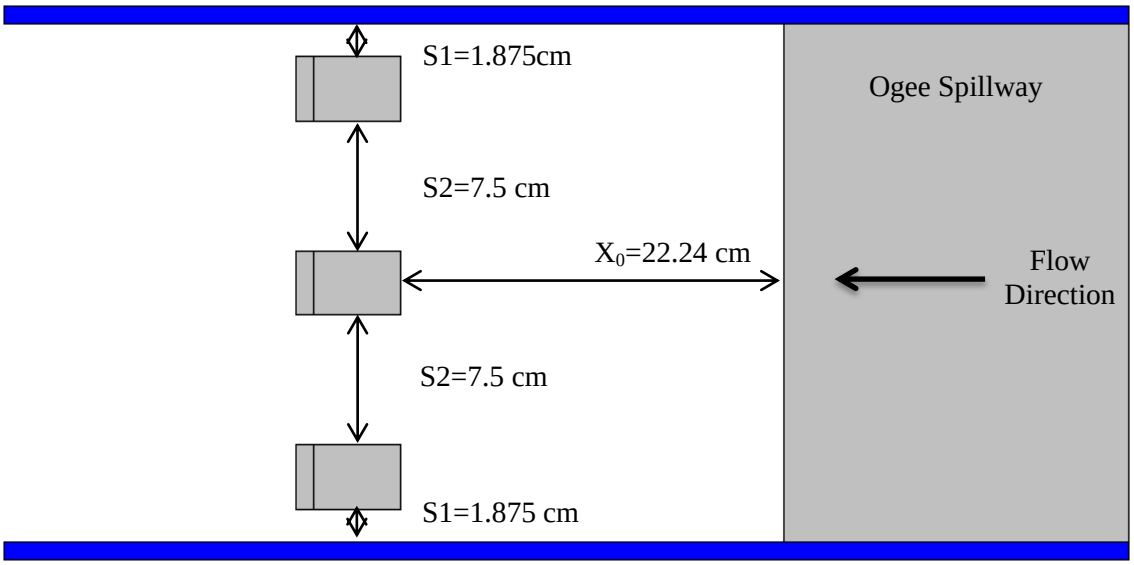

Figure 3.6: Baffle blocks arrangements-A2 one row

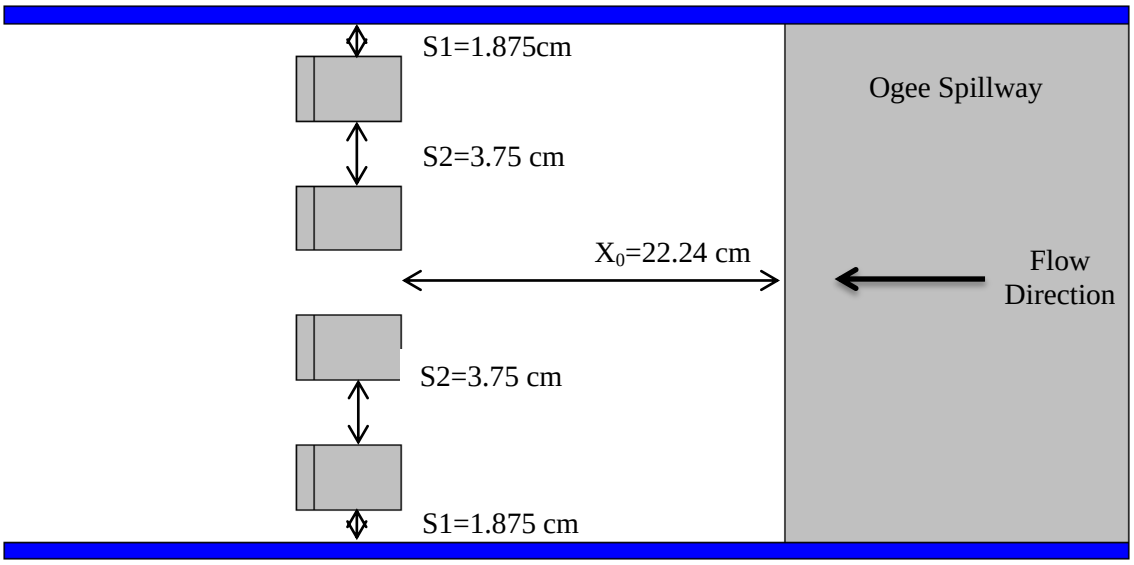

Figure 3.7: Baffle blocks arrangements-A3 one row.

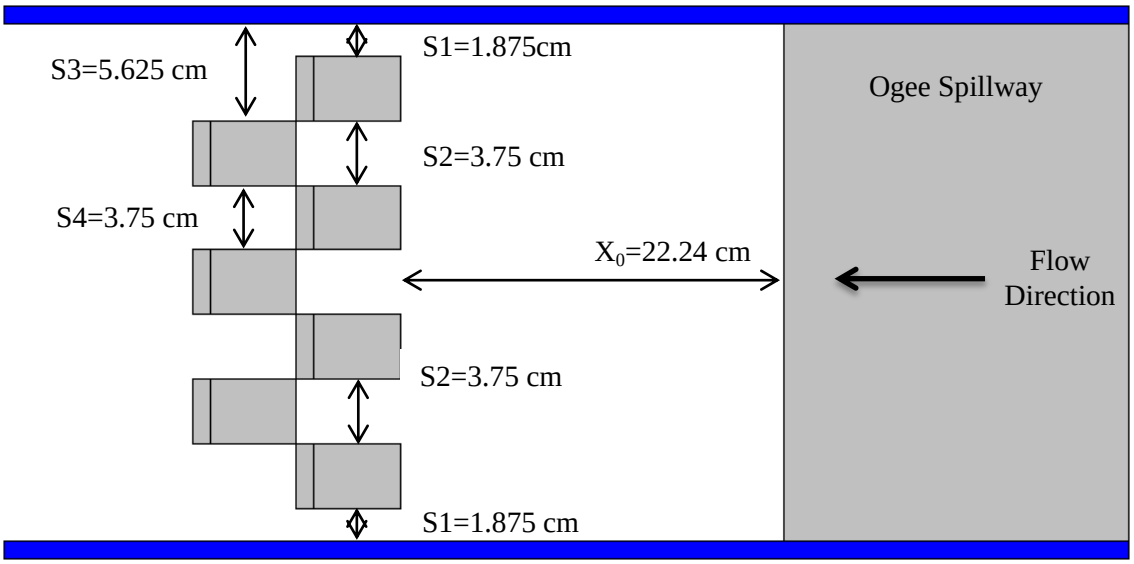

Figure 3.8: Baffle blocks arrangement-B1 two rows.

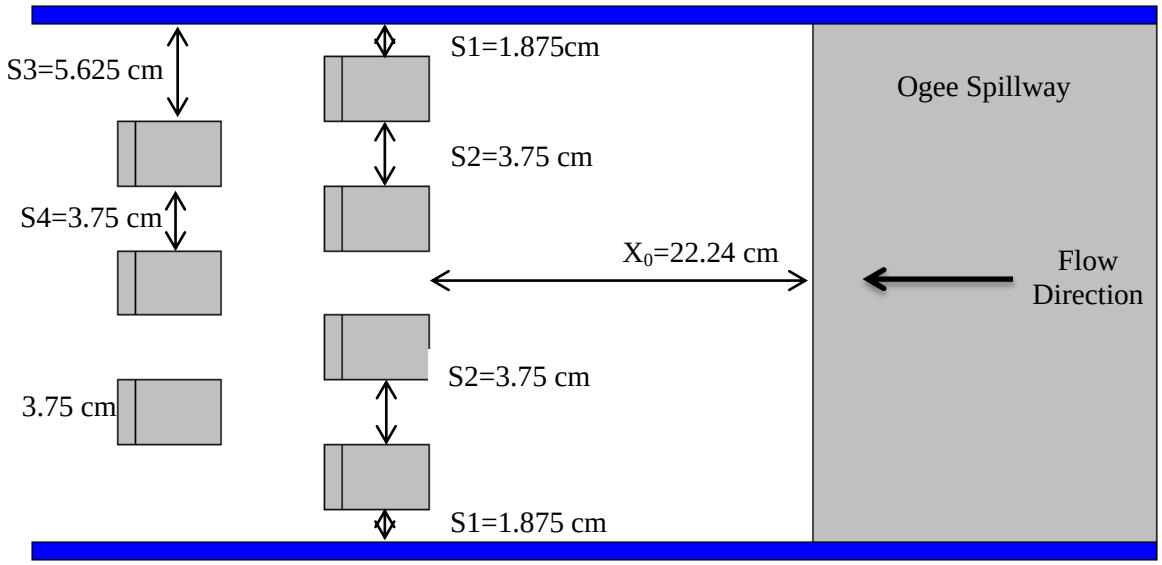

Figure 3.9: Baffle blocks arrangement-B2 two rows.

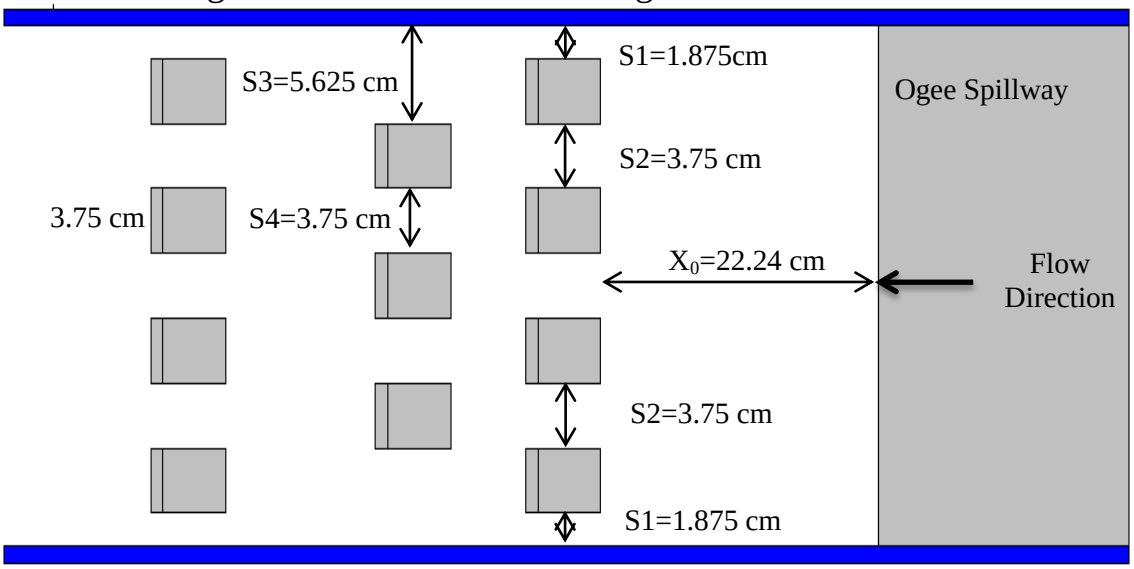

Figure 3.10: Baffle blocks arrangement-C1 two rows.

Figure 3.11: Laboratory test of baffle blocks.

3.5.2 Stepped Blocks

It was proposed to dissipate the energy of water by using three rows of stepped blocks. The blocks were made from timber fixed at the height of 5cm for the entire Froude number range so that the width is 3.75 cm, and the length of the base is manufactured at 6 cm, as presented in Figure (3.12). The configuration of the arrangement of the stepped blocks was shown in Table (3.3) and Figures (3.13 to 3.18).

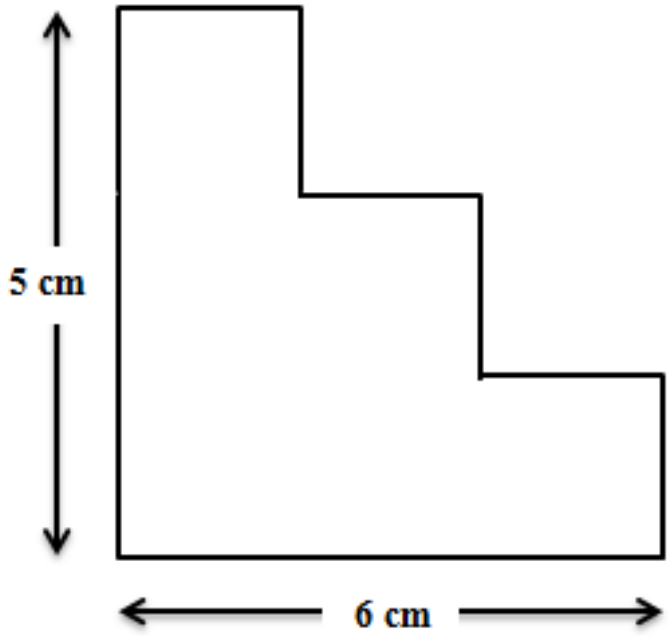

Figure 3.12: The configuration and dimensions of stepped blocks.

Figure (3.19) presents the view of configuration-B2 for the two-row configuration. The blockage ratio of 37.5 % was used with the two configurations on the single row. The same number of blocks have been used for configuration C1 but there was a difference in spacing.

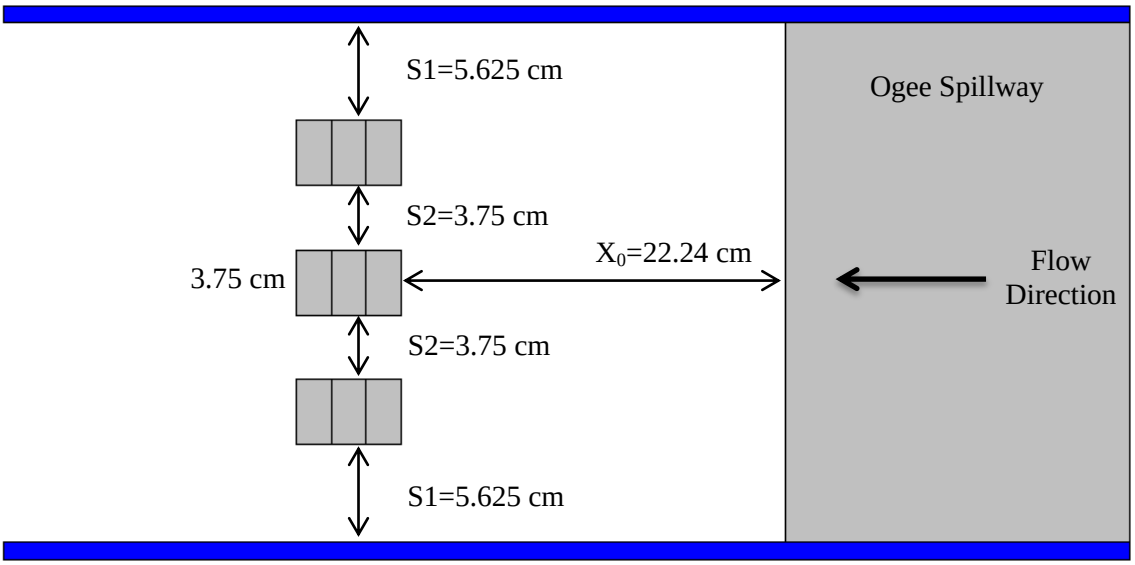

Figure 3.13: Stepped blocks arrangements-A1 one row, η=37.5-I %.

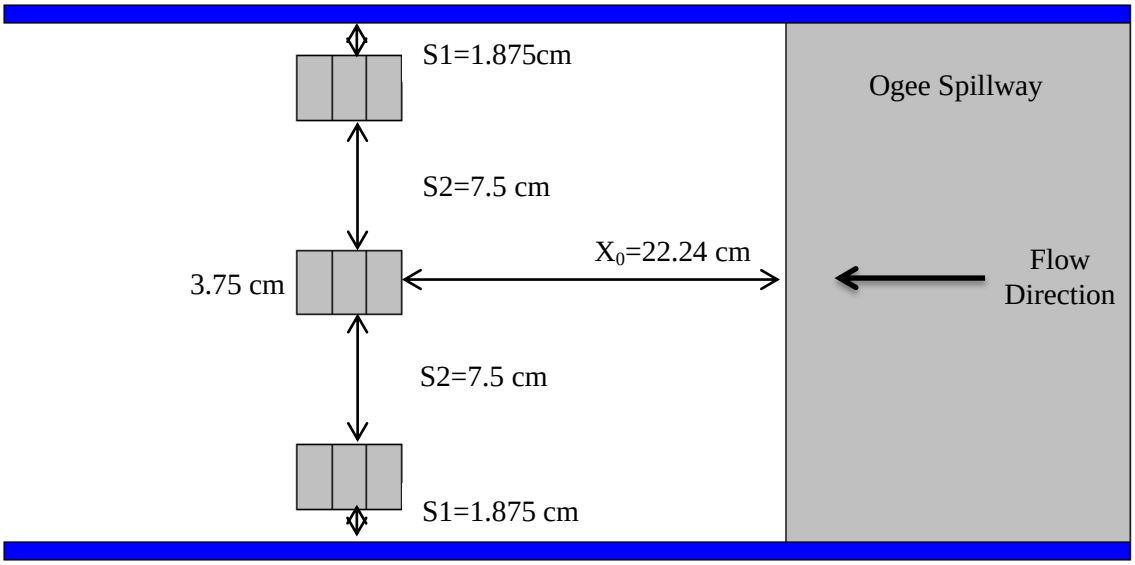

Figure 3.14: Stepped blocks arrangements-A2 one row, η=37.5-I %.

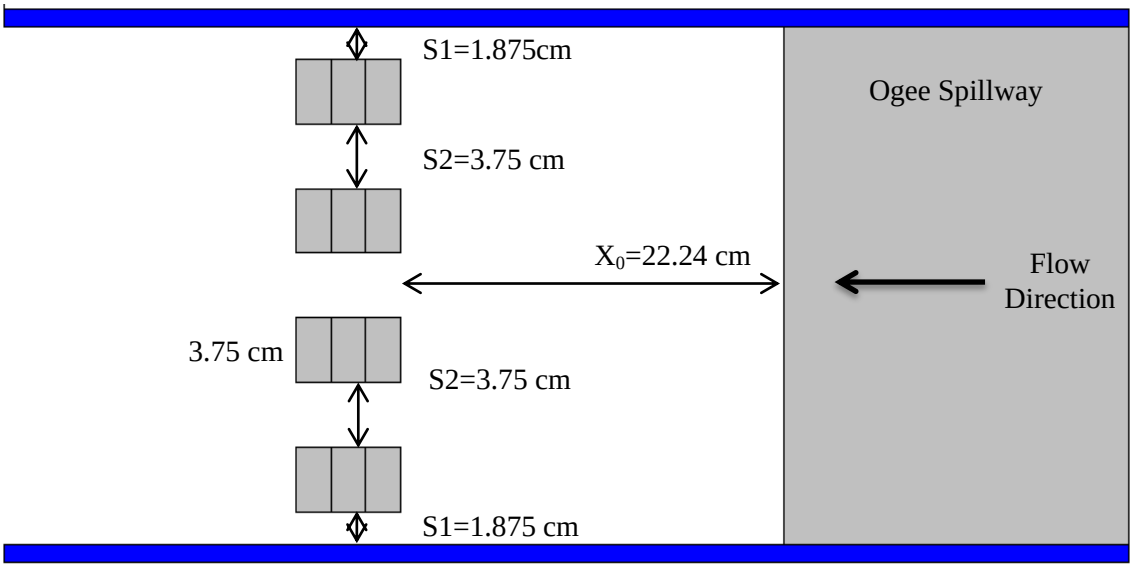

Figure 3.15: Stepped blocks arrangements-A3 one row, η=50 %.

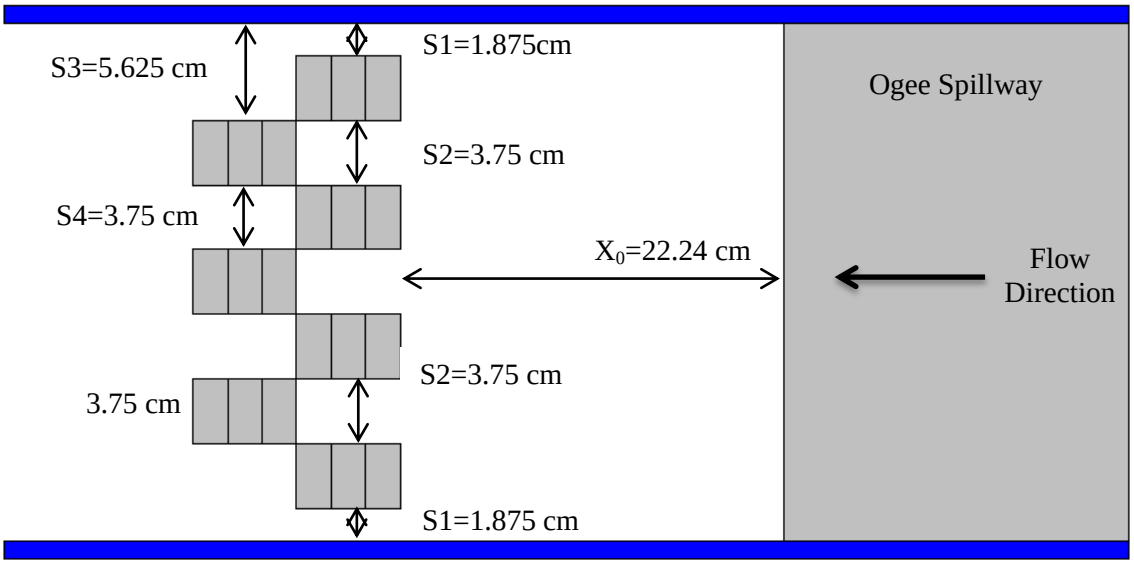

Figure 3.16: Stepped blocks arrangement-B1 two rows, $\bar{X}$ /b =1and η=50&37.5%II.

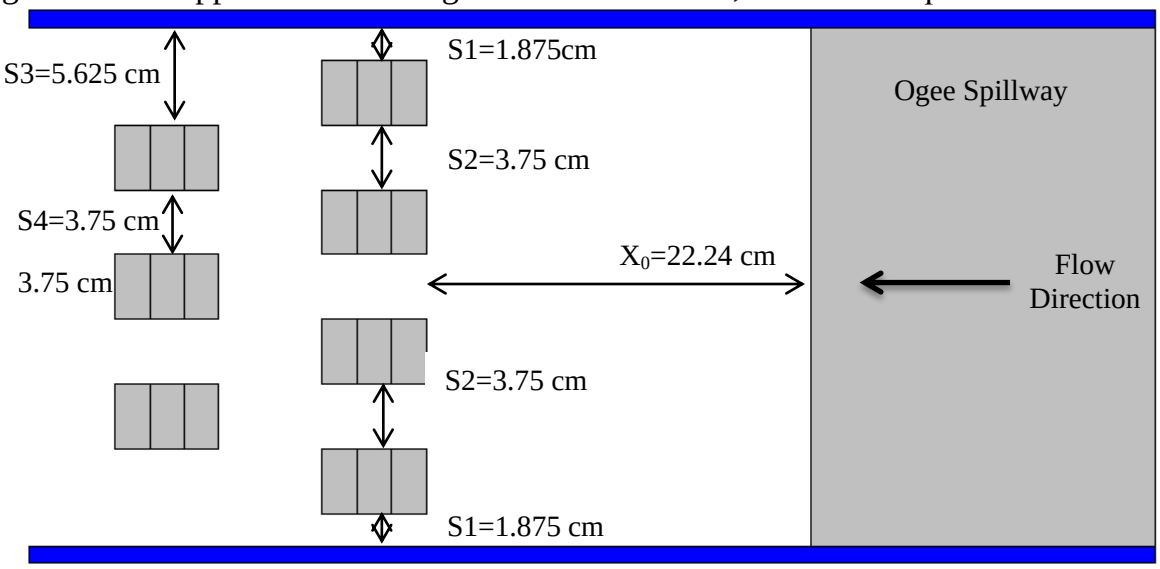

Figure 3.17: Stepped blocks arrangement-B2 two rows, $\bar{X}$ /b=2and η=50&37.5%II.

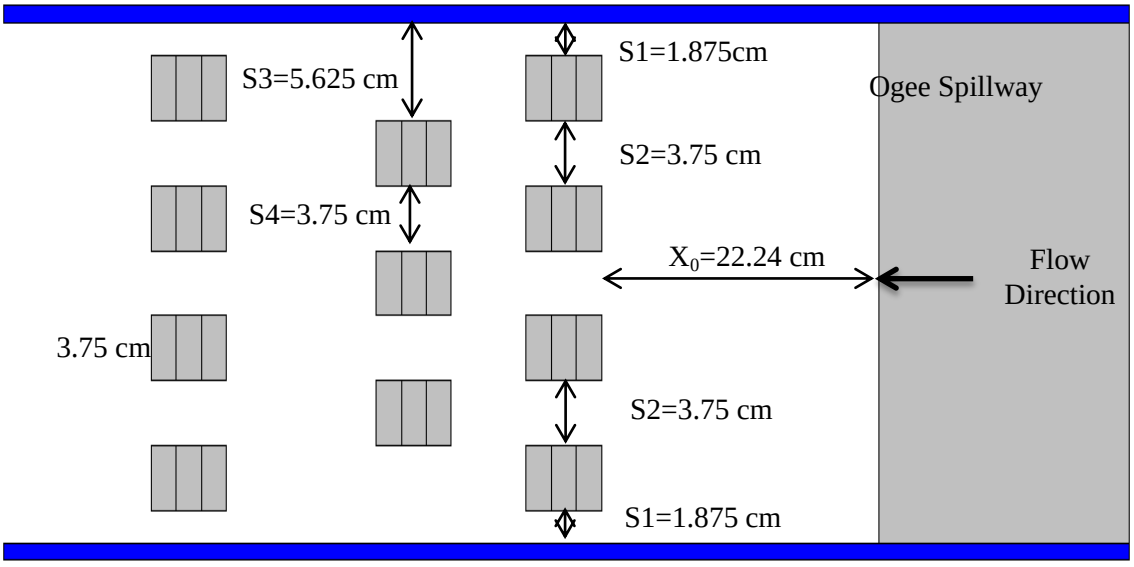

Figure 3.18: Stepped blocks arrangement-C1 three rows, $\bar{X}$ /b=2and η=50&37.5%II.

Figure 3.19: Laboratory test of stepped blocks.

3.5.3 Triangle Blocks

Also, it was attempted to dissipate the energy of water along the stilling basin, using triangle blocks. The blocks were made from timber fixed at the height of 5cm for the entire Froude number range so that the width is 3.75 cm, and the length of the base is manufactured at 6 cm, as presented in Figure (3.20). The configuration of the triangle block arrangement was discussed in Table (3.3) and Figures (3.21 to 3.26).

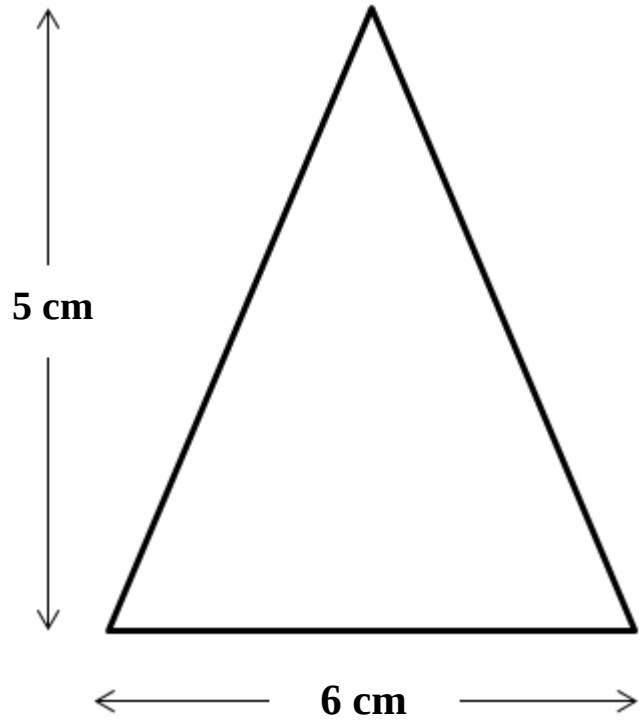

Figure 3.20: The configuration and dimensions of triangle blocks.

The blockage ratio of 37.5 % was used with the two configurations on the single row, as shown in Figure (3.27). The same number of blocks have been used for configuration C1 but there was a difference in spacing.

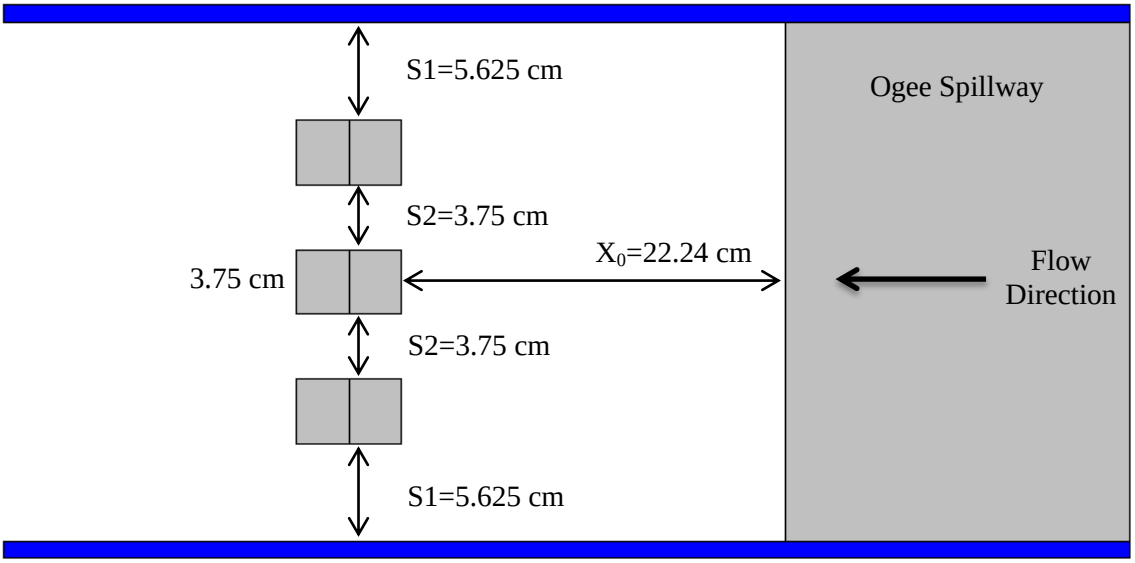

Figure 3.21: Triangle blocks arrangements-A1 one row, η=37.5-I %.

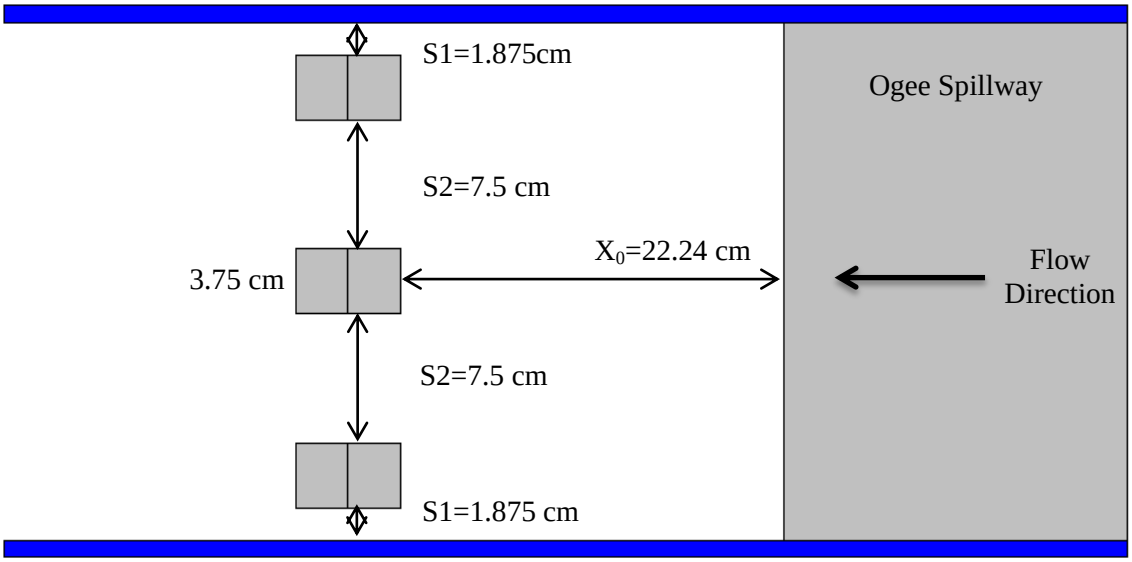

Figure 3.22: Triangle blocks arrangements-A2 one row, η=37.5-I %.

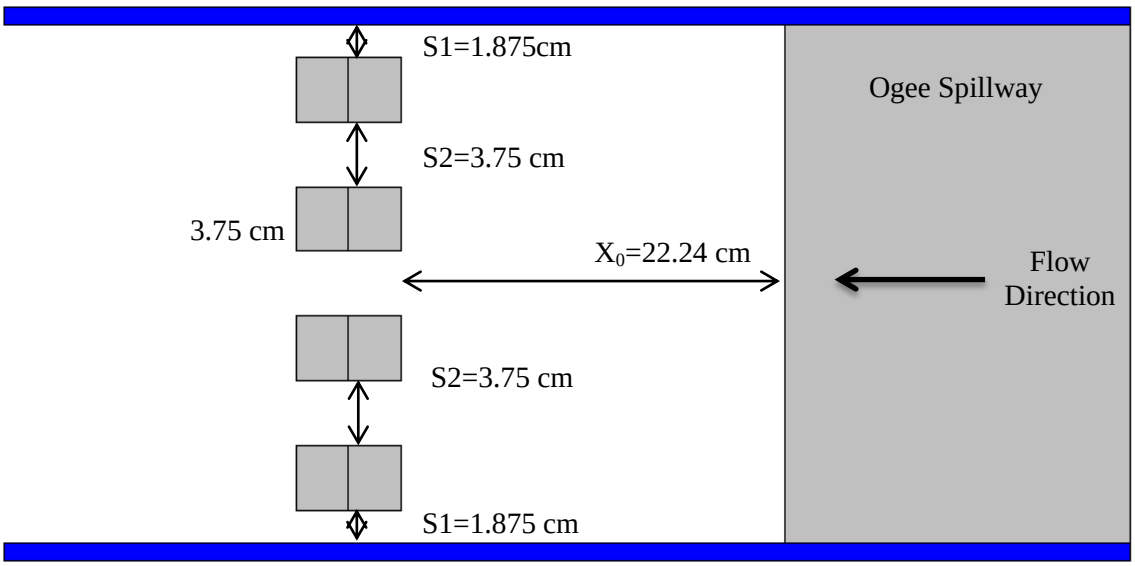

Figure 3.23: Triangle blocks arrangements-A3 one row, η=50 %.

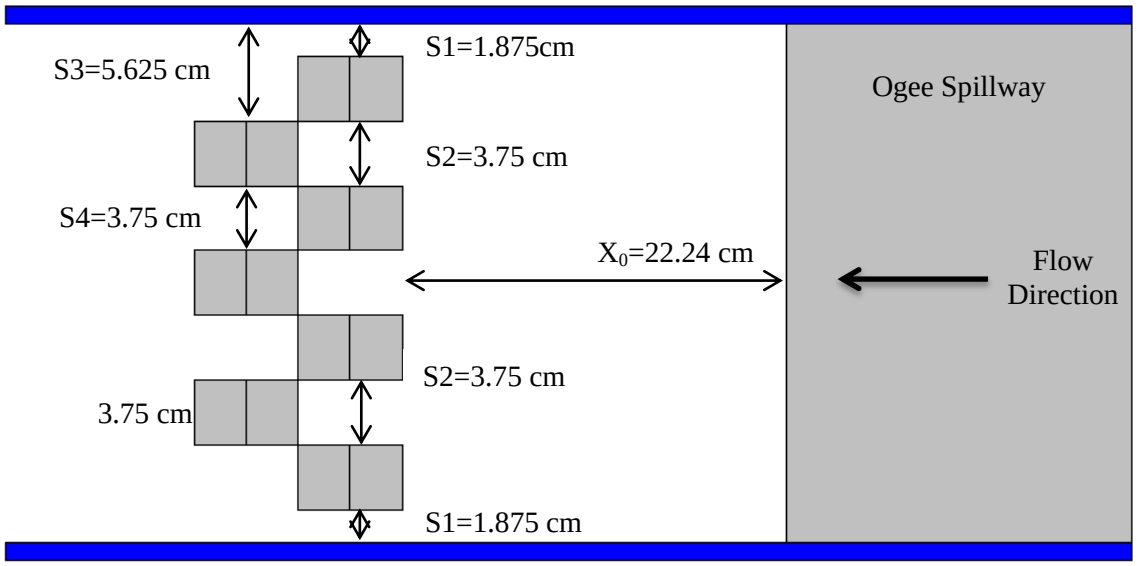

Figure 3.24: Triangle blocks arrangement-B1 two rows, $\bar{X}$ /b =1and η=50&37.5%II.

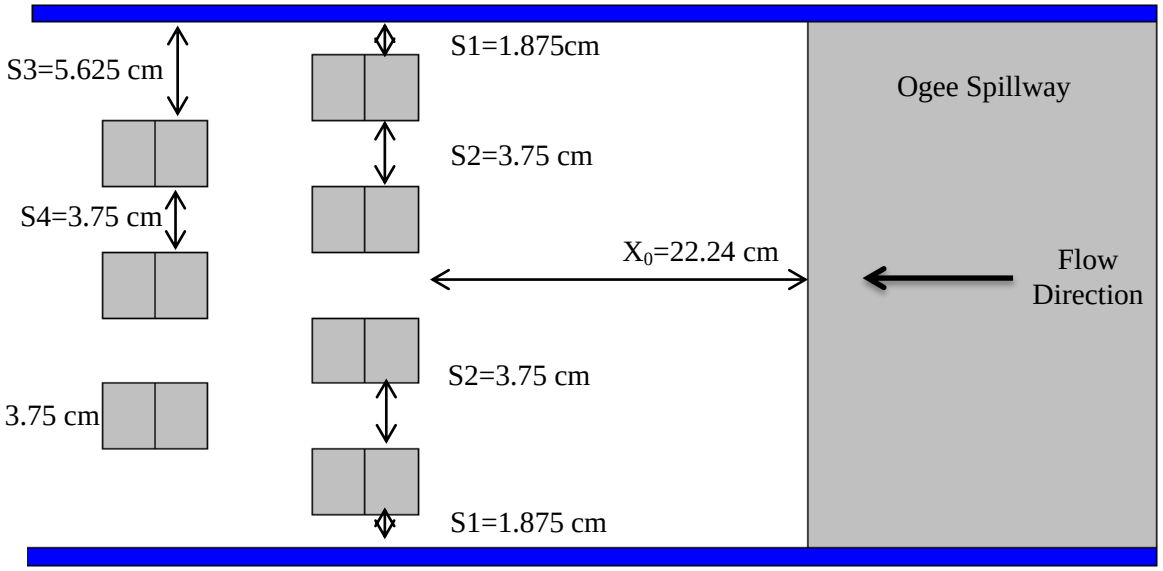

Figure 3.25: Triangle blocks arrangement-B2 two rows, $\bar{X}$ /b=2and η=50&37.5%II.

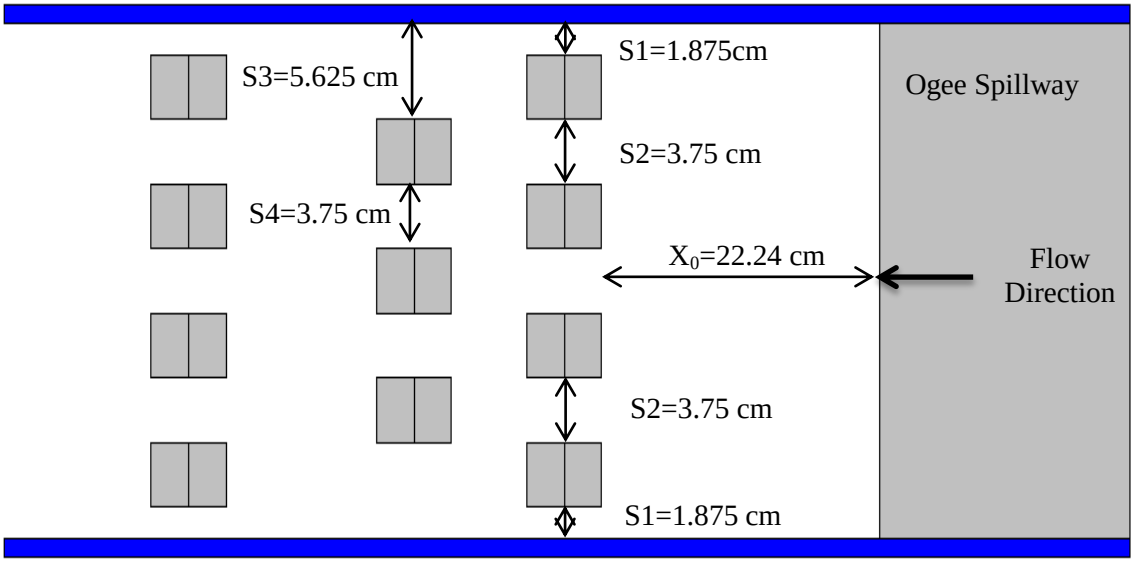

Figure 3.26: Triangle blocks arrangement-C1 three rows, $\bar{X}$ /b=2and η=50&37.5%II.

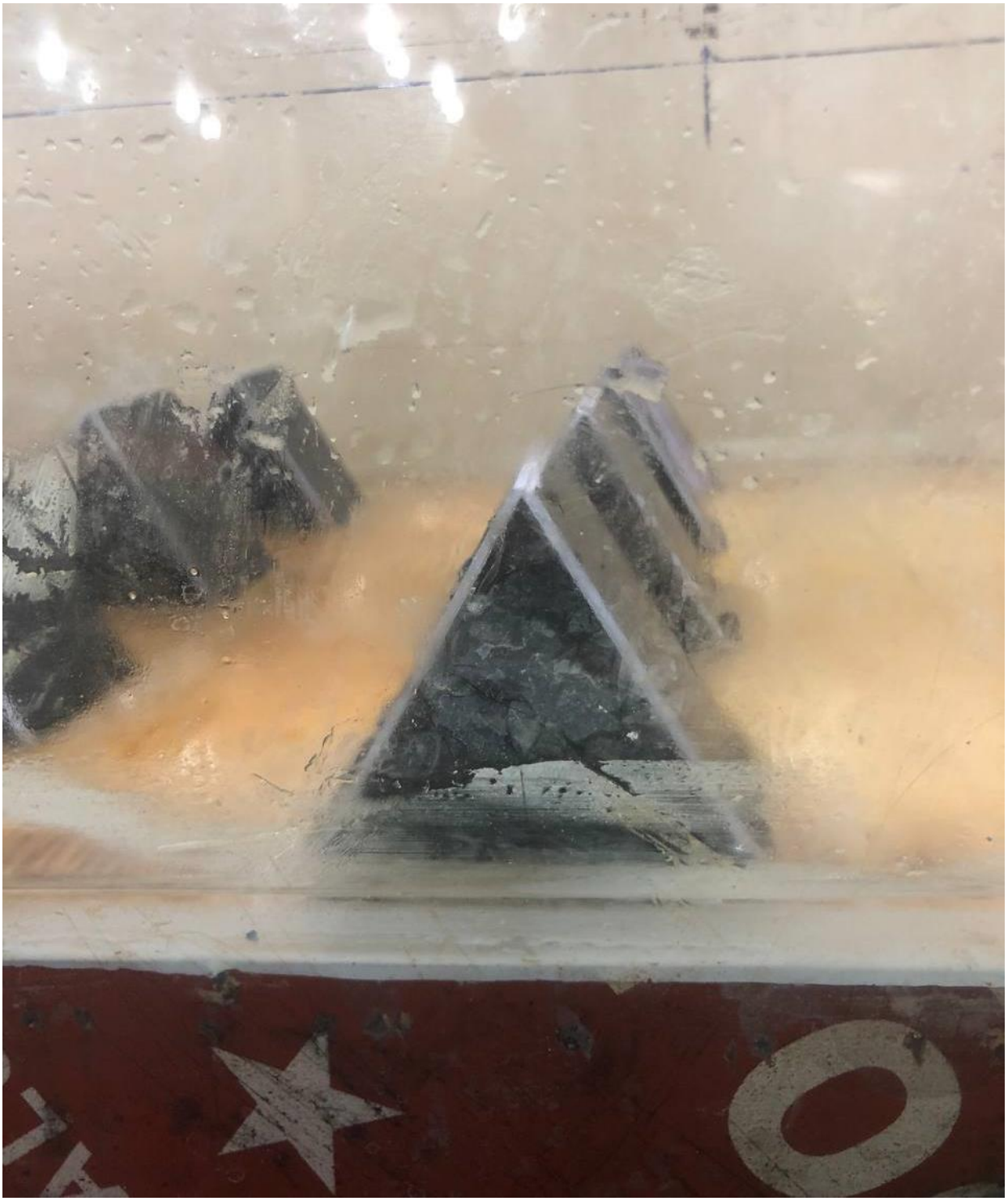

Figure 3.27: Laboratory test of triangle blocks.

3.6 Scour and Stilling Basin

Stilling basin is a structure that has a function of energy minimizing downstream of the spillway. One of the parts of the stilling basin is the end-sill. The end-sill was useful to inhibit the supercritical flow from the crest of the spillway which falling down to the stilling basin so that change to be the subcritical flow behind the end sill structure. Therefore the end sill also uses as an energy damper in the stilling basin. Since the flow in the stilling basin changed from the supercriticl to the subcritical flow caused by the end sill, then stream pattern in stilling basin also altered. In another word, the hydraulic jump is generated in the stilling basin and sketched in Figure (3.28 a, b, and c).

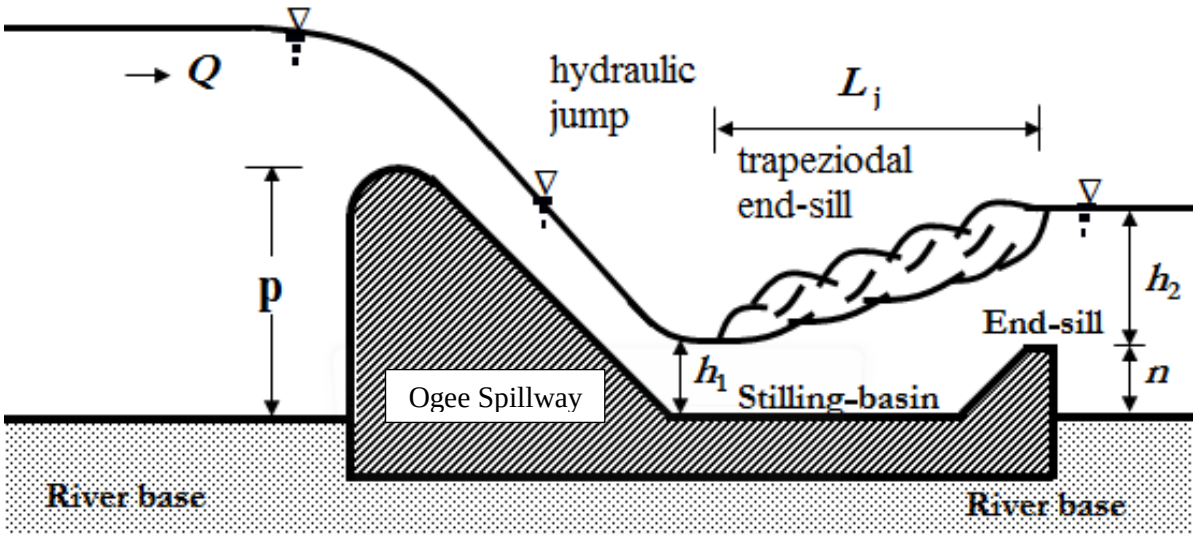

(a): Sketch of the stilling basin.

Where h_1 is the upstream depth, h_2 is the downstream depth over the end-sill, L_j is the length of the hydraulic jump, p is the crest high of the weir, n is the high of the end-sill, and Q is stream discharge.

(b): Photo for laboratory work.

(c):

Figure 3.28: Hydraulic jump on stilling basin.

Three types of stepped blocks (A1, A2, and A3) with end sill are used to evaluate the minimized velocities and hydraulic jump. The tailwater depth of flow was controlled by one-row blocks fixed at the end of the spillway (Figure 3.29). The mobile bed of sand was extended to 150cm with 10cm thickness. The model sand is non-uniform (uniformity coefficient =D60/D10= 1.8) with D50= 1.7mm, and geometric mean =D85/D15 =1.69. The grain size analysis of bed soil was tabulated in Table (3.4).

The experimental study was started by studying the effect of scour characteristics with a different number of steps.

Figure 3.29: Sieve analysis of the sand at end of spillway.

Table 3.4: Grain size analysis (Weight of dry sand sample = 1000 gm).

Sieve opening (mm)	Retained weight (gm)	Retained percentage %	Cumulative weight (gm)	Cumulative percentage %	Pass percentage %
1.18	0	0	0	0	100
0.85	82	8.2	82	8.2	91.8
0.6	828	82.8	910	91	9
0.420	85	8.5	995	99.5	0.5
0.3	2	0.2	997	99.7	0.3
0.15	1	0.1	998	99.8	0.2
0.074	0.5	0.05	998.5	99.85	0.15
pan	1.5	0.15	1000	100	0

3.7 Flow parameters

During the planning phase, the flow conditions for various tests had to be determined. The discharge over the spillway section was determined using Equation 2.2, found in **Section 2.4.5**, and each discharge was determined with respect to the following major variables:

- Head over the crest (H_e)
- Discharge coefficients (C)

Based on USBR (1987), the coefficients of discharge for different heads other than the design head and the rating curve showing the relationship between the discharge Q (m^3/s) and head (m), respectively, are presented in Figure (3.30).

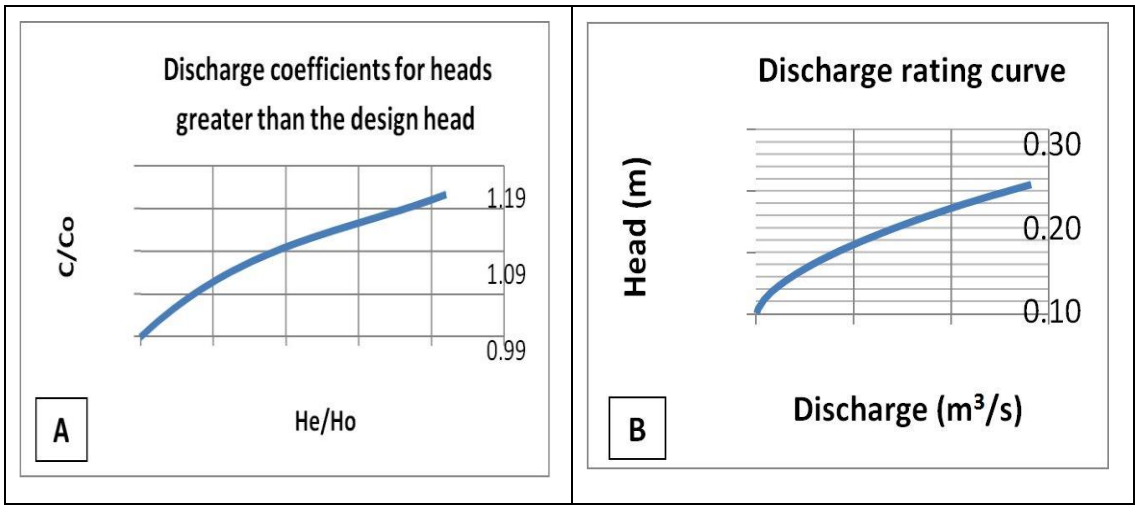

Figure 3.30: Discharge characteristics of the physical model: A: Discharge coefficients, B: Discharge rating curve.

3.8 Measuring Equipment and Techniques

During the physical modeling, much attention was paid to the necessary instrumentation. A typical test procedure consisted of a selected discharge being allowed to pass. The tailgate was adjusted until a jump is formed just downstream of the spillway. Starting test time of the run was recorded, and water surface profiles were measured and recorded during the test. Once the stability conditions were reached, flow rate, length of the jump, water depths upstream and at the vena contract downstream of the spillway, the sequent depth of the jump, and the tailwater depth are recorded. After 120 minutes the pump was stopped. After the sand was drained from the water, the maximum scour depth, the maximum deposition, their locations, and also a survey of the scour hole mesh were measured. These steps were repeated for different discharges until the required ranges of the parameters being under investigation were covered.

CHAPTER FOUR

RESULTS AND DISCUSSION

4.1 General

The tests performed in the laboratory as experimental works were found to select the most efficient type of block for improving the characteristics of a hydraulic jump such as depth ratio, transverse velocity distribution, and scour downstream of the stilling basin.

4.2 Baffle Block Results

4.2.1 Baffle Block Velocities

The comparison between the different baffle distribution block results in terms of sequent depths and velocity distributions is shown in Figure (4.1) and Figure (4.2), respectively. It is evident through these figures that better results were achieved by using A3 in terms of reducing the sequent depth ratio and flow velocities, which provided more uniformity in distribution, especially with the range of Froude number 4.5-9.25.

However, good stability of the hydraulic jump was observed when using A3, while this was difficult to achieve by using both A1 and A2. More turbulence was observed, which lead to the dissipation of more energy and, therefore, reduced sequent depth y_2. On the other hand, there is a greater possibility to divide the incoming flow into almost equal sections, suggesting more regularity in the distribution of velocity, especially with higher Froude numbers. This efficient performance of configuration A3 leads to its further use in other run series as opposed to using both A1 and A2.

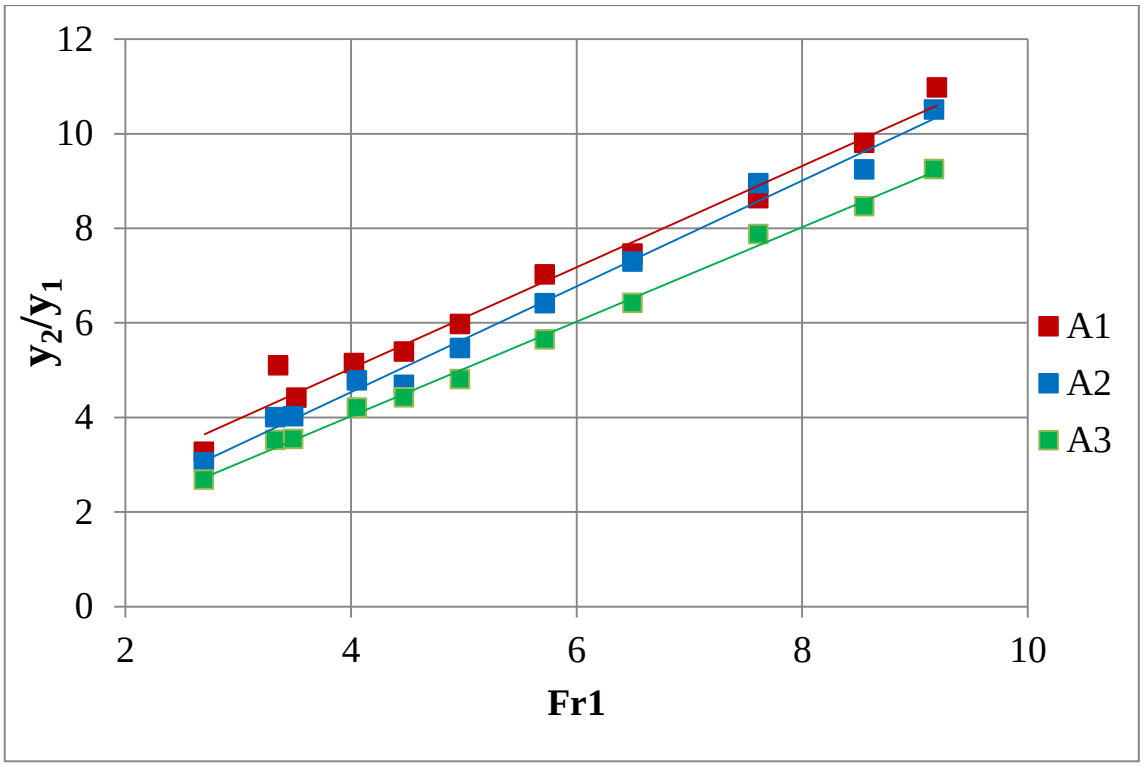

Figure 4.1: The variation of y_2/y_1 with baffle block configurations of single row.

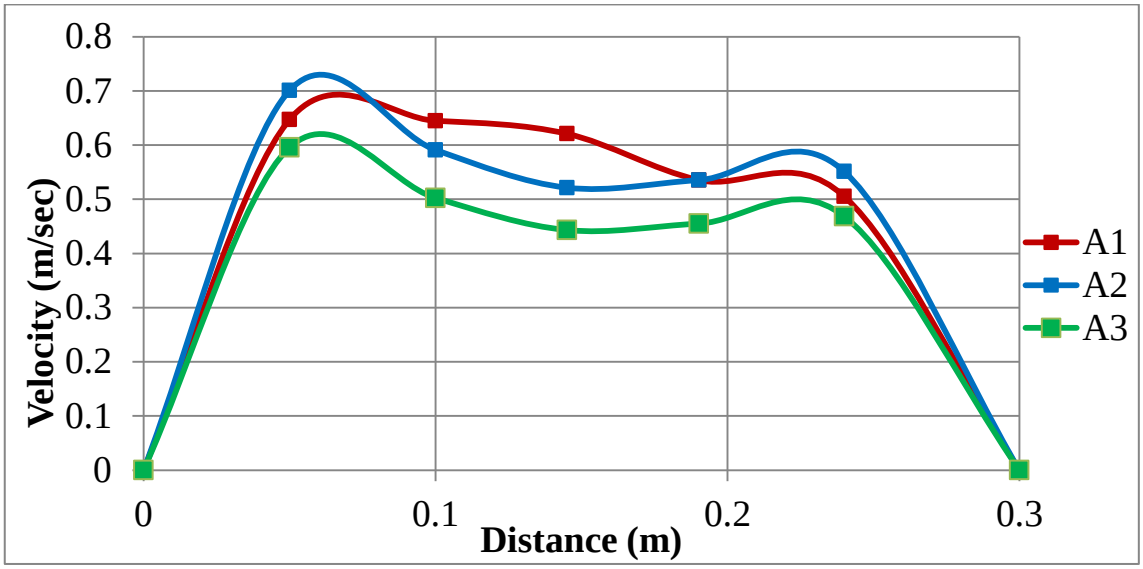

(a): Fr_1=2.75

Figure 4.2: Transverse velocity distribution for baffle block configurations, continue.

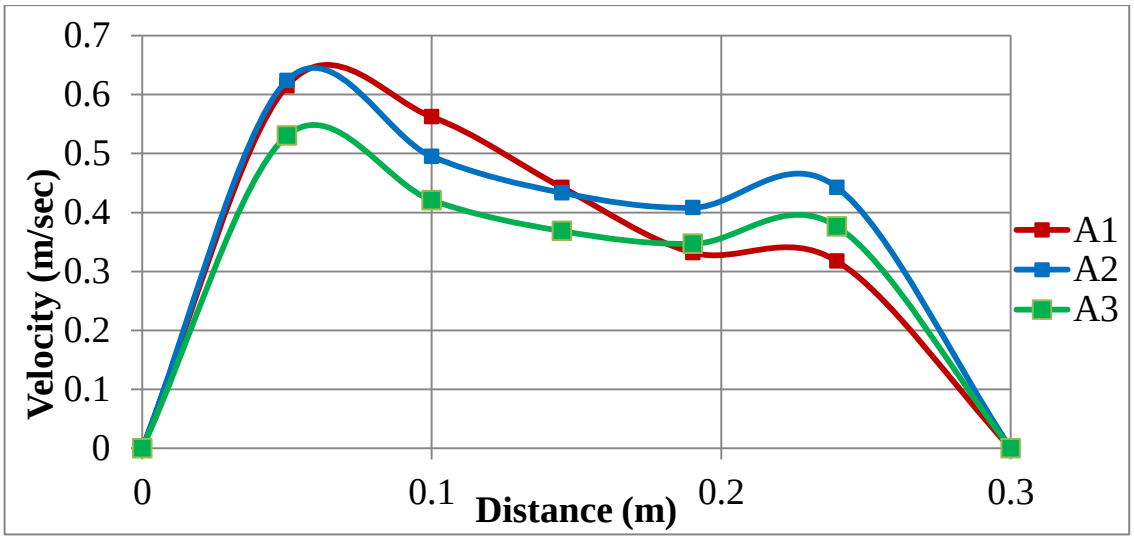

(b): Fr_1=3.50

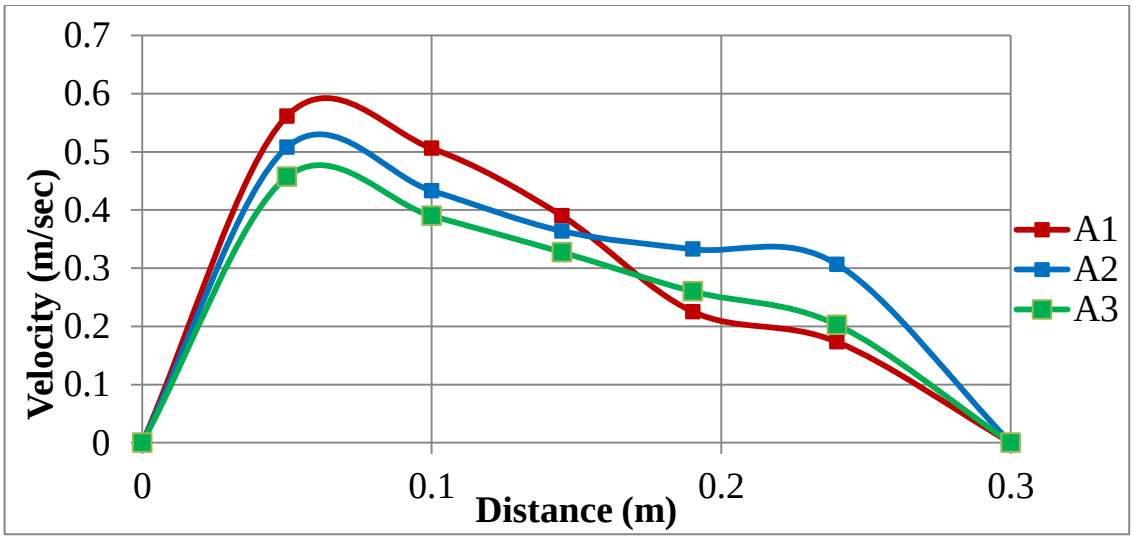

(c) Fr_1=4.50

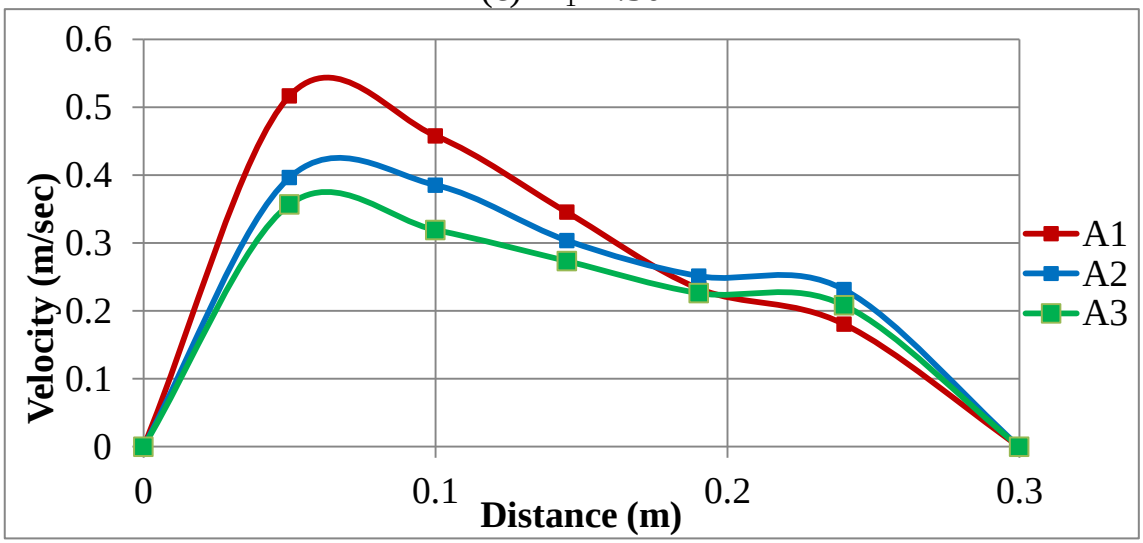

(d) Fr_1=5.75

Figure 4.2: Transverse velocity distribution for baffle block configurations, continue.

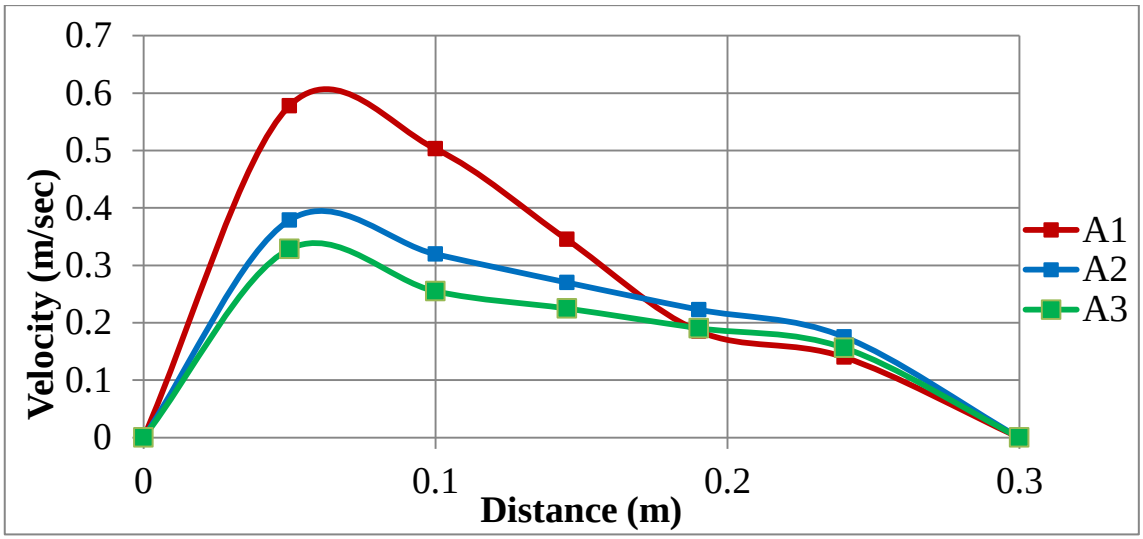

(e) Fr_1=6.50

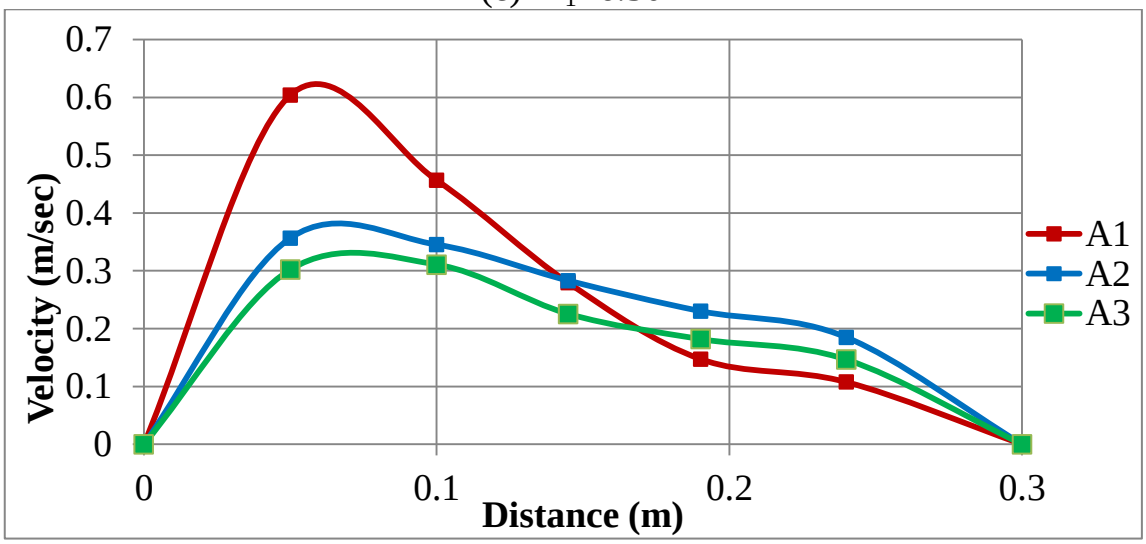

(f) Fr_1=7.75

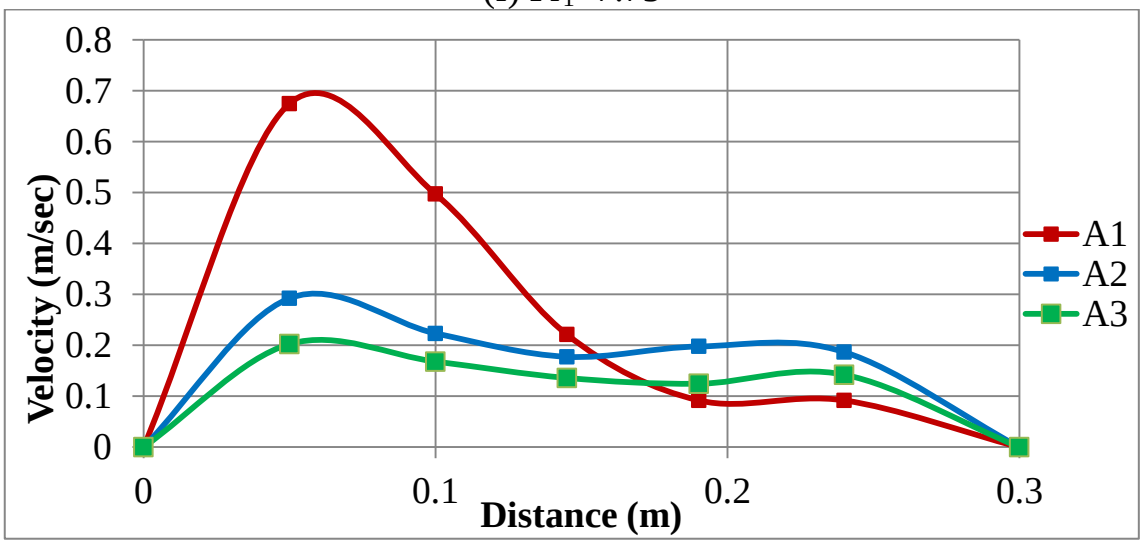

(g) Fr_1=8.50

Figure 4.2: Transverse velocity distribution for baffle block configurations, continue.

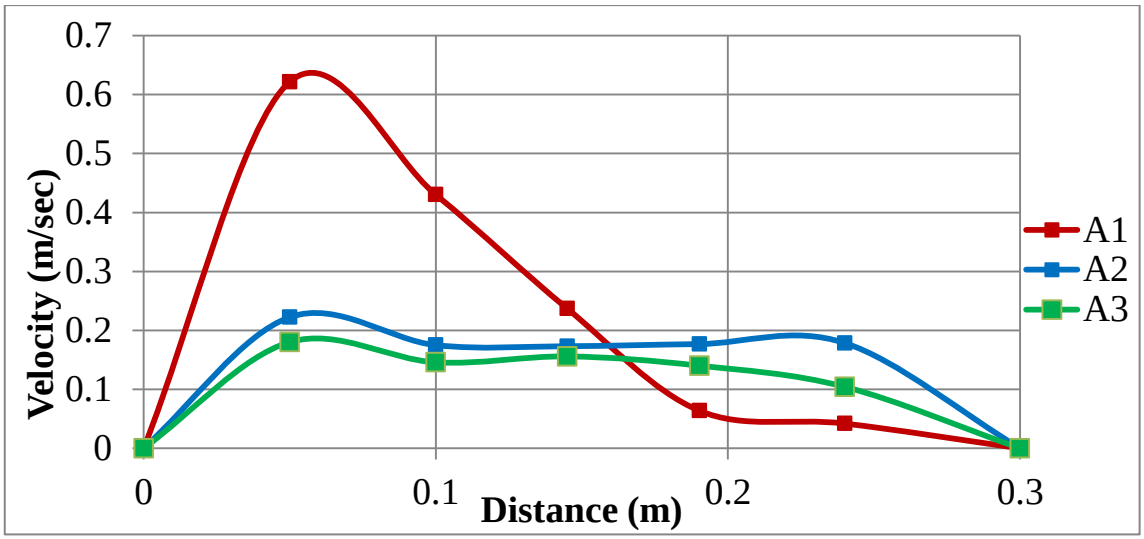

(h) Fr_1=9.25

Figure 4.2: Transverse velocity distribution for baffle block configurations.

4.2.2 Baffle Block Sequent Depth Ratio

As mentioned previously, equipping the bed of the channel that contains the hydraulic jump by appurtenances (e.g., baffle blocks) eventually has an appreciable effect through the decrease in the sequent depth ratio (y_2/y_1). This decrease is a pointer to the hydraulic performance improvement. Figure (4.3) shows the variation of the sequent depth ratio (y_2/y_1) with the initial Froude number for all models of configurations A, B and C. In this figure, the line that represents the sequent depth ratio of a free jump of the Belanger equation is also shown. As observed, the sequent depth ratio in the rough bed stilling basin (i.e. equipped with baffle block) for all blockage ratios was smaller than that achieved for the classical jump (Belanger equation). However, the configuration-C1 gives a better performance in reducing the sequent depth (y_2) compared to the other configurations.

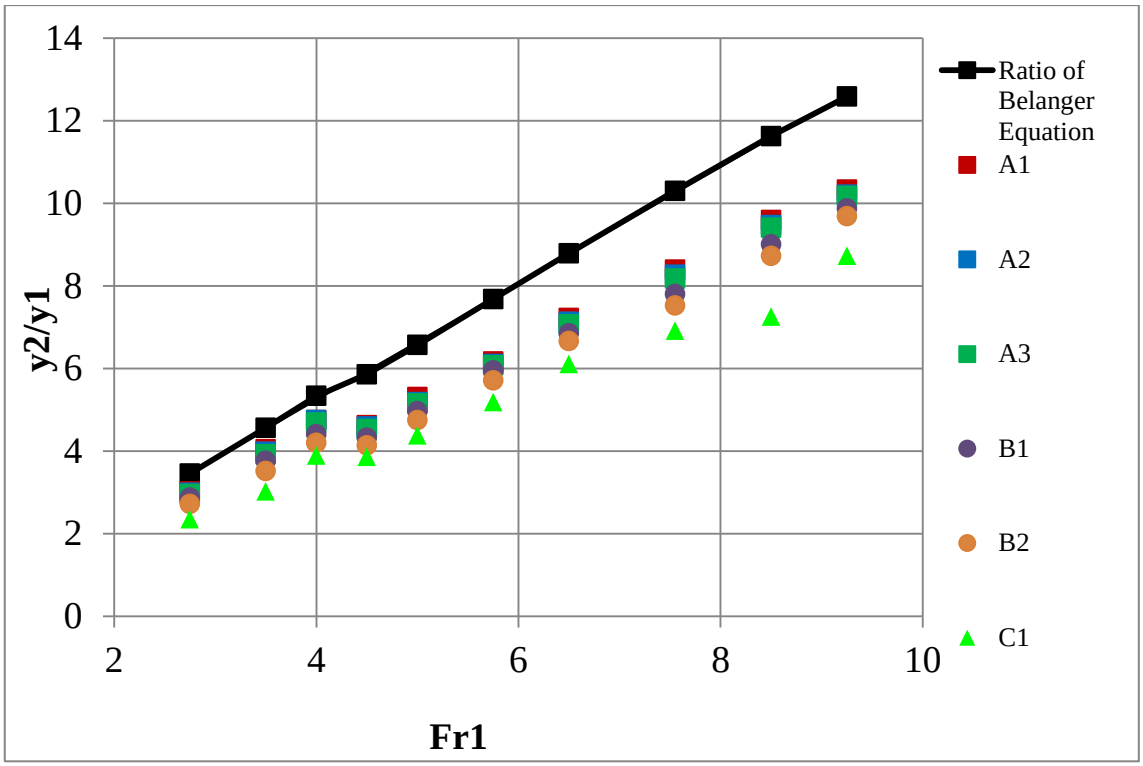

Figure 4.3: Sequent depth ratio for all configurations of baffle blocks.

To verify the accuracy of the results obtained from the experiments conducted in the laboratory. The results of configuration-B1 have been compared with the results of those previously presented by Eloubaidy et al. (1999) (for curved in-plan baffle block), Ellayn and Sun (2012) (for wedge-shaped baffle block) and Maatooq, and Taleb (2018) (for wedge-shaped baffle block). Figure (4.4) illustrates this comparison and shows the same trend between the results of the present study and those of the previous works. At the same time, however, less sequent depth ratios are associated with using the configuration-B1, which indicates that the hydraulic jump performance improved with the use of this configuration compared with one row. The percent improvement in the reduction of y_2/y_1 relative to the results of Eloubaidy (1999), Ellayn and Sun (2012), and Maatooq, and Taleb (2018), are 65%, 35%, and 20%, respectively. Consequently, it could construct a new relationship between the sequent depth ratio and the

Froude number for the best configuration-B1 with correlation R^2 equal to 0.981.

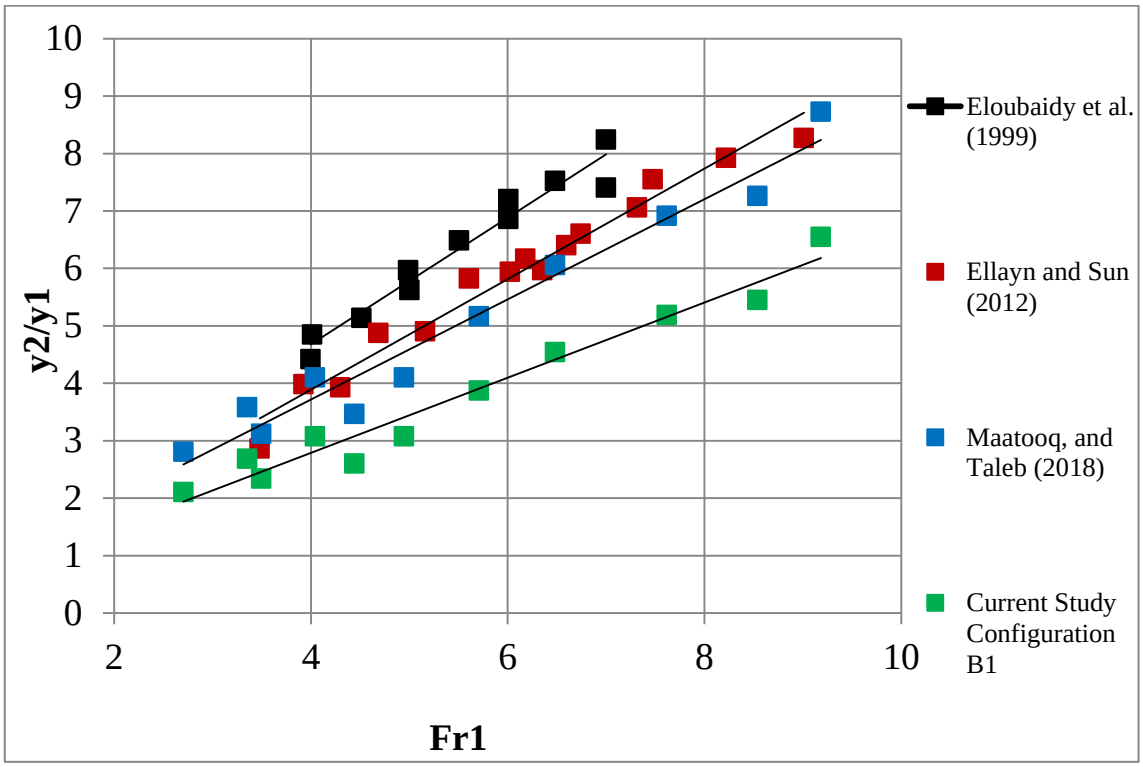

Figure 4.4: Comparison of the sequent depth ratio for baffle block configuration B1, with previous studies.

4.3 Triangle Block Results

4.3.1 Triangle Block Velocities

Figures (4.5) and (4.6a to h) compared the outcomes and demonstrate the contrast. These figures clearly show that utilizing A3 produced superior outcomes in terms of reducing the sequent depth ratio and the flow velocities, which produced a more uniform distribution, notably in the Froude number range of 5.75–9.25. However, the hydraulic jump's stability was noted when utilizing A3, but both A1 and A2 had difficulty achieving this characteristic.

Due to the triangular blocks in configuration A3 being closer together than those in configurations A1 and A2, performance with this configuration of model A3 may be explained. More turbulence was seen, which caused more energy to be lost and lowered the subsequent depth y_2. Due to the A3 configuration's effective performance, it was chosen for usage in additional run series rather than both A1 and A2.

It is important to note that this type of block (Triangle block) fails to reduce the speed compared to the previous type (Baffle block), as it can be seen that there is an increase in velocities up to 1.15% for most of the user configurations (A1, A2, A3, B1, B2, and C1).

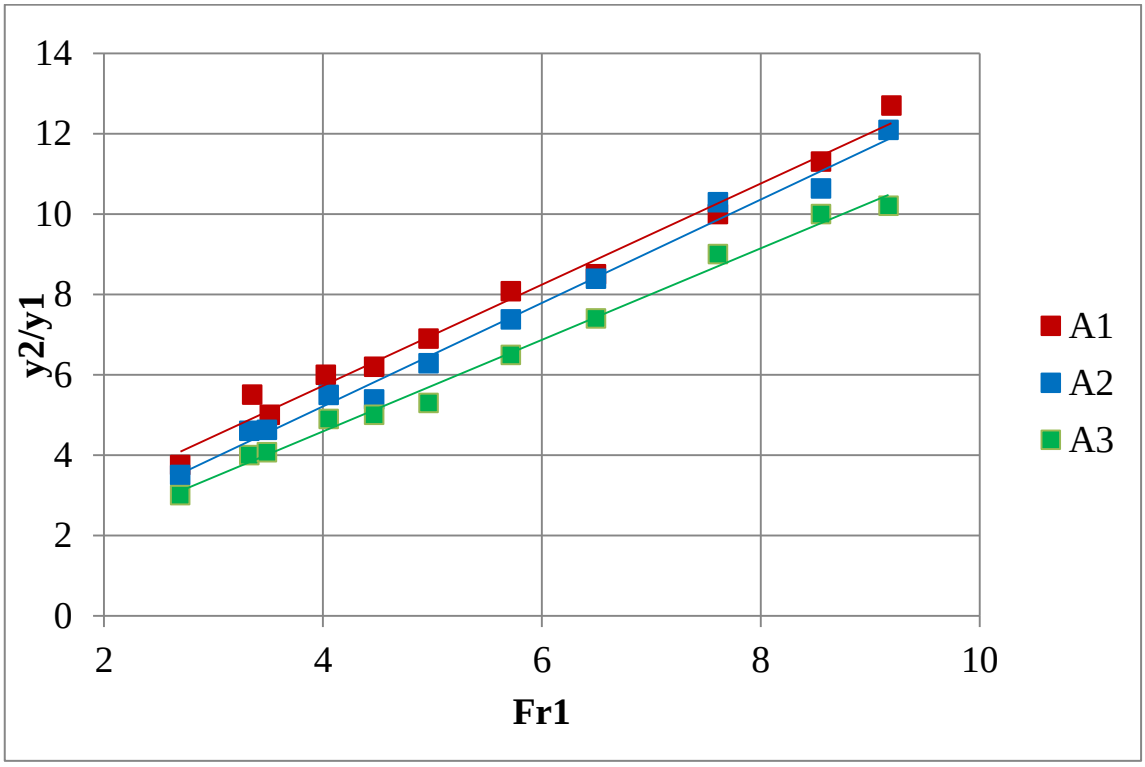

Figure 4.5: The variation of y_2/y_1 with triangle block configurations of single row.

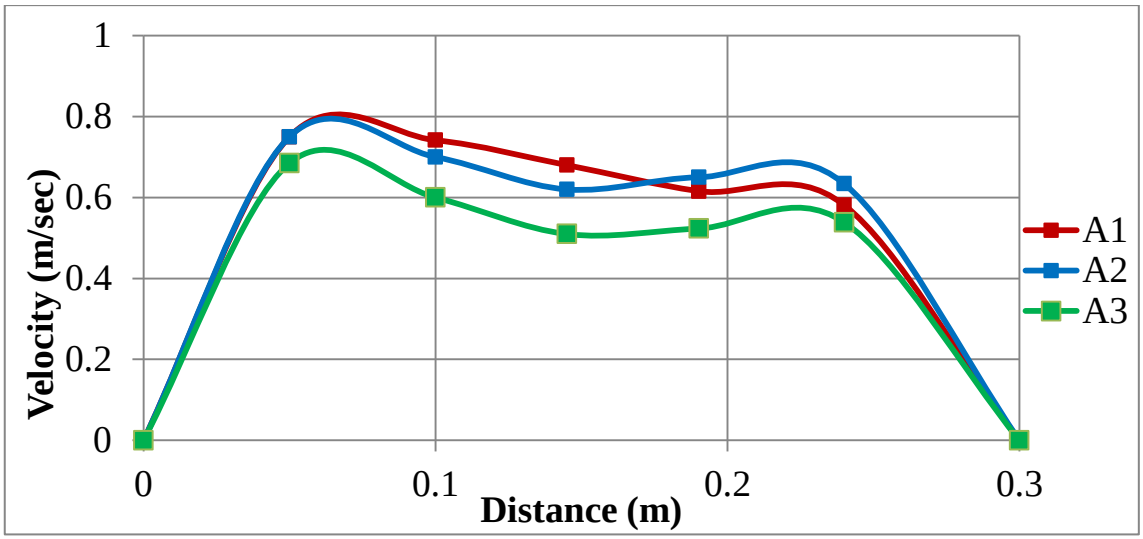

(a): Fr_1=2.750

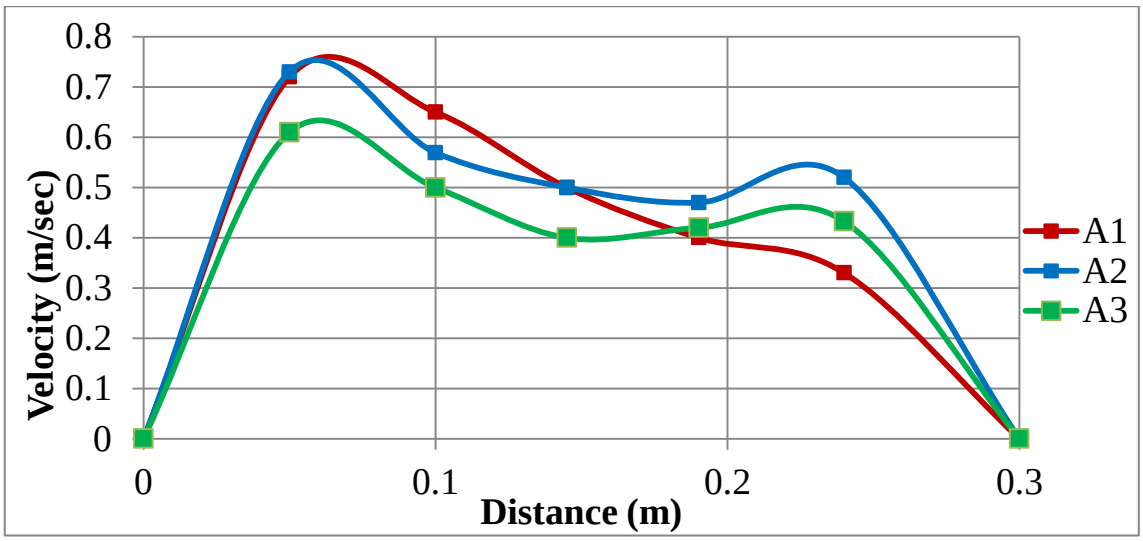

(b): Fr_1=3.50

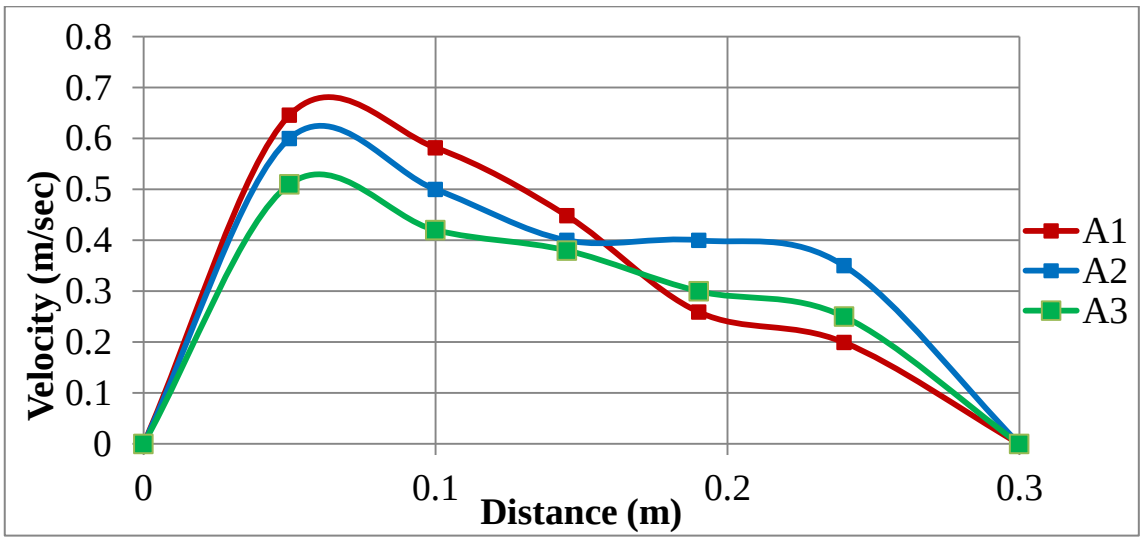

(c) Fr_1=4.50

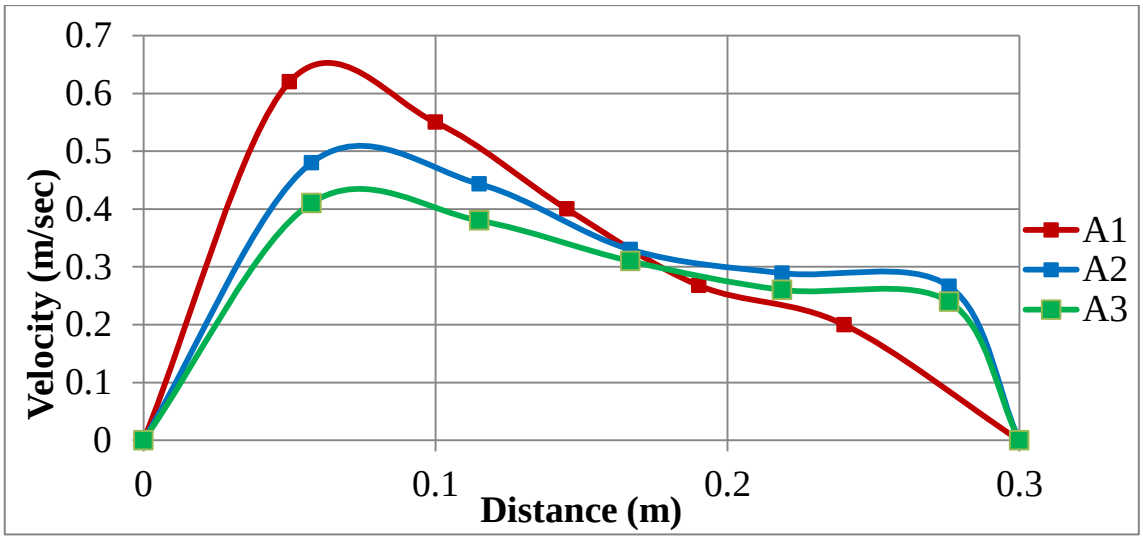

(d) Fr_1=5.75

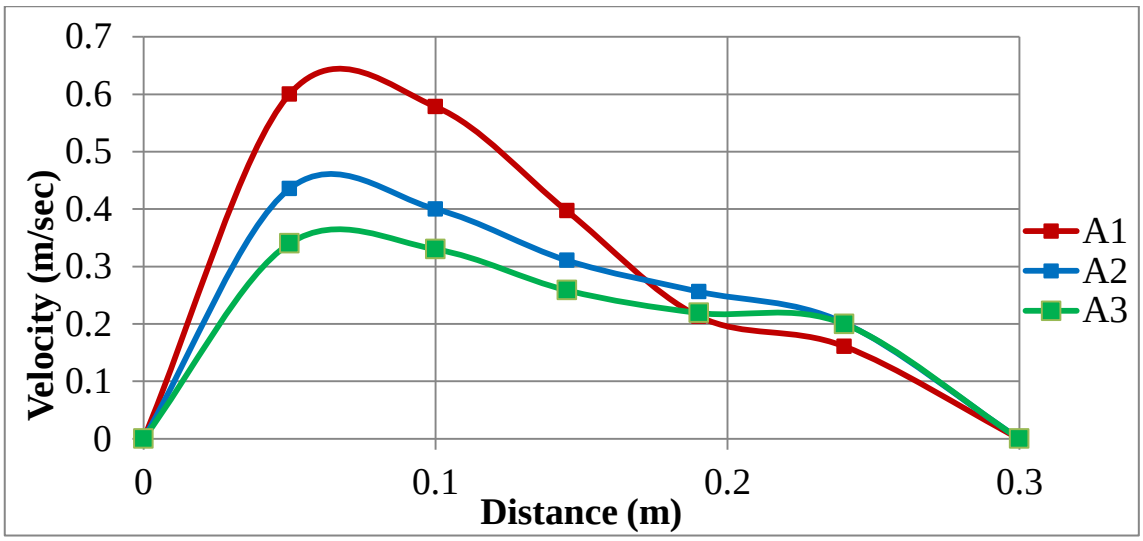

(e) Fr_1=6.50

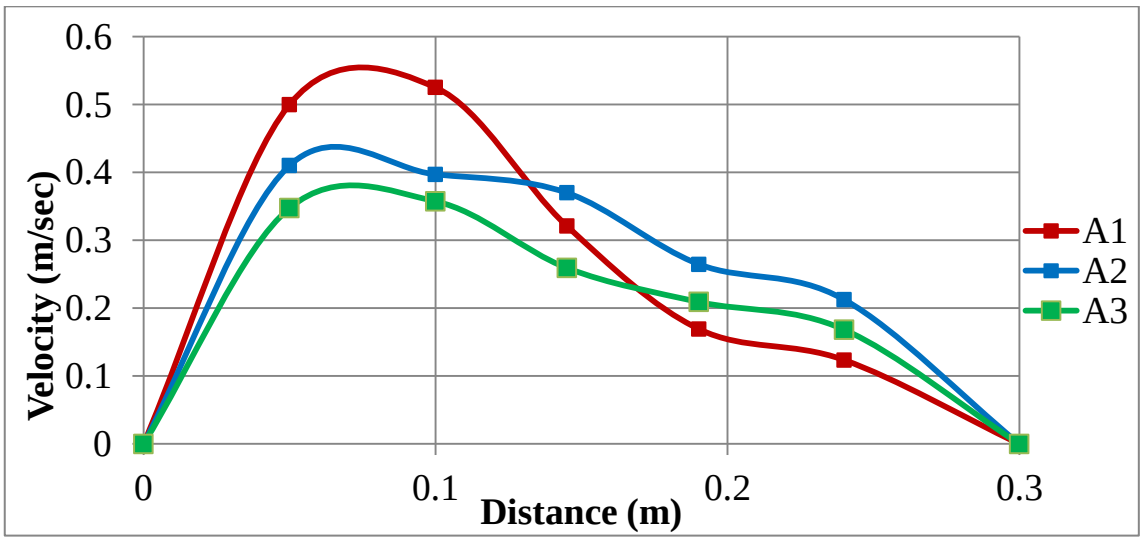

(f) Fr_1=7.75

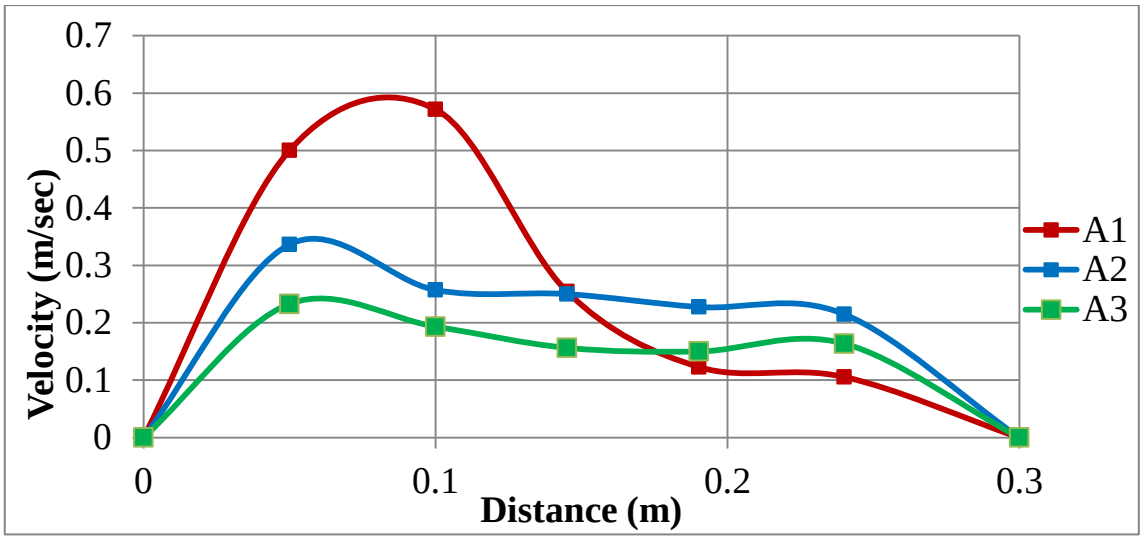

(g) Fr_1=8.50

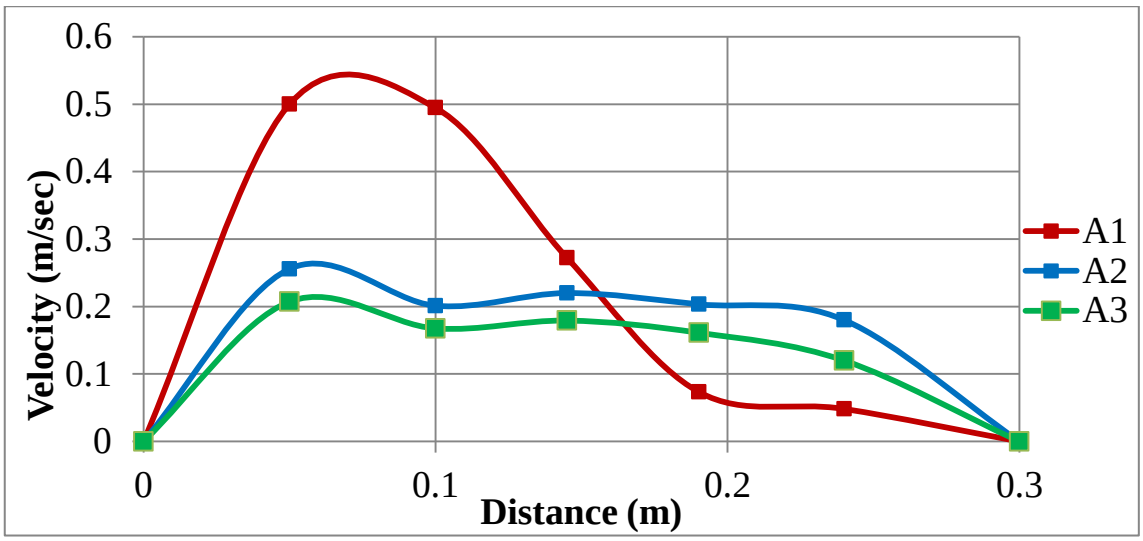

(h) Fr_1=9.25

Figure 4.6: (a to h) Transverse velocity distribution for triangle block configurations A1, A2 and A3 under Fr_1 (2.75-9.25).

4.3.2 Triangle Block Sequent Depth Ratio

As mentioned previously, equipping the bed of the channel that contains the hydraulic jump by appurtenances (e.g., triangle blocks) eventually has an appreciable effect through the decrease in the sequent depth ratio (y_2/y_1). This decrease is a pointer to the hydraulic performance improvement. Figure (4.7) shows the variation of the sequent depth ratio (y_2/y_1) with the initial Froude number for all models of configurations A, B

and C. In this figure the line that represents the sequent depth ratio of a free jump of the Belanger equation is also shown. As observed from the figure, generally, the sequent depth ratio in the rough bed stilling basin (i.e. equipped with a triangle block) for all blockage ratios was smaller than that achieved for the classical jump (Belanger equation). However, the configuration-C1 gives a better performance in reducing the sequent depth (y_2) compared to the other configurations. The observations refer that this configuration has led to lengthening the roller region. This, consequently, increases energy dissipation. However, it increases from the length of the stilling basin.

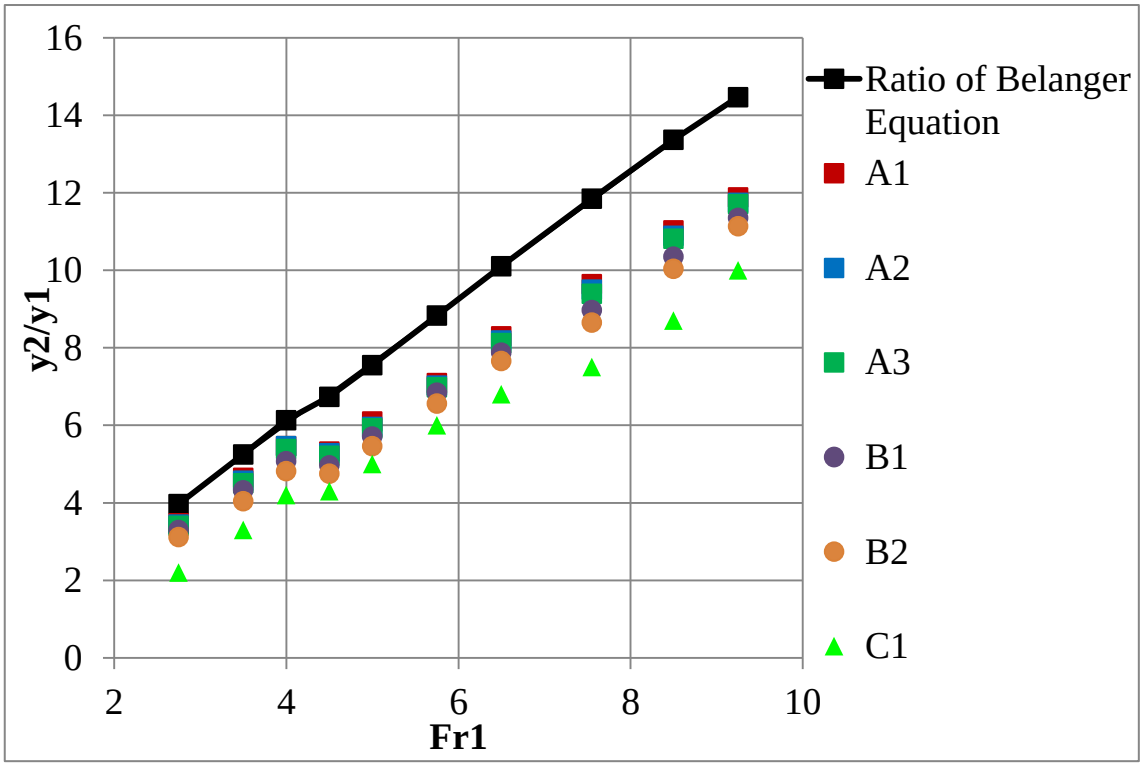

Figure 4.7: Sequent depth ratio for all configurations of triangle blocks.

4.4 Stepped Block Results

4.4.1 Stepped Block Velocities

The comparison between the results is shown in Figures (4.8 and 4.9). It is evident through these figures that better results were achieved by using

A3 in terms of reducing the depth ratio and reducing the velocities in width, which provided more uniformity in distribution, with the range of Froude number 2.75-9.25. However, good stability of the hydraulic jump was observed when using A3, while this feature was semi-difficult to achieve by using both A1 and A2.

The performance with the configuration of model A3 can be attributed to the closer distance between the stepped blocks of configuration A3.

More turbulence was observed, which lead to the dissipation of more energy and, therefore, reduced sequent depth y_2. On the other hand, there is a greater possibility to divide the incoming flow into almost equal sections, suggesting more regularity in the distribution of velocity, especially with higher Froude numbers. This efficient performance of configuration A3 leads to its further use in other run series as opposed to using both A1 and A2.

It is important to note that this type of block (Stepped block) is characterized by reducing the velocities compared to the baffle block and triangle block, as it can be seen that there is a decrease in velocities up to (73-85) % for most of the used configurations (A1, A2, A3, B1, B2 and C1).

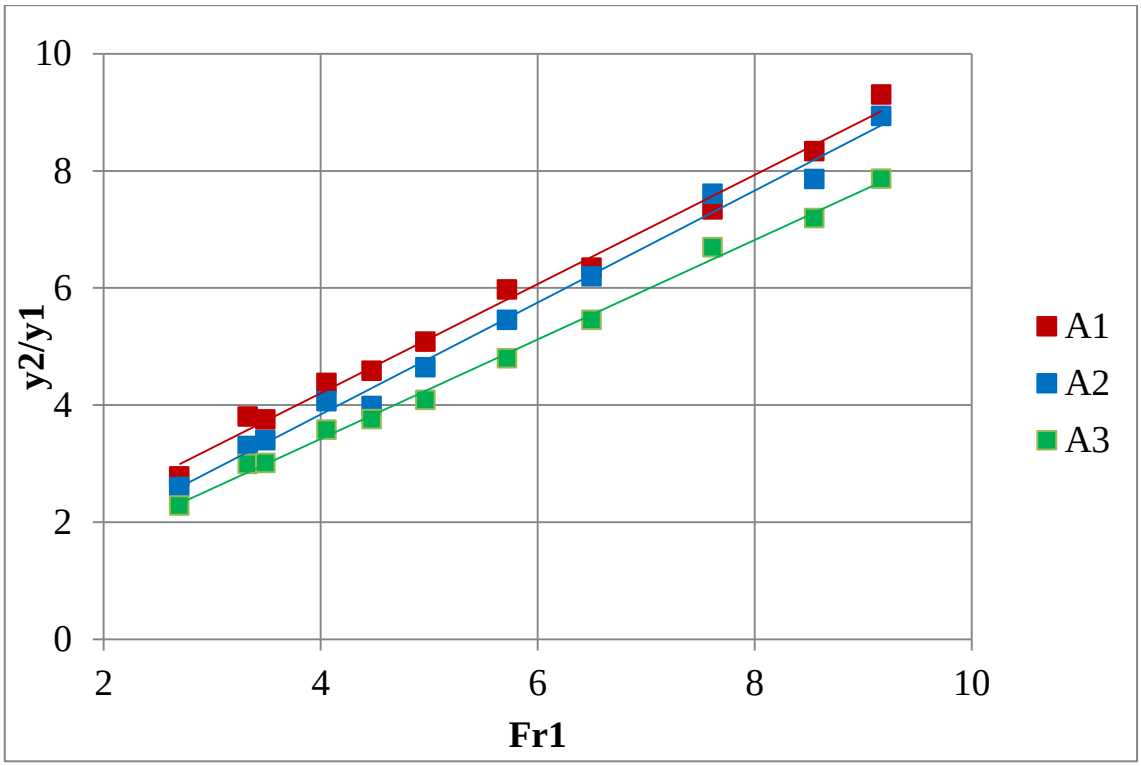

Figure 4.8: The variation of y_2/y_1 with stepped block configurations of single row.

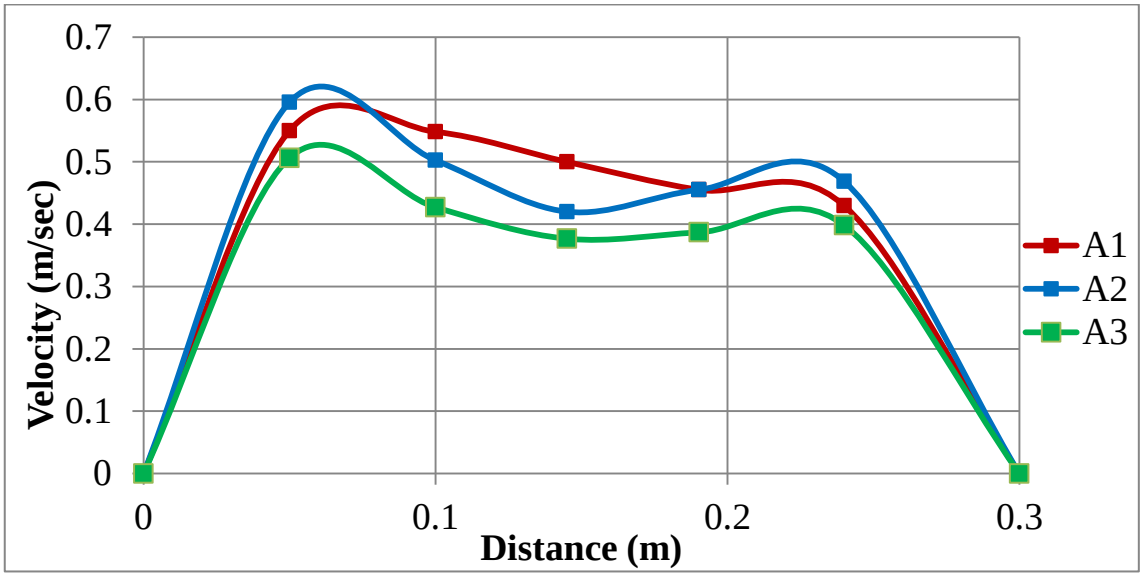

(a): Fr_1=2.750

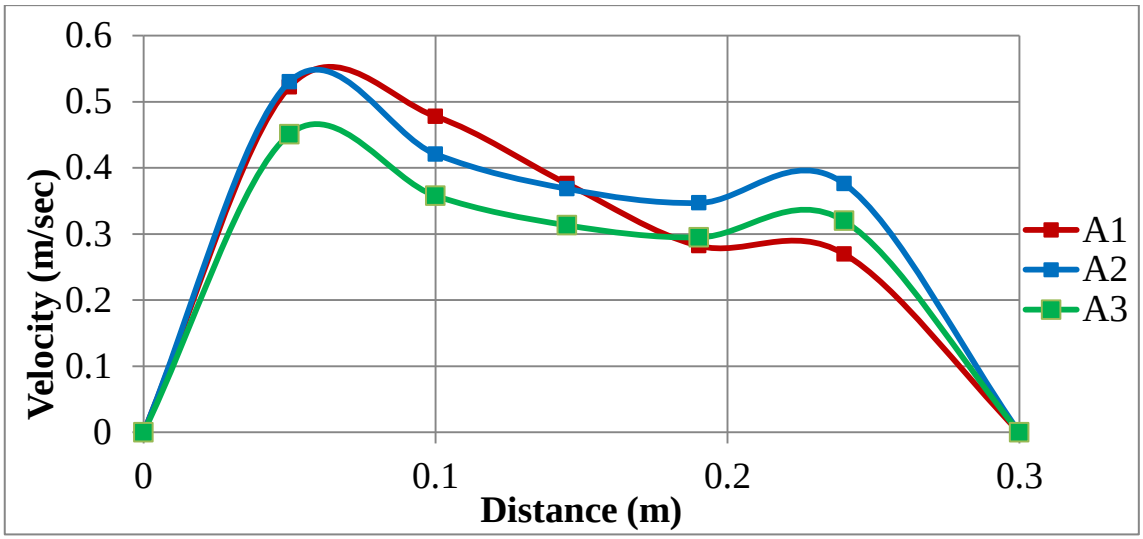

(b): Fr_1=3.50

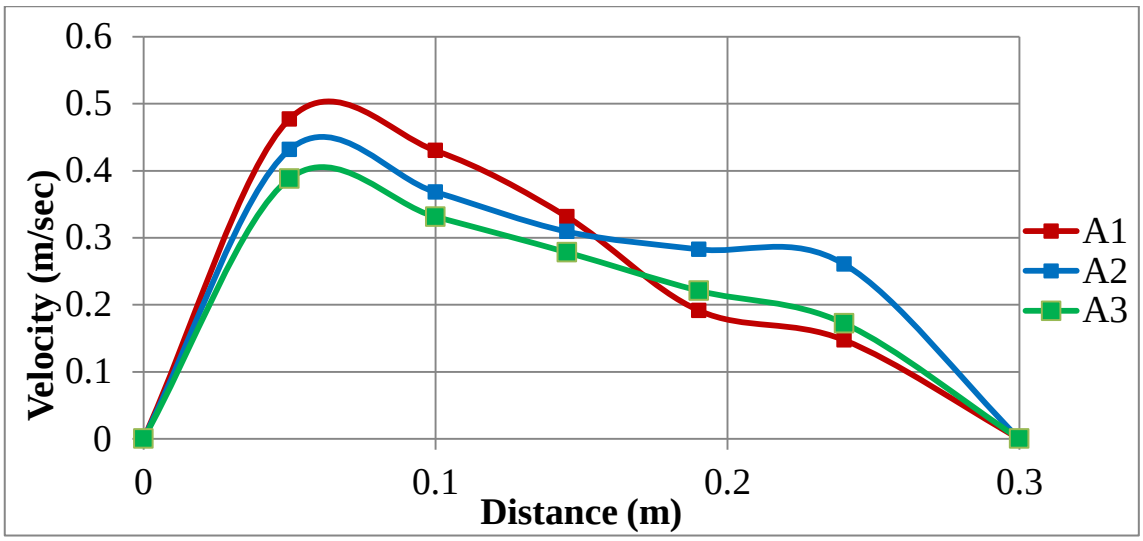

(c) Fr_1=4.50

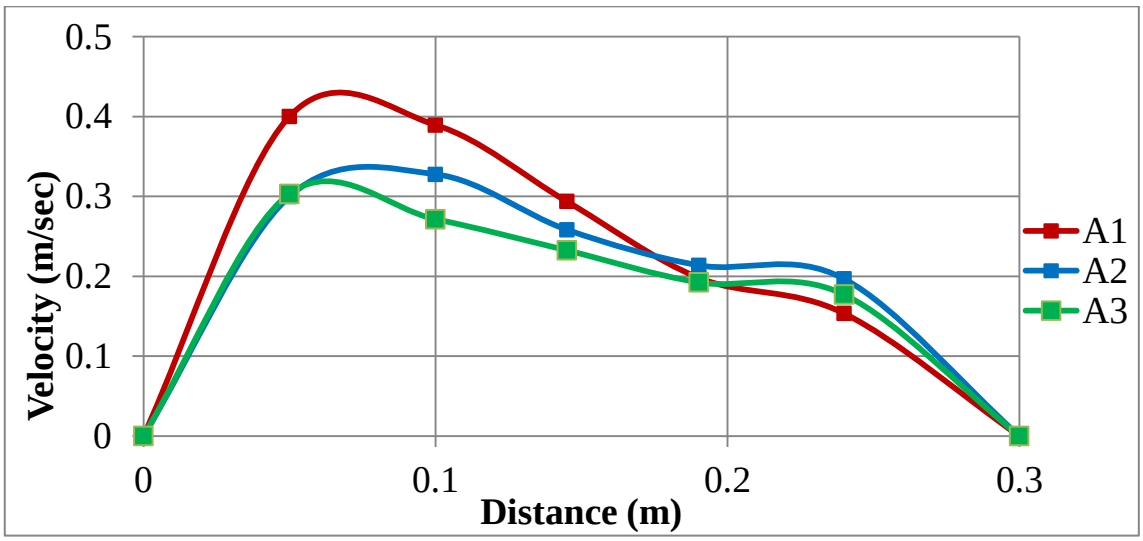

(d) Fr_1=5.75

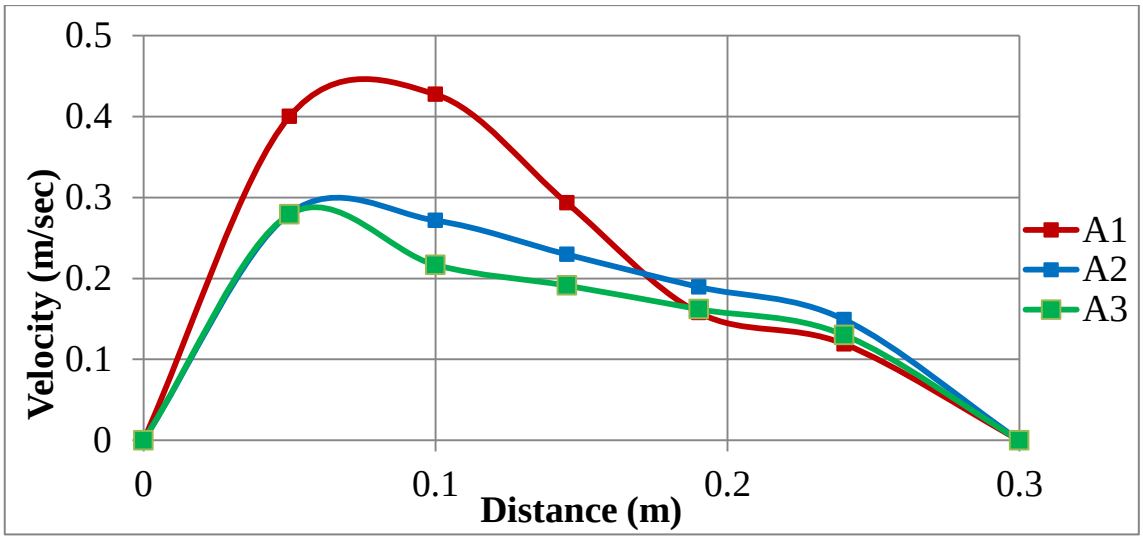

(e) Fr_1=6.50

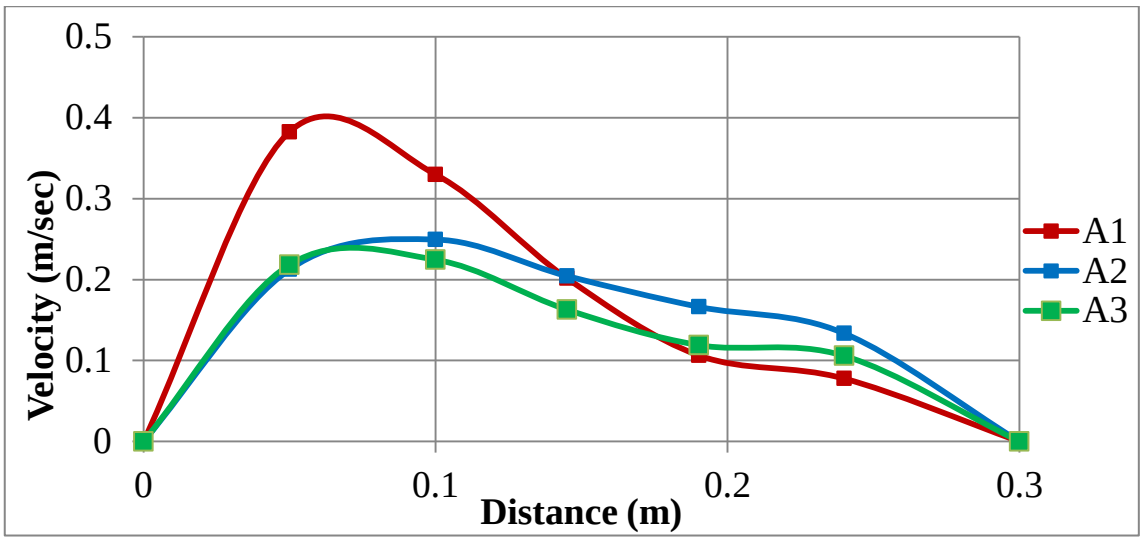

(f) Fr_1=7.75

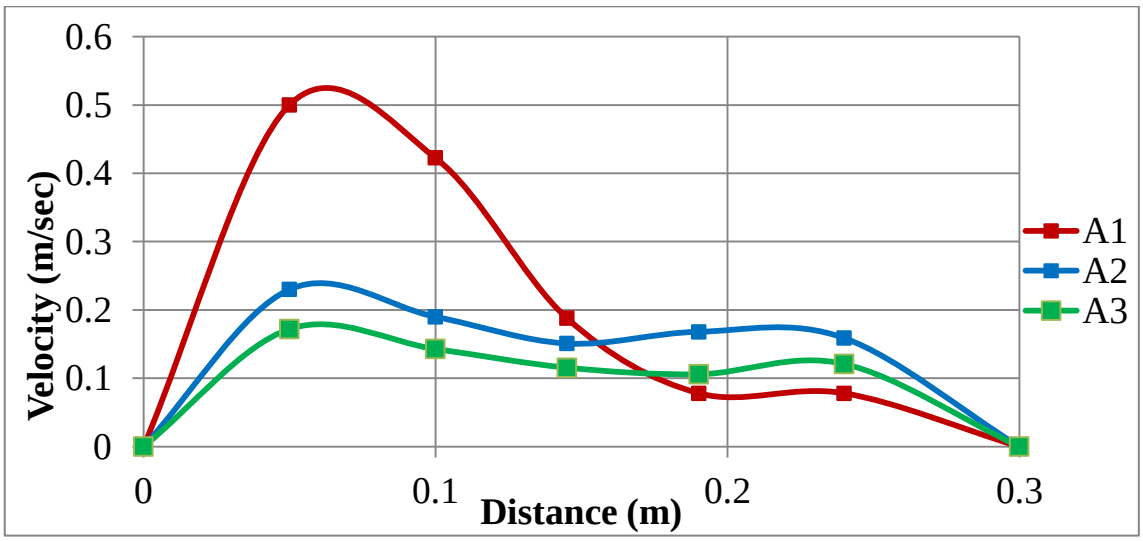

(g) Fr_1=8.50

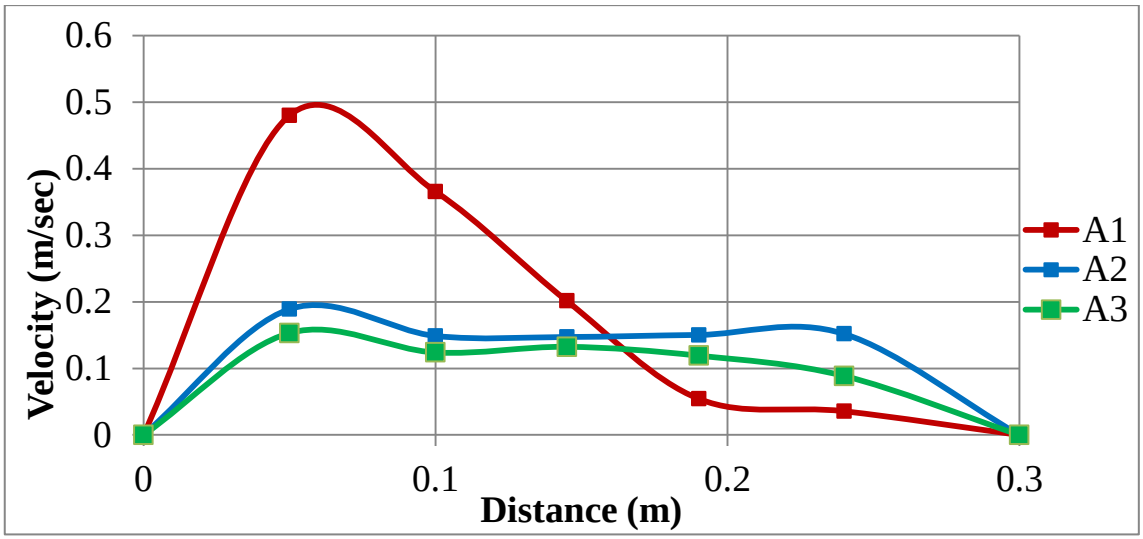

(h) Fr_1=9.25

Figure 4.9: (a to h) Transverse velocity distribution for stepped block configurations A1, A2 and A3 under Fr_1 (2.75-9.25).

4.4.2 Stepped Block Sequent Depth Ratio

As mentioned previously, equipping the bed of the channel that contains the hydraulic jump by appurtenances (e.g., triangle blocks) eventually has an appreciable effect through the decrease in the sequent depth ratio (y_2/y_1). This decrease is a pointer to the hydraulic performance improvement. Figure (4.10) shows the variation of the sequent depth ratio (y_2/y_1) with the initial Froude number for all models of configurations A, B and C. In this figure, the line that represents the sequent depth ratio of a free jump of the Belanger equation is also shown. As observed from the figure, generally, the sequent depth ratio in the rough bed stilling basin (i.e. equipped with a stepped block) for all blockage ratios was smaller than that achieved for the classical jump (Belanger equation). However, the configuration-C1 gives a better performance in reducing the sequent depth (y_2) compared to the other configurations. The observations refer that this configuration has led to lengthening the roller region. This, consequently, increases energy dissipation. However, it increases from the length of the stilling basin.

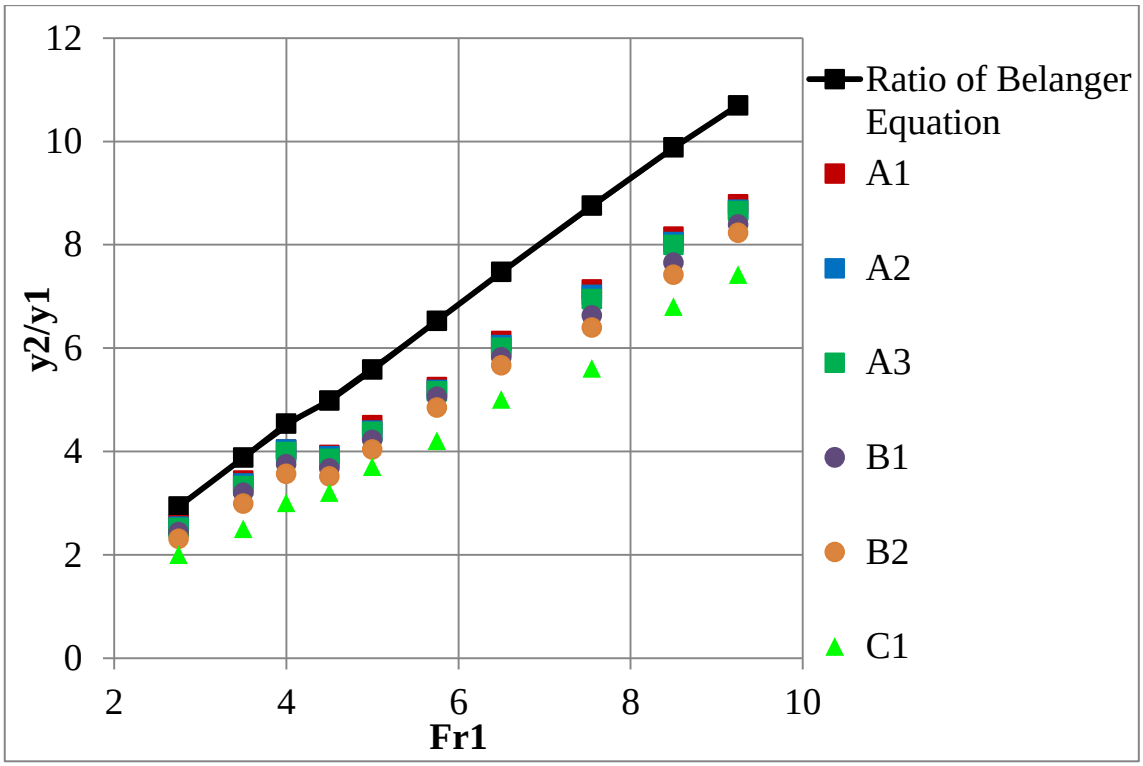

Figure 4.10: Sequent depth ratio for all configurations of stepped blocks.

4.5 Relative Dissipation of Energy and Efficiency

The performance of the forced hydraulic jump can be measured by noting the increase in the amount of kinetic energy dissipation. There are two indicators for its good performance: the relative loss of energy ΔE/E1 and the efficiency E2/E1. Where ΔE is a difference between the specific energy at the supercritical flow before jump E1 (at the location of y_1) and the specific energy at the subcritical flow after jump E2 (at the location of sequent depth y_2). The higher value of the first term indicates the great percentage of energy dissipation through the jump. However, the less value of the second indicator refers to better efficiency of energy dissipation. These two indicators have been calculated for all configurations adopted in this study, and the average value for each model is listed in Table (4.1). As evident from the values, the higher loss of energy with high efficiency has been achieved by using configuration C1.

Table 4.1: Average values of the relative loss of energy and efficiency of force hydraulic jump with different configurations undertaken.

Relative loss	Single row			Two row		Three row
	A1	A2	A3	B1	B2	C1
ΔE/E1 (%)	50.9	52.75	55.56	59.24	63.45	69.88
E2/E1 (%)	48.2	47.5	45.45	42.55	40.64	37.85

4.6 Transverse Local Velocity Distribution

The Local velocity over the flume bed has been measured by the current meter across the flume width at the end section of the jump to show the feature of velocity distribution transversely. Ninety-nine runs were conducted with used block configurations installed for testing. The aim is to get a uniform distribution of velocity across the width at the end of the stilling basin along with reducing its value. Approaching this aim is considered a positive indicator in terms of minimizing the ability to scour and preventing its negative effect downstream.

Figure (4.11) illustrates the lateral velocity distribution with different block configurations with the incoming Froude number range of 2.5-9.25. the results showed a little disagreement both in the amounts and features of velocity distribution between single and double rows. However, with the double-row configurations, the velocity tends towards the uniform distribution across the channel width. The most symmetrical distribution along with the less amount of velocity registers with the use of configuration A1 and to a lesser degree, with A2 and A3. Whereas at a higher Froude number (within a range of steady jump), the inverse situation was observed, and the best distribution was registered with configurations B1 and B2.

Even though the configuration-C1's values appear to be higher than those seen with the other configurations, the velocity distribution when employing it tends to become more uniform throughout the breadth across the whole range of flow. By limiting the concentration of the flow at one side, which, if it happens, increases the risk of the collapse, this has relevance for reducing the possibility of scour downstream.

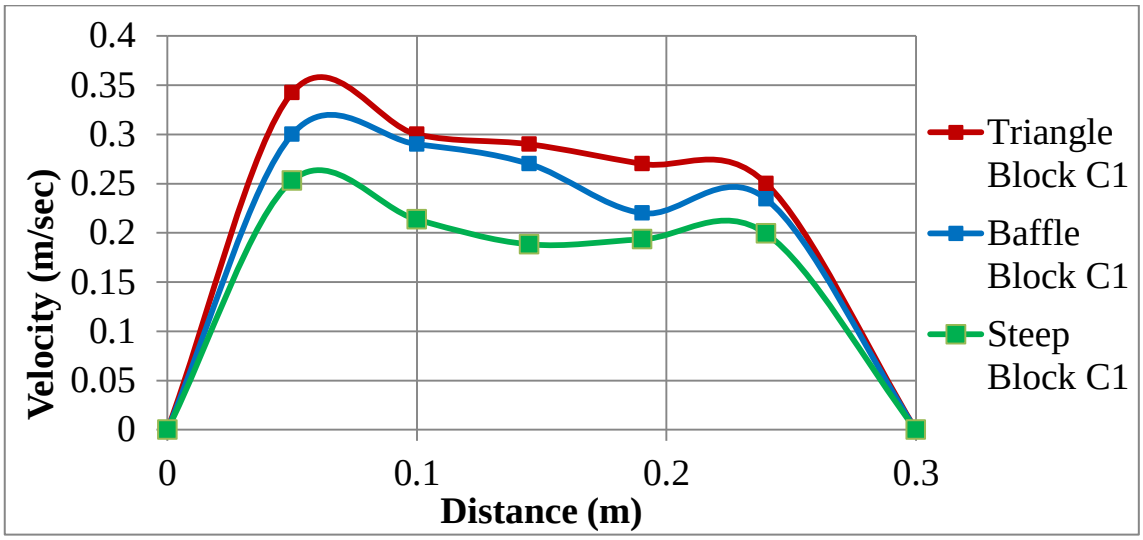

(a): Fr_1=2.750

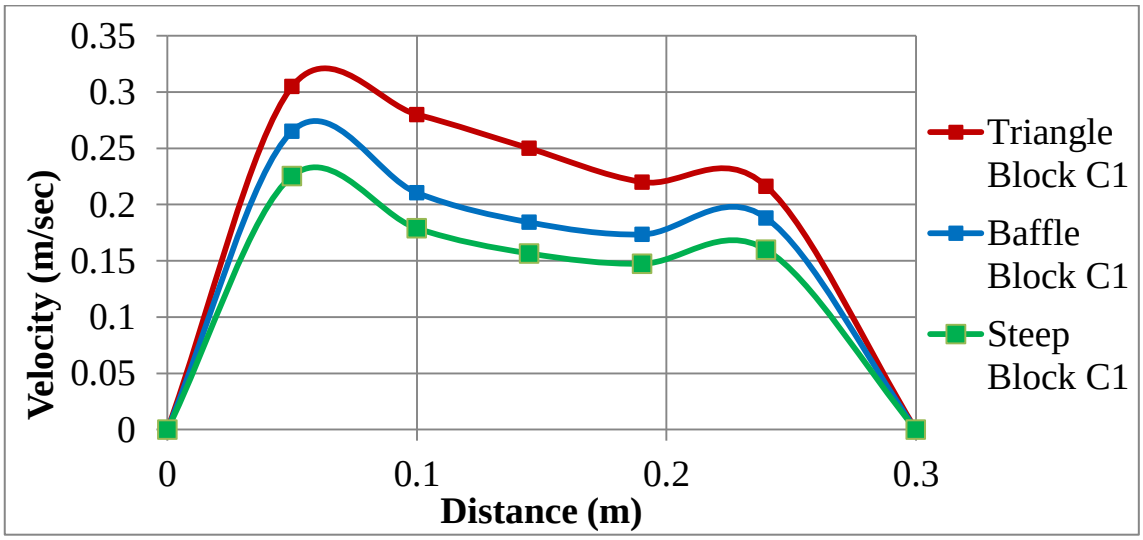

(b): Fr_1=3.50

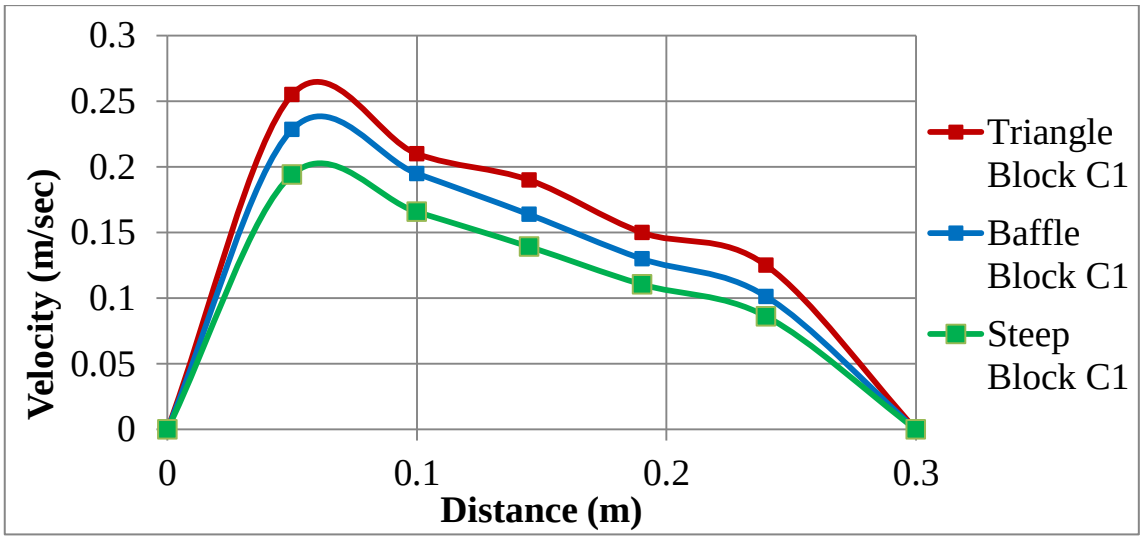

(c) Fr_1=4.50

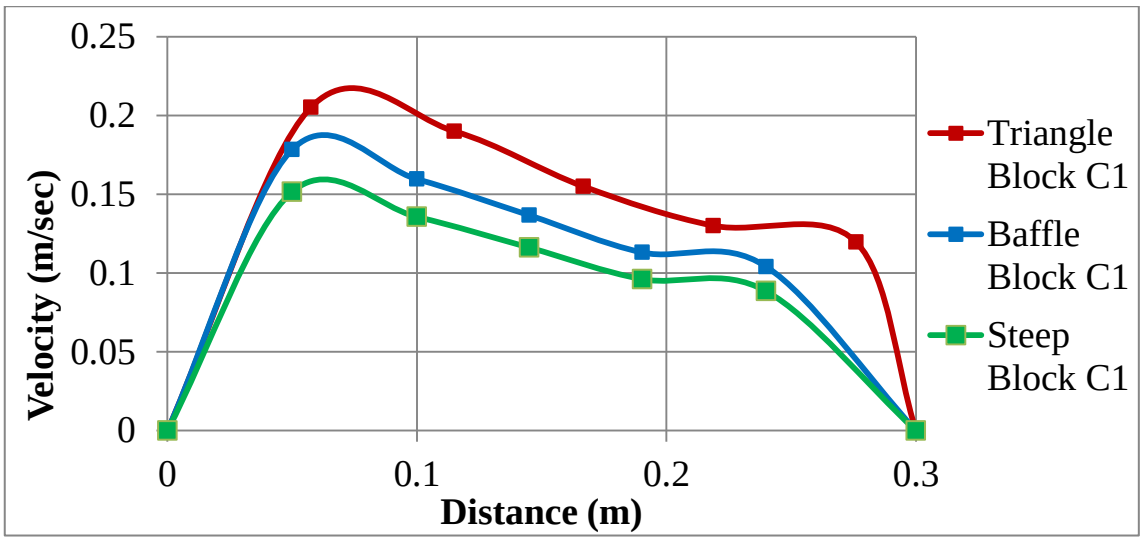

(d) Fr_1=5.75

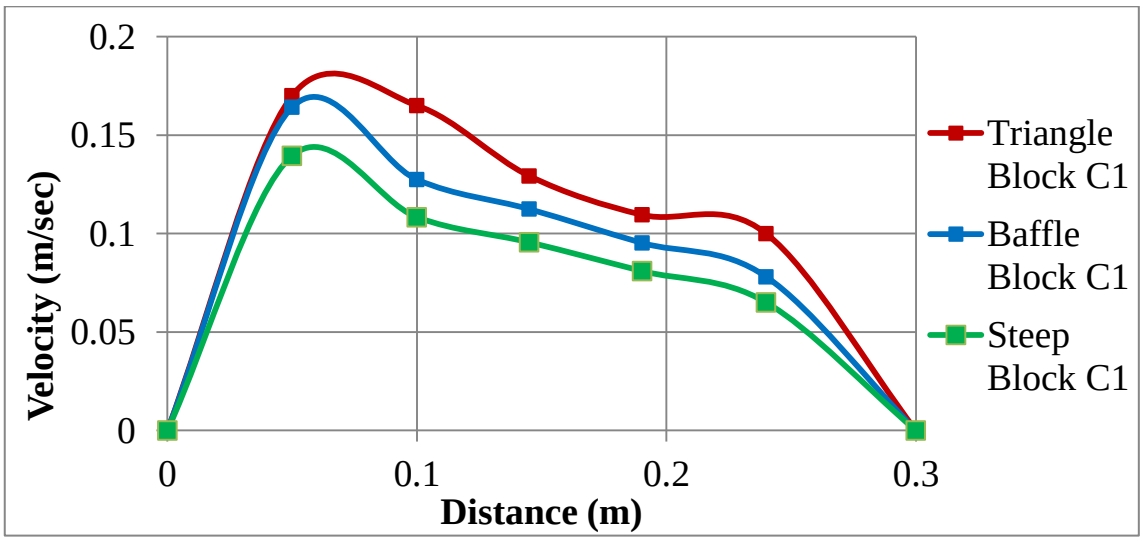

(e) Fr_1=6.50

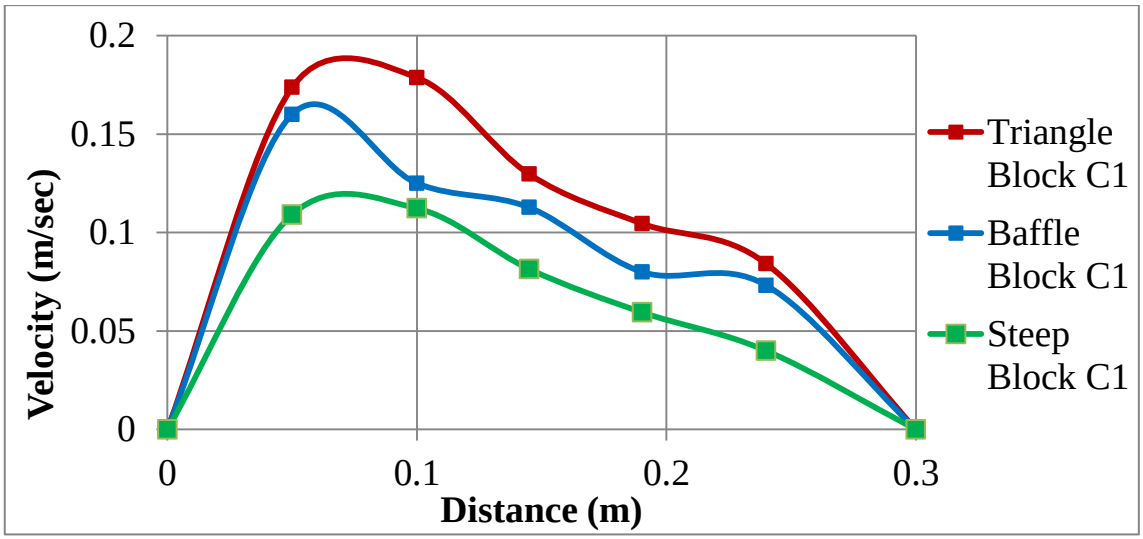

(f) Fr_1=7.75

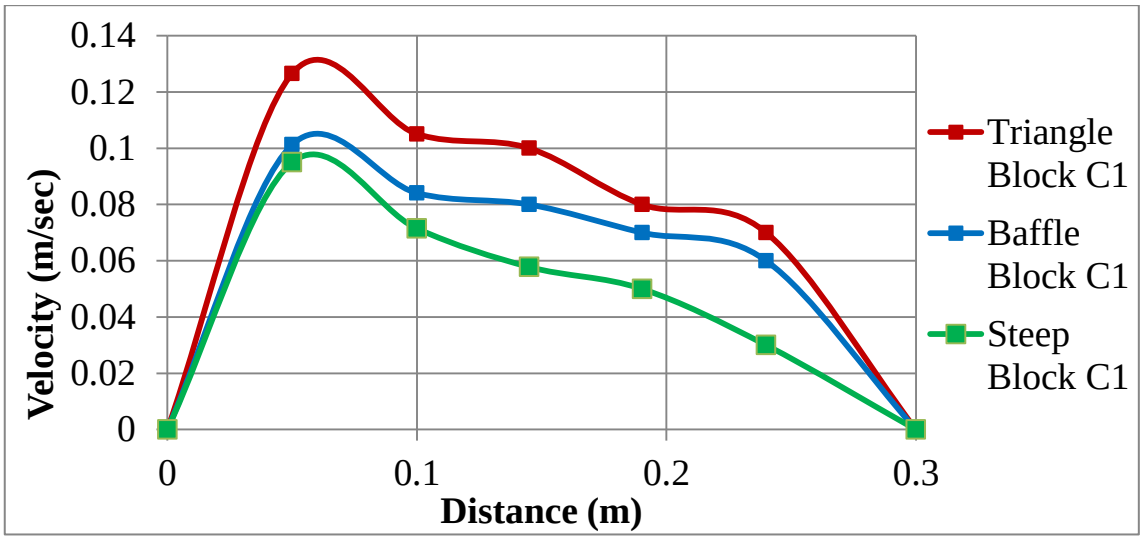

(g) Fr_1=8.50

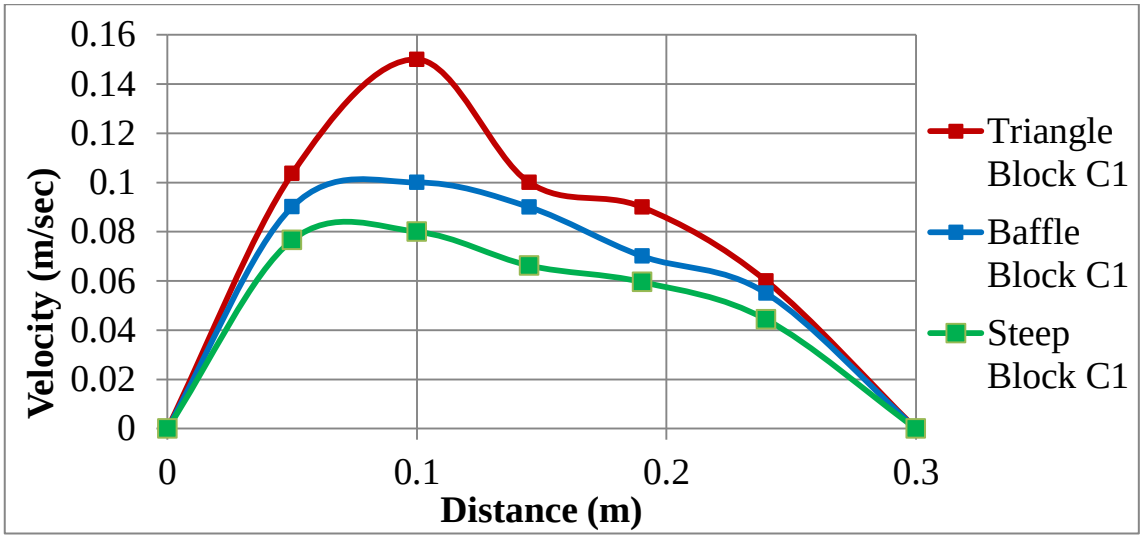

(h) Fr_1=9.25

Figure 4.11: (a to h) Variation of transverse local velocity with different configurations for steady jump Fr_1under (2.750-9.25).

4.7 Stilling Basin With End Sill

The hydraulic characteristics of the jump are measured and compared with the classical hydraulic jump under variable discharges. The results of the experiments confirmed the significant effect of the sill on the dissipation of energy. The five quantitative measured discharges are gauged by the bend for each of the end-sill models.

The parameters of the hydraulic jump measured are upstream depth (y_1) and downstream depth (y_2), velocities (V_1 and V_2), energy dissipated with the hydraulic jump ΔE, sediment height Δs, sediment affected length L_s, minimum sediment affected length L_{min}, water depth at upstream Yup, and water depth at downstream Y_d. The result of hydraulic jump characteristics measurement for the three previously mentioned tests (A1, A2 and A3).

By analyzing the results, it can be said that the use of type A3 increases the height of the water column upstream, which reduces the velocity on the same side, and thus reduces the effects of the hydraulic jump and reduces soil erosion in the stilling basin. It can be concluded from the results that the proposed type (A3) is better than the other two types A2 and A1 in terms of reducing soil erosion and hydraulic jump effects (Figures 4.12 to 4.19).

However, it is possible to notice that there is a relatively large amount of runoff that eroded a considerable amount of soil behind the stilling basin, as presented in Figure (4.19). This in itself needs other studies to reduce these effects.

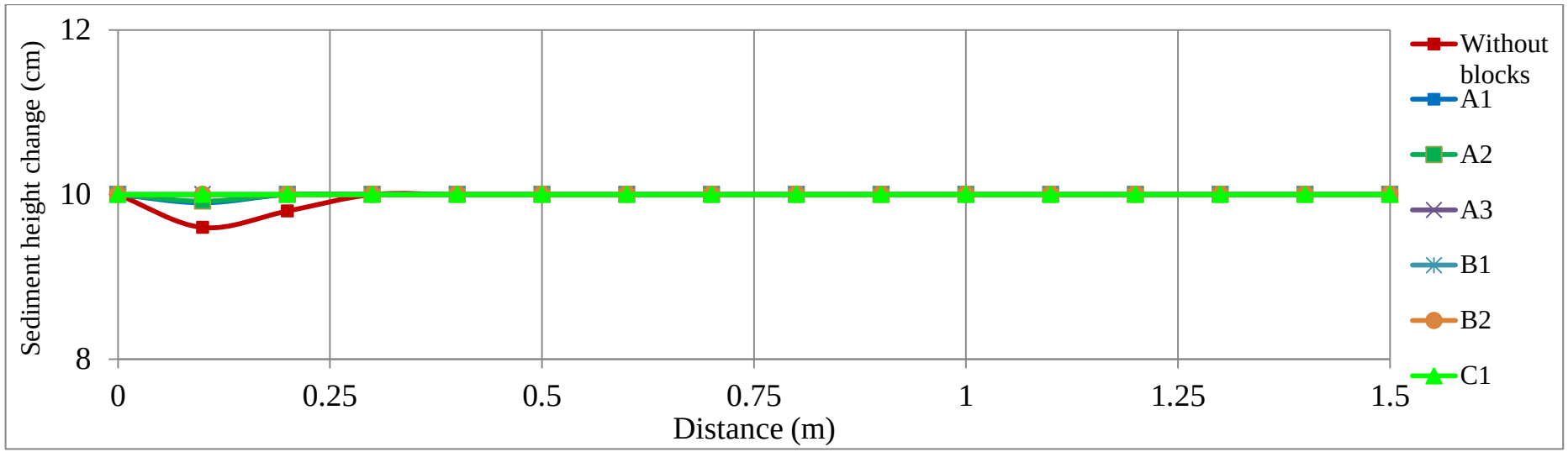

Figure 4.12: Scour profiles at downstream flows of stilling basin under Fr_1=2.75.

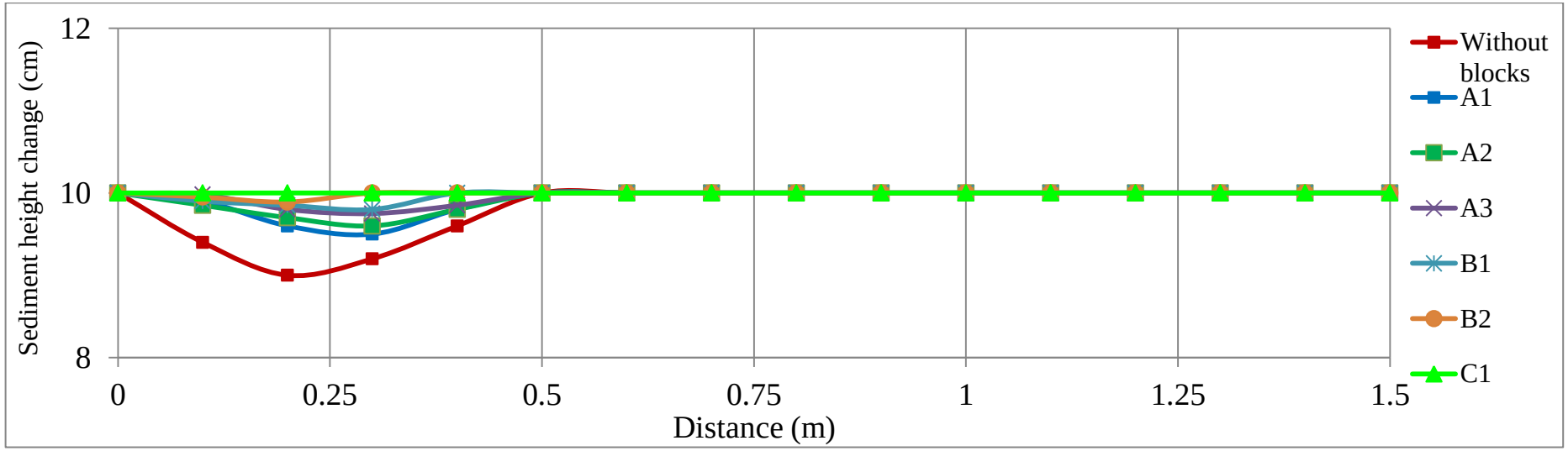

Figure 4.13: Scour profiles at downstream flows of stilling basin under Fr_1=3.5.

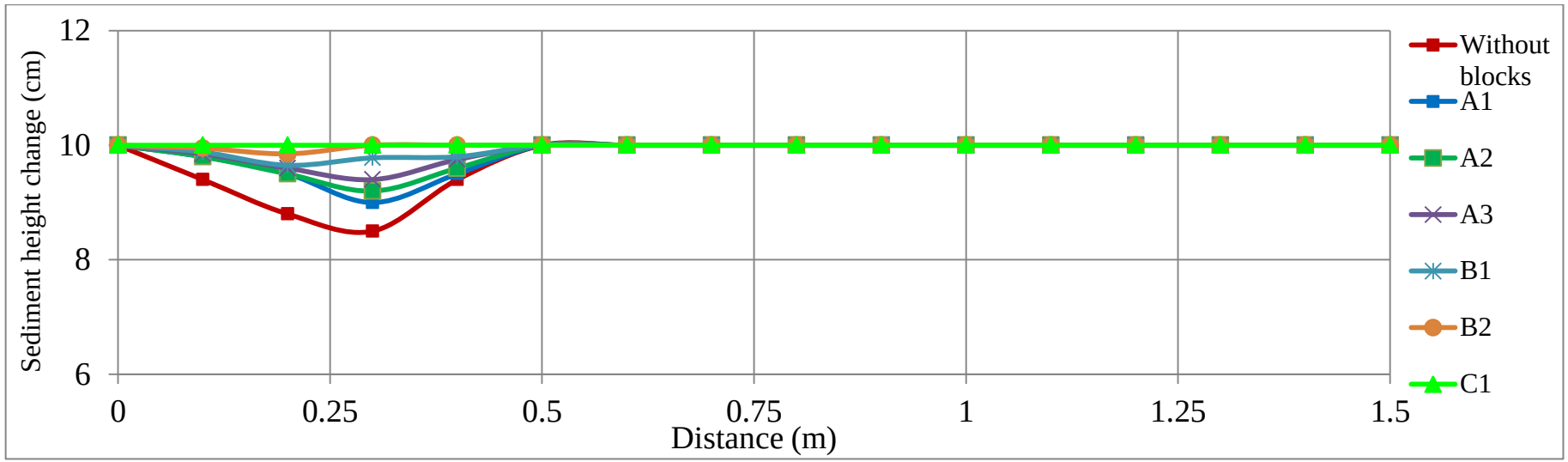

Figure 4.14: Scour profiles at downstream flows of stilling basin under Fr_1=4.5.

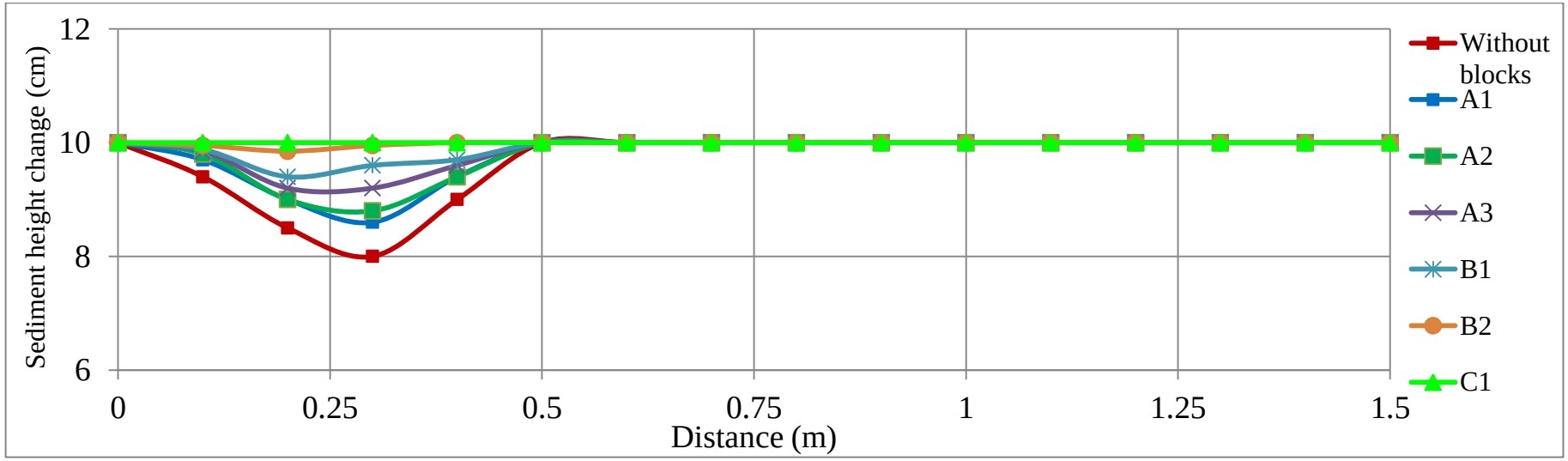

Figure 4.15: Scour profiles at downstream flows of stilling basin under Fr_1=5.75.

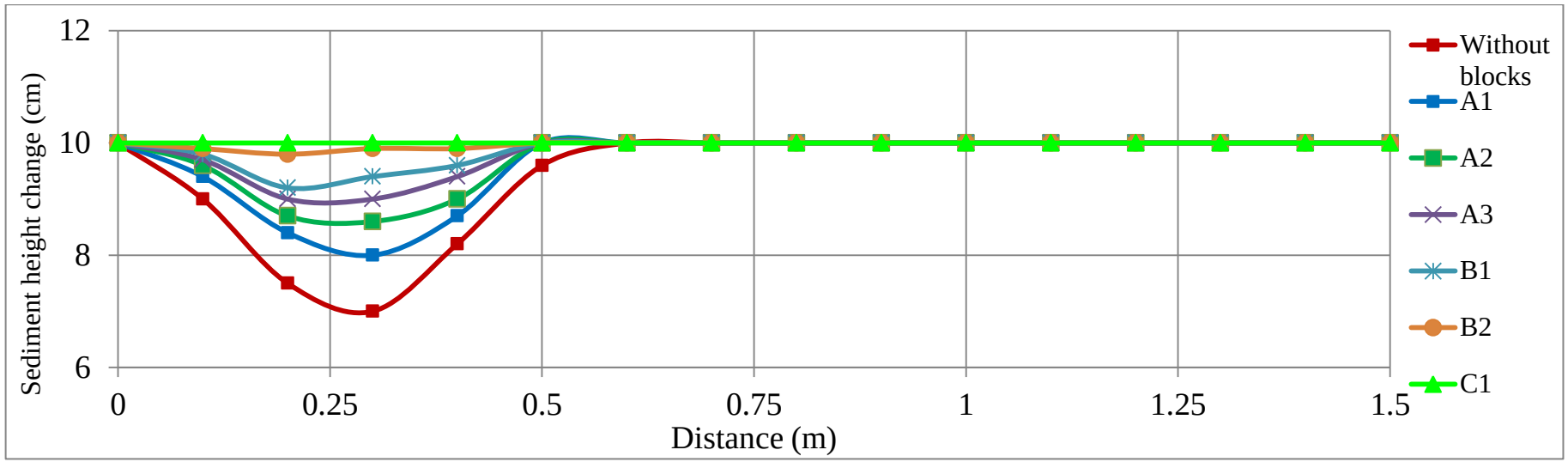

Figure 4.16: Scour profiles at downstream flows of stilling basin under Fr_1=6.5.

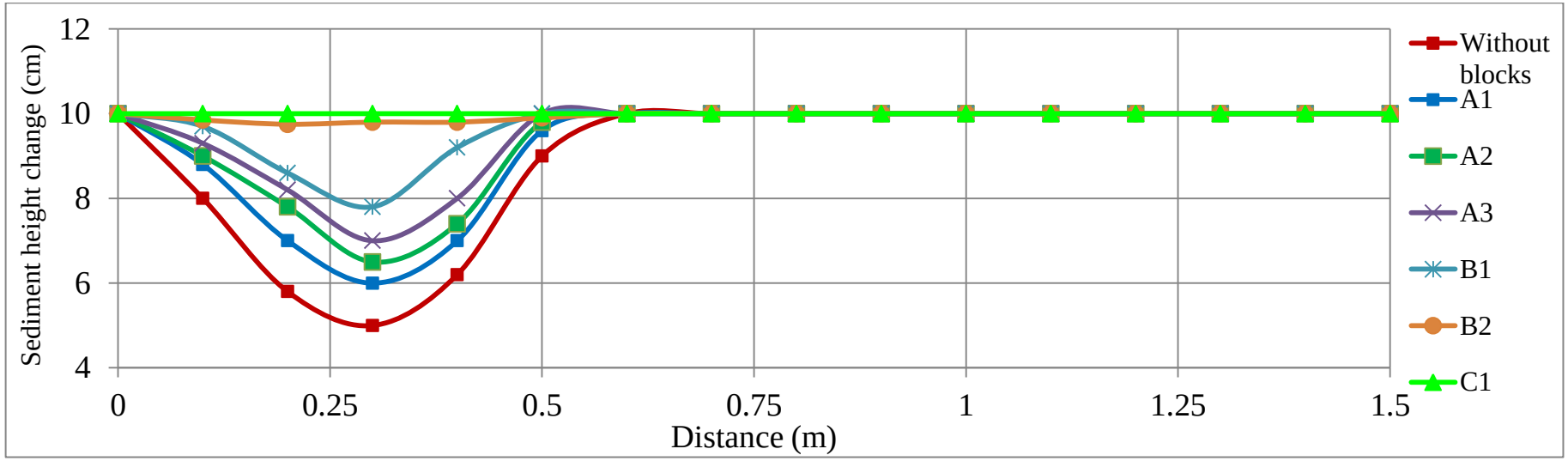

Figure 4.17: Scour profiles at downstream flows of stilling basin under Fr_1=7.75.

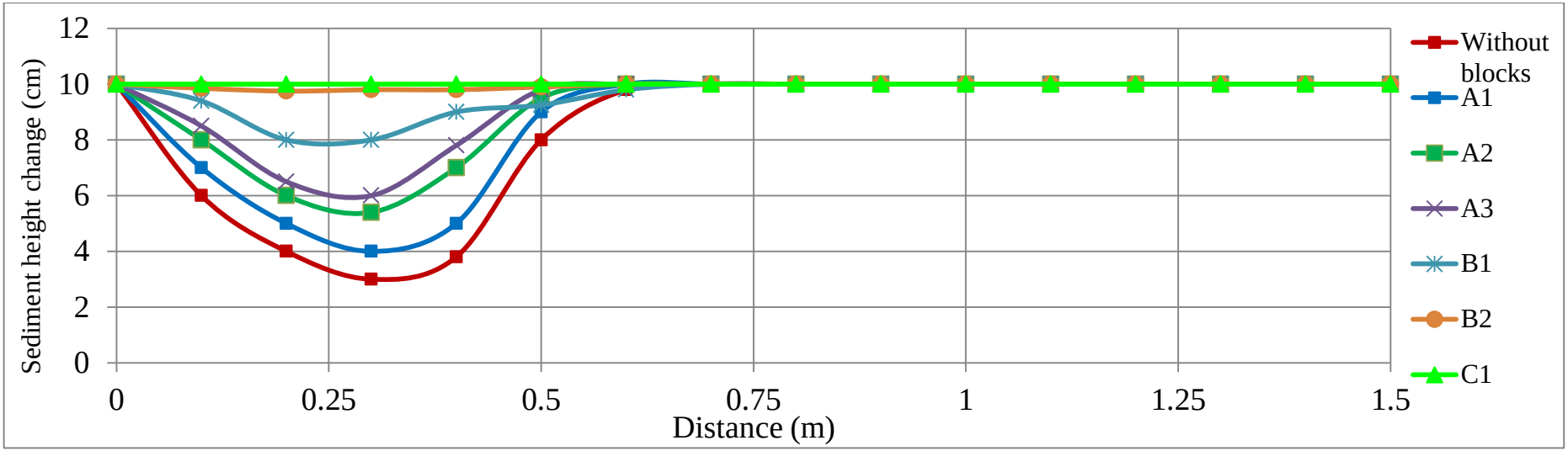

Figure 4.18: Scour profiles at downstream flows of stilling basin under Fr_1=8.5.

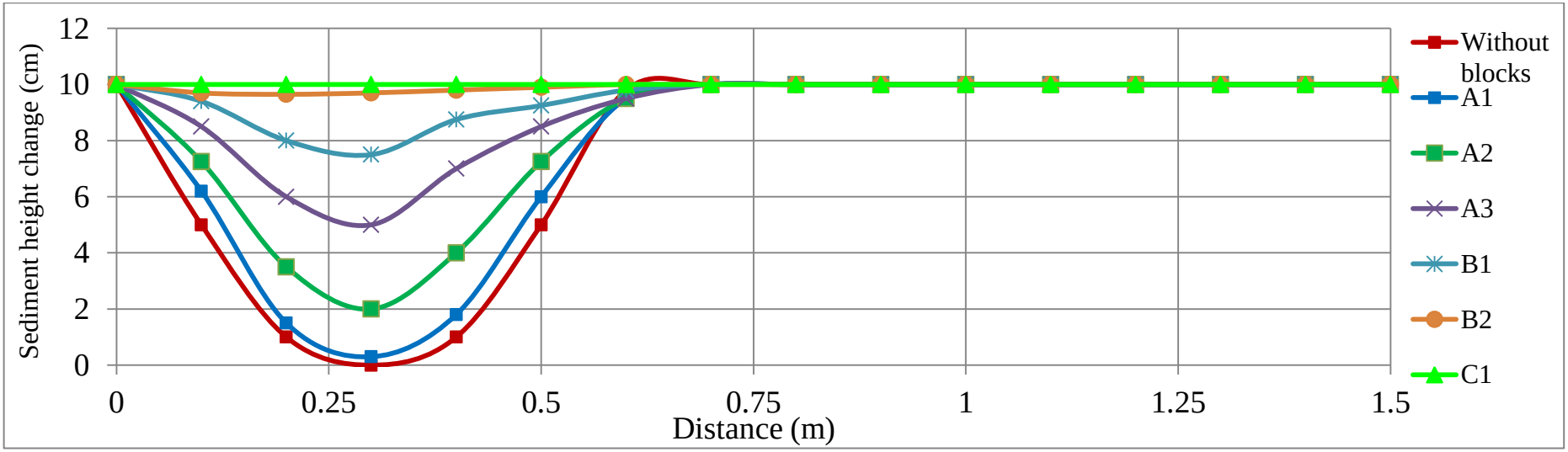

Figure 4.19: Scour profiles at downstream flows of stilling basin under Fr_1=9.25.

CHAPTER FIVE

CONCLUSIONS AND RECOMMENDATIONS

5.1 General

Experimental modelling plays a capital role in the design and analysis of hydraulic structures. However, this often necessitates physical models, considered the most established form of hydraulic modelling, to ensure reasonable accuracy of the results. This study was devoted to carrying out experimental tests to select the most efficient type of blocks for improving the characteristics of a hydraulic jump such as depth ratio, transverse velocity distribution, and scour downstream of the stilling basin. To achieve this objective, three distinct ogee spillway configurations (baffle block, block, triangle and stepped block) were adopted with different proposed distributions (A1, A2, A3, B1, B2 and C1) as comparison baseline.

Based on the results obtained from both experimental models, conclusions are presented and recommendations for future research are conducted in this chapter.

5.2 Conclusions

1. Baffle block distribution (A3) appeared with good results of reducing flow velocities and hydraulic jump within the stilling basin, compared with A1 and A2 distributions, especially with the range of Froude number 4.5-9.25.
2. The variation of the sequent depth ratio (y_2/y_1) with the initial Froude number for all baffle block distributions A, B, and C, proved that block distribution C1 was efficient in decreasing the sequent depth ratio compared to the other distributions.

3. The utilization of the A3 triangle block distributions proved that this distribution produces a uniform flow along the stilling basin, with a range of 5.75–9.25 of the Froude number.
4. The triangle block fails to reduce the flow velocity compared to the Baffle block type, as it can be seen that there is an increase in flow velocities up to 1.15% for most of the used configurations (A1, A2, A3, B1, B2, and C1).
5. The comparison between the stepped block distribution (A1, A2 and A3), cleared that the A3 distribution appeared with better results in reducing the sequent depth ratios and the flow velocities.
6. The stepped block is characterized by reducing the flow velocities compared to the baffle block and triangle block, as it can be seen that there is a decrease in velocities up to 0.85% for all used distributions.
7. The transverse local velocity distribution across the flume width when using the C1 distribution tends to become more uniform across the width while these values seem greater than those that were observed with the other distributions.
8. Compared with A1 and A2 distributions, the A3 distribution is distinct with reduces the velocity on the stilling basin upstream and thus reduces the effects of the hydraulic jump and soil erosion downstream of the stilling basin.
9. According to the results of scour, hydraulic jump, and energy dissipation in the stilling basin, C1 was distinguished in improving mentioned items, followed by the distribution of B2, B1, A3, A2 and A1, respectively.

5.3 Recommendations

1. This study sought to validate the uncontrolled ogee spillway hydraulics using experimental works. The same validation is advised for a

controlled ogee spillway to examine the usage of flume in the design and testing procedures of this particular kind.

2. Other types of turbulence models should be assessed to determine their capabilities for turbulence and multiphase modelling.

References

Abdel-Mageed, N. B., Mobasher, A., Abdul-Muttalib, M. A., and Salih, M. H. (2019). Review of The Energy Dissipation Over Stepped Weir. *Engineering Research Journal-Faculty of Engineering (Shoubra)*, *42*(1), 132-137.

Abdul-Mehdi, T. R., Al-Mussawy, H. A., and Al-Madhhachi, A. S. T. (2016). A laboratory study attempt of flow and energy dissipation in stepped spillways. *Journal of Engineering*, *22*(12), 48-64.

Al Zubaidy, R. Z., Khedher, K. I., and Darweesh, A. N. (2016). Energy Dissipation on the Ogee Spillways by Using Direction Diverting Blocks. *Journal of Engineering*, *22*(3), 77-88.

Al-Husseini, T. (2015). Experimental study of increasing energy dissipation on stepped spillway. *journal of kerbala university*, *11*(1), 87-100.

Alwan, H. H., Kamonna, H. H., and Hashim, N. A. (2016). Evaluation of local scour development downstream an apron of different angles for an ogee spillway. *Kufa Journal of Engineering*, *7*(3).

Al-Zubaidy, R., Al-Murshidi, K. R., and Khlif, T. H. (2014). Energy dissipation by using different sizes and configurations of direction diverting blocks on spillways. *Journal of Babylon University/Engineering Sciences*, (2).

Asadi, M. E., Naeeni, S. T. O., and Kerachian, R. (2022). The effects of splitters on the downstream scour hole of overflow spillways: application of support vector regression. *Water Supply*, *22*(2), 1905-1929.

Aydin, M. C., and Ulu, A. E. (2018). Effects of different shaped baffle blocks on the energy dissipation and the downstream scour of a

regulator. *Bitlis Eren University Journal of Science and Technology*, *8*(2), 69-74.

Azmathullah, H. M. D., Deo, M. C., and Deolalikar, P. B. (2006). Estimation of scour below spillways using neural networks. *Journal of Hydraulic Research*, *44*(1), 61-69.

Baghal, S. R., and Khodashenas, S. R. (2022). Fuzzy risk-based technique for the design of an ogee spillway in a diversion dam based on hydrological return period discharge and the resistance-load theory. *Journal of Hydrology*, 129004.

Banerjee, D. (2018). *Numerical modelling of ogee spillway hydrualics using cfd and its validation through physical model tests* (Doctoral dissertation).

Bhajantri, M. E., and Deolalikar, P. (2006). Hydrodynamic modelling of flow over a spillway using a two-dimensional finite volume-based numerical model. *Sadhana*, 743-754.

Blight, G. E., Robinson, M. J., and Diering, J. A. (2010). The Flow of Slurry from a breached tailings dams. *Journal of The South African Institute of Mining and Metallurgy*, Johannesburg.

Brater, F. E., King, W. H., Lindell, J., and Wei, Y. C. (1996). *Handbook of Hydraulics.* New York: MC Graw - Hill.

Chanson, H. (2002). *The Hydraulics of stepped chutes and spillways.* Lisse, Netherlands: Balkema.

Chanson, H. (2004). Air-water flows in water engineering and hydraulic structures. Basic processes and metrology. *Proceedings of the international conference on hydraulics of dams and River structures*, (pp. 3-21). Tehran - Iran.

Chanson, H. (2022). Energy dissipation on stepped spillways and hydraulic challenges—Prototype and laboratory experiences. *Journal of Hydrodynamics*, *34*(1), 52-62.

Chatila, J., and Tabbara, M. (2020). Finite Analytic Method in Flows and Heat Transfer. *Computers and Structures 82*, 1805-1812.

Chow, V. T. (1959). *Open-Channel Hydraulics.* New York: McGraw Hill Book Company INC.

Chung, T. (2002). Computational fluid dynamics. *The press syndicate of the University of Cambridge*, 1036.

Daneshfaraz, R., Ghaderi, A., Akhtari, A., and Di Francesco, S. (2020). On the effect of block roughness in ogee spillways with flip buckets. *Fluids*, *5*(4), 182.

Ellayn, A. F., and Sun, Z. L. (2012). Hydraulic jump basins with wedge-shaped baffles. *Journal of Zhejiang University SCIENCE A*, *13*(7), 519-525.

Elnikhely, E. A. (2018). Investigation and analysis of scour downstream of a spillway. *Ain Shams Engineering Journal*, *9*(4), 2275-2282.

Eloubaidy, A. F., Al-Baidhani, J. H., and Ghazali, A. H. (1999). Dissipation of hydraulic energy by curved baffle blocks. *Pertanika Journal Science Technology*, *7*(1), 69-77.

Foroudi, A., and Barati, R. (2022). Experimental study of cavitation index in an ogee spillway by considering convergence angle of sidewalls. *Water Supply*, *22*(6), 5729-5738.

Frizell K.W. and Svoboda C.D. 2012. “Performance of Type III Stilling Basins – Stepped Spillway Studies”Hydraulic Laboratory Report HL-2012-02, US Bureau of Reclamation, Denver, USA.

Frizell K.W. and Svoboda C.D. 2012. “Performance of Type III Stilling Basins – Stepped Spillway Studies”Hydraulic Laboratory Report HL-2012-02, US Bureau of Reclamation, Denver, USA.

Ghaderi, A., Abbasi, S., and Di Francesco, S. (2021). Numerical study on the hydraulic properties of flow over different pooled stepped spillways. *Water*, *13*(5), 710.

Ghaderi, A., Daneshfaraz, R., Torabi, M., Abraham, J., and Azamathulla, H. M. (2020). Experimental investigation on effective scouring parameters downstream from stepped spillways. *Water supply*, *20*(5), 1988-1998.

Hariri-Ardebili, M. A., and Nuss, L. K. (2018). Seismic risk prioritization of a large portfolio of dams: Revisited. *Advances in Mechanical Engineering*, *10*(9), 1687814018802531.

Hong, S. H., Kim, S. J., Sturm, T. W., Stoesser, T., and González-Castro, J. A. (2010). Effect of low tailwater during drought on scour conditions downstream of an ogee spillway. *River Flow 2010*, 1193-1200.

ICOLD. (2001). Risk of Dangerous occurences: Lessons learnt from practical experiences. *Bulletin of Tailings Dams*.

Jafari-Asl, J., Seghier, M. E. A. B., Ohadi, S., and Plevris, V. (2021). Soft computing framework for the uncertainty-based optimization of the length and height of ogee-crested spillway.

Jamel, A. A. J. (2018). Numerical simulation for estimating energy dissipation over different types of stepped spillways and evaluate the performance by Artificial Neural Network. *Tikrit Journal of Engineering Sciences*, *25*(2), 18-26.

Khatsuria, R. (2005). *Hydraulics of spillways and energy disspators.* New York: Marcel Dekker.

Kositgittiwong, D. (2012). *Validation of numerical model of flow behaviour through smooth and stepped spillways using Large - Scale Physical model.* Thon Buri: King Mongkut's University of Technology Thon Buri.

Kote, A. S., and Nangare, P. B. (2019). Hydraulic model investigation on stepped spillway's plain and slotted roller bucket. *Engineering, Technology and Applied Science Research*, *9*(4), 4419-4422.

Kuriqi, A., Koçileri, G., and Ardiçlioğlu, M. (2020). Potential of Meyer-Peter and Müller approach for estimation of bed-load sediment transport under different hydraulic regimes. *Modeling Earth Systems and Environment*, *6*(1), 129-137.

Lihe, J., Mazin, E., Natalya, S., Dudley, R., and Sukumar, A. (2011). Ruskin Dam spillway shocrete assessed. *Concrete Internationwithpermission of American Concrete Institute*, 7.

Loftin, M. (1999). *Water Resources Engineering",.* The McGraw-Hill Companies, Inc.

Lueker M.L., Mohseni O., Gulliver J.S., Schulz H. and Christopher R.A. 2008. "The Physical Model Study of the Folsom Dam Auxiliary Spillway System" University of Minnesota, St. Anthony Falls Laboratory Project Report 511, Minneapolis, Minnesota.

Maatooq, J. S. (2006). Stepped spillway hydraulic model investigation. *Tikrit Journal of Engineering Sciences*, *13*(3), 103-120.

Maatooq, J., and Taleb, E. (2018). The effects of baffle blocks locations and blockage ratio on the sequent depth and velocity distribution of forced hydraulic jump.

Mohammed, J. R., and Qasim, J. M. (2012). Comparison of one-dimensional HEC-RAS with two-dimensional ADH for flow over

trapezoidal profile weirs. *Caspian Journal of Applied Sciences Research*, *1*(6), 1-12.

Mohtar, W. H. M. W., Sharil, S., Samion, M. K. H., Mohamad, M. F., Hamzah, S. B., Razali, S. F. M., ... and Desa, S. M. (2020). Assessment of dam appurtenant structures under multiple flow discharge scenarios. *Ain Shams Engineering Journal*, *11*(4), 913-922.

Morales, V., Tokyay, T. E., and Garcia, M. (2012). Numerical modeling of ogee crest spillway and tainter gate structure of a diversion dam on Canar River, Ecuador. In *INTERNATIONAL CONFERENCE ON WATER RESOURCES CMWR* (Vol. 19).

Muhsun, S. S., and Al-Sharify, Z. T. (2018). Experimental work and CFD model for flowrate estimating over ogee spillway under longitudinal slope effect. *International Journal of Civil Engineering and Technology*, *9*(13), 430-439.

Murrone, A., and Villedieu, P. (2011). Numerical Modeling of Dispersed Two-Phase Flows. *Aerospace Lab*.

Nabil B., and Rezak A.A. 2002. "Effect of Baffle Blocks with Sloping Front Face on the Length of the Jump"Journal of Civil Engineering the Institute of Engineers, Bangladesh 30(2):101-108.

Nasralla, T. H. (2022). Experimental and numerical investigation of scour downstream contracted spillways. *Journal of Water and Land Development*, 53-59.

Nikseresht, A., Alishahi, M., and Emdad, H. (2008). Complete Flow Field Computation around an ACV (Air Cushion Vehicle) Using 3-D VOF with Lagrangian Propagation in Computational Domain. *Computer and structures Vol. 86, ,* No7-8.

Nou, M. R. G., Zolghadr, M., Bajestan, M. S., and Azamathulla, H. M. (2021). Application of ANFIS–PSO hybrid algorithm for predicting the dimensions of the downstream scour hole of ski-jump spillways. *Iranian Journal of Science and Technology, Transactions of Civil Engineering*, *45*, 1845-1859.

Peltier, Y., Dewals, B., Archambeau, P., Pirotton, M., and Erpicum, S. (2018). Pressure and velocity on an ogee spillway crest operating at high head ratio: experimental measurements and validation. *Journal of Hydro-environment Research*, *19*, 128-136.

Peterka, A. J., (1978). "Hydraulic Design of Stilling Basins and Energy Dissipators." United States Department of the Interior, Bureau of Reclamation, Engineering Monograph No. 25, Denver CO, 4th revised printing.

Rajaa, A. I., and Kamela, A. H. (2020). Performance study of fluent-2D and flow-3D platforms in the CFD modeling of a flow pattern over ogee spillway. *Anbar Journal for Engineering Sciences*, *8*(4), 317-328.

Ribeiro, D. B., Simões, A. L. A., Da Luz, L. D., Mangieri, L. S. G., and Schulz, H. E. (2020). Stability of solids in stepped flume nappe flows: Subsidies for human stability in flows. *Journal of Applied Fluid Mechanics*, *14*(3), 681-690.

Saki, N., and Shafai Bejestan, M. (2022). Experimental Investigation of the Wedge-Shaped Deflector Installation Position Effects on the Flip Bucket Spillway Energy Dissipation. *Journal of Hydraulics*, *17*(2), 87-106.

Salmasi, F. (2021). Effect of downstream apron elevation and downstream submergence in discharge coefficient of ogee weir. *ISH Journal of Hydraulic Engineering*, *27*(4), 375-384.

Samadi, M., Jabbari, E., Azamathulla, H. M., and Mojallal, M. (2015). Estimation of scour depth below free overfall spillways using multivariate adaptive regression splines and artificial neural networks. *Engineering Applications of Computational Fluid Mechanics*, *9*(1), 291-300.

Saneie, M., SheikhKazemi, J., and Azhdary Moghaddam, M. (2016). Scale effects on the discharge coefficient of ogee spillway with an arc in plan and converging training walls. *Civil Engineering Infrastructures Journal*, *49*(2), 361-374.

Savage, M., and Johnson, M. (2001). Flow over Ogee Spillway: Physical and Numerical model Case Study. *Journal of Hydraulic Engineering 127(8)* , 640-649.

Şentrürk, F. (1994). *Hydraulics of Dams and reservoirs.* Toulouse: Water ressources publications.

Sorensen, R.M. 2020. “Stepped Spillway Hydraulic Model Investigation.” Journal of Hydraulic Engineering, ASCE, 111(12): 1461-1472.

Tuna, M. (2012). "Effect Of Offtake Channel Base Angle Of Stepped Spillway On Scour Hole." Iranian Journal of Science and Technology. Transactions of Civil Engineering 36.

U.S.B.R. (1973). *Design of Small Dams.* United States Department of Interior - Bureau of Reclamation.

U.S.B.R. (1987). *Design of Small Dams.* United States Department of Interior - Bureau of Reclamation.

Ulu, A. E., Aydın, M. C., and Işık, E. (2021). Energy dissipation potential of flow separators placed in spillway flip bucket. *Advanced Engineering Science*, *2*, 60-66.

USACE. (1990). *Hydraulic design of spillways.* Washington: Department of the U.S Army corps of Engineers.

Valero, D., Bung, D. B., and Crookston, B. M. (2018). Energy dissipation of a Type III basin under design and adverse conditions for stepped and smooth spillways. *Journal of Hydraulic Engineering*, *144*(7), 04018036.

Versteeg, H., and Malalasekera, W. (2007). *An introduction to Computational Fluid Dynamics: The finite volume method*. England: Prentice Hall.

Wendet, F. J. (2009). *Computational Fluid Dynamics: An Introduction, 3rd Edition*. Eagle River, WI, USA: Springer.

Wilhelms, S. C., and Gulliver, J. S. (2005). Bubbles and waves description of self-aerated spillway flow. *Journal of hydraulic research*, *43*(5), 522-531.

Yildiz, A., Yarar, A., Kumcu, S. Y., and Marti, A. I. (2020). Numerical and ANFIS modeling of flow over an ogee-crested spillway. *Applied Water Science*, *10*(4), 1-10.

Young, M.F. 2022. "Feasibility Study of a Stepped Spillway." Proceedings, Hydraulics Division Speciality Conference, ASCE, New York, 96-106.

المستخلص

يعتبر مفيض (Spillway) تصريف المياه أحد أهم مكونات السد لضمان السلامة أثناء الفيضان. يعد تحديد الخصائص الهيدروليكية لمجرى المفيض مسألة صعبة لأنه يتعرض لأنواع مختلفة من الجريان طوال فترة خدمته. يعتبر مفيض أوجي (Ogee) أهم أنواع مجاري الصرف ، نظرًا لاستخدامه على نطاق واسع في العديد من السدود الترابية والخرسانية ، فضلاً عن أنه يحتاج إلى تفاصيل تصميم دقيقة ومعقدة. مشكلة النحر (Scour) الناتجة عن حركة الماء في مناطق المصب للهياكل الهيدروليكية هي مشكلة شائعة. من أجل منع حدوث هذا النحر، يتم وضع أنواع مختلفة من مشتتات الطاقة في اتجاه مجرى النهر للهياكل الهيدروليكية، خاصة في أحواض السكون (Stilling Basin). تلعب عوامل متنوعة مثل نوع الرواسب وسرعة تيار الجريان ونظام التدفق دورًا مهماً في معالجة النحر والتعرية. لذلك من المهم جداً تبديد طاقة الماء المتدفق قبل الالتقاء بالرواسب.

تهدف الدراسة الحالية إلى تقليل كمية النحر التي تحدث في اتجاه مجرى مفيض أوجي باستخدام أشكال هندسية مختلفة للكتل مثل كتلة الحاجز (Baffle block)، والكتلة المثلثية (Triangle block ، والكتلة المتدرجة (Stepped block). تم توزيع هذه الكتل في حوض السكون بثلاثة أنواع مقترحة جديدة للتوزيعات، مثل صفوف واحد ، وصفان ، وثلاثة صفوف.

تم فحص عمليات التدفق والنحر على قناة التصريف في المختبر كأعمال تجريبية.

تم اختبار كل تكوين وفقًا لأرقام Froude التي تتراوح من 2.75 إلى 9.25 حيث تم جعل القفزة الهيدروليكية ضمن وصف القفزة المتذبذبة والثابتة. خلال الاختبارات ، تم قياس العمق المتسلسل وتوزيع السرعة العرضية. تمت مقارنة النتائج تبعاً للتوزيعات المقترحة للكتل وتمت مناقشة النتائج في هذا الصدد.

أظهرت النتائج أن تكوين البلوك الحاجز ظهر بنتائج جيدة في تقليل سرعات التدفق داخل حوض التسكين وفقًا للتوزيعات المقترحة ، خاصة مع نطاق رقم Froude الذي يتراوح بين 4.5-9.25. علاوة على ذلك ، أثبت استخدام توزيعات كتلة المثلث أن هذا التوزيع ينتج تدفقًا منتظمًا على طول حوض التسكين ، بمدى 5.75-9.25 من رقم Froude. ظهر توزيع الكتلة المتدرجة بنتائج أفضل في تقليل نسب العمق المتسلسلة وسرعات التدفق مقارنةً بالكتلة الحاجزة وكتلة المثلث ، حيث يمكن ملاحظة أن هناك انخفاضًا في السرعات يصل إلى 0.85٪. يميل توزيع السرعة المحلية المستعرضة عبر عرض القناة عند استخدام تكوين الكتلة المتدرجة بينما تبدو هذه القيم أكبر من تلك التي لوحظت مع التكوينين الآخرين.

جمهورية العراق
وزارة التعليم العالي والبحث العلمي
جامعة بابل
كلية الهندسة
قسم الهندسة المدنية

تحري فعالية كتل مختلفة في تشتيت الطاقة ضمن أحواض التهدئة

رسالة

مقدمة الى كلية الهندسة/ جامعة بابل وهي من متطلبات الحصول على درجة الماجستير في الهندسة المدنية/ هندسة الموارد المائية

من قبل

محمد جواد كاظم الفتلاوي

بكالوريوس 2016

أشراف

الأستاذ الدكتور عبد الحسن خضر الشكر

1444